JET CONTROL WITH MICROJETS

By

PRAMEET S. NARULA

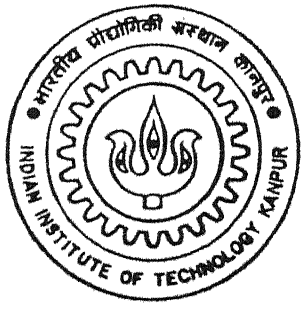

DEPARTMENT OF AEROSPACE ENGINEERING
INDIAN INSTITUTE OF TECHNOLOGY KANPUR
JANUARY, 2001

JET CONTROL WITH MICROJETS

A Thesis Submitted in Partial Fulfillment of the Requirements
For the Degree of

MASTER OF TECHNOLOGY

by

PRAMEET S. NARULA

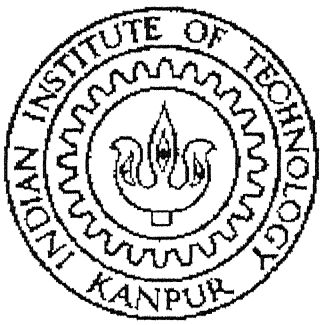

Department of Aerospace Engineering
Indian Institute of Technology Kanpur, India
January, 2001

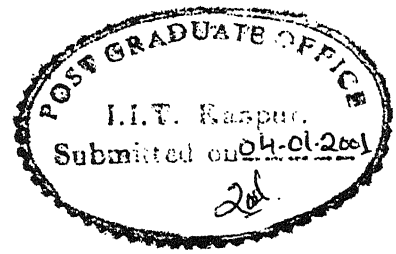

CERTIFICATE

It is certified that the work contained in the thesis entitled **"JET CONTROL WITH MICROJETS"** by Prameet S. Narula, has been carried out under my supervision and that this work has not been submitted elsewhere for a degree.

January 4, 2000

Prof. E Rathakrishnan
Department of Aerospace Engineering
Indian Institute of Technology Kanpur

To

My Beloved Parents

&

Sweet Sister

ACKNOWLEDGMENT

I take this opportunity to express my deep sense of gratitude for *Prof. E. Rathakrishnan* for his exemplary supervision, complete support, unlimited freedom, constant encouragement immense patience and benevolence. A mere word of gratitude is insufficient to express my regard and respect to him. It was a privilege to be associated with him, which was a rich, memorable and cherishing experience.

A special word of thanks to *Mr. Suresh Mishra* who always supported me to the best of his ability.

Prof. S.A. Khan's light minded cheerfulness acted as a refreshner and his sense of humor created a warm atmosphere in the lab.

I thank *Mr. S.S. Chauhan* of Aerospace workshop for his extended help in fabricating of my models.

I would like to acknowledge *Mr. Shishupal Singh* and *Mr. Sharad Chauhan* for their whole-hearted co-operation.

I would also like to thank my friends desai, gullu, rizvi, vivek, sourish, anuj and all others for their help and co-operation.

The blessings of my mother, love of my sister and encouragement of my uncle have been a constant source of inspiration for me.

Above all I would like to thank The Almighty God whose omnivorous presence helped in surpassing all the hurdles throughout the tenure.

Prameet S.Narula

CONTENTS

Nomenclature

ADC	Analog to Digital Converter
D_e	Nozzle exit diameter
M	Nozzle exit Mach number
NPR	Nozzle Pressure Ratio (P_o/P_a)
OASPL	Overall Sound Pressure Level in dB
P	Centreline pitot pressure
P_a	Ambient pressure
P_o	Stagnation pressure in the settling chamber
PRV	Pressure Regulating Valve
PSI	Pressure System Inc.
X	Co-ordinate perpendicular to nozzle exit plane
Y	Co-ordinate parallel to the horizontal 2 microjets
Z	Co-ordinate parallel to the vertical 2 microjets

JET CONTROL WITH MICROJETS

A Thesis Submitted in Partial Fulfillment of the Requirements
For the Degree of

MASTER OF TECHNOLOGY

by

PRAMEET S. NARULA

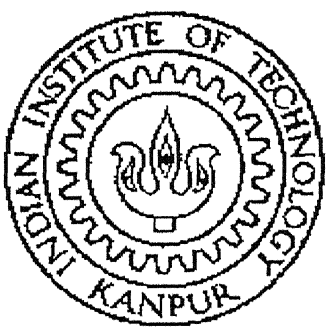

Department of Aerospace Engineering
Indian Institute of Technology Kanpur, India
January, 2001

ABSTRACT

The effectiveness of microjets as active controls for controlling the mixing characteristics of Mach 2 axisymmetric jet has been investigated experimentally. The microjets employed were sonic jets with different levels of under-expansion. Two diametrically opposite microjets and four microjets located on orthogonal diameters were investigated in the present study. In addition to a level of under-expansion, the radial locations of microjets were also studied. For 2 and 4 microjets of Mach 1, exiting orifices of diameter 0.5 mm were employed. In the present study, the operating NPRs for main jet and microjet were the same. Jet centerline decay, pressure survey in grid points across the jet and flow visualization with shadowgraph technique have been carried out to understand the jet propagation process. The present results indicate that the active controls in the form of microjets is most effective in reducing the core-length at correctly expanded operation compared to under- and over-expanded conditions. It is interesting to note that in the nearfield, the microjets act as a shield and protect the shocks in the core. Even though some kind of non-circular shape in the form of elliptical cross-section was observed from the isobaric contour results, a clear axis-switching typical of non-circular jet was not present in the jets. But, there is some far-field manipulation present when the microjets are employed which diffuses the weak shocks beyond certain axial distance for every NPR tested, resulting in a significantly shorter core for the controlled jet compared to uncontrolled one. As high as $6D_e$ reduction in core-length was achieved for a certain combination of parameters of the present study.

Chapter 1

Introduction

Jets are free shear flows driven by the momentum introduced at the exit of, usually, a nozzle or an orifice. Jet flow plays a central role in research aimed at improving our understanding of the fundamental physics of turbulent shear flows in general. High speed jet research is one of the fascinating areas for researchers owing to its wide range of applications starting from house-hold appliances to hi-tech rockets. Research on high-speed jets is mainly focused on the aerodynamic mixing and aeroacoustic characteristics of jets. Decrease of jet core length and noise level is desirable in many application areas of jets. With the above objectives in mind, many control techniques have been studied by a vast number of researchers.

1.1 Jet Control

The diverse nature of applicability of jets demand that they be made suitable for their specific applications by controlling them. Control may be defined as the ability to modify the flow characteristics in such a way as to achieve better engineering efficiency, technological ease, economy, adherence to standards etc. Jet controls may be broadly classified into active and passive controls. In active control, an auxiliary power source (like microjets and acoustic excitation) is used to control the jet characteristics. The other method, termed passive control does not require any additional energy for achieving control. Both active and passive controls mainly aim at modifying the flow and acoustic characteristics of jets to result in enhanced mixing and reduced noise.

1.1.1 Flow Control

Jet flows are an important part of various mixing devices and propulsive systems, wherein enhanced rates of mixing or thrust augmentation is desirable. The jet decay is an important phenomenon. A rapid jet decay implies faster mixing. A typical jet-velocity decay pattern associated with the correctly expanded and "wave dominated" (incorrectly expanded) jets are shown schematically in Fig. 1.1. In combustion chambers with space

constraint, the entire mixing process has to be completed within a short distance. In certain other cases, a jet might be required to entrain more ambient mass. This feature becomes more important for fighter aircraft and missiles where faster mixing of hot gases with ambient cold air causes a rapid jet decay, this rapid decay of jet plume makes the detection of jet more difficult for the infrared sensors commonly used in surface-to-air and air-to-air missiles. This helps in increasing the stealth capabilities of fighter aircraft and missiles.

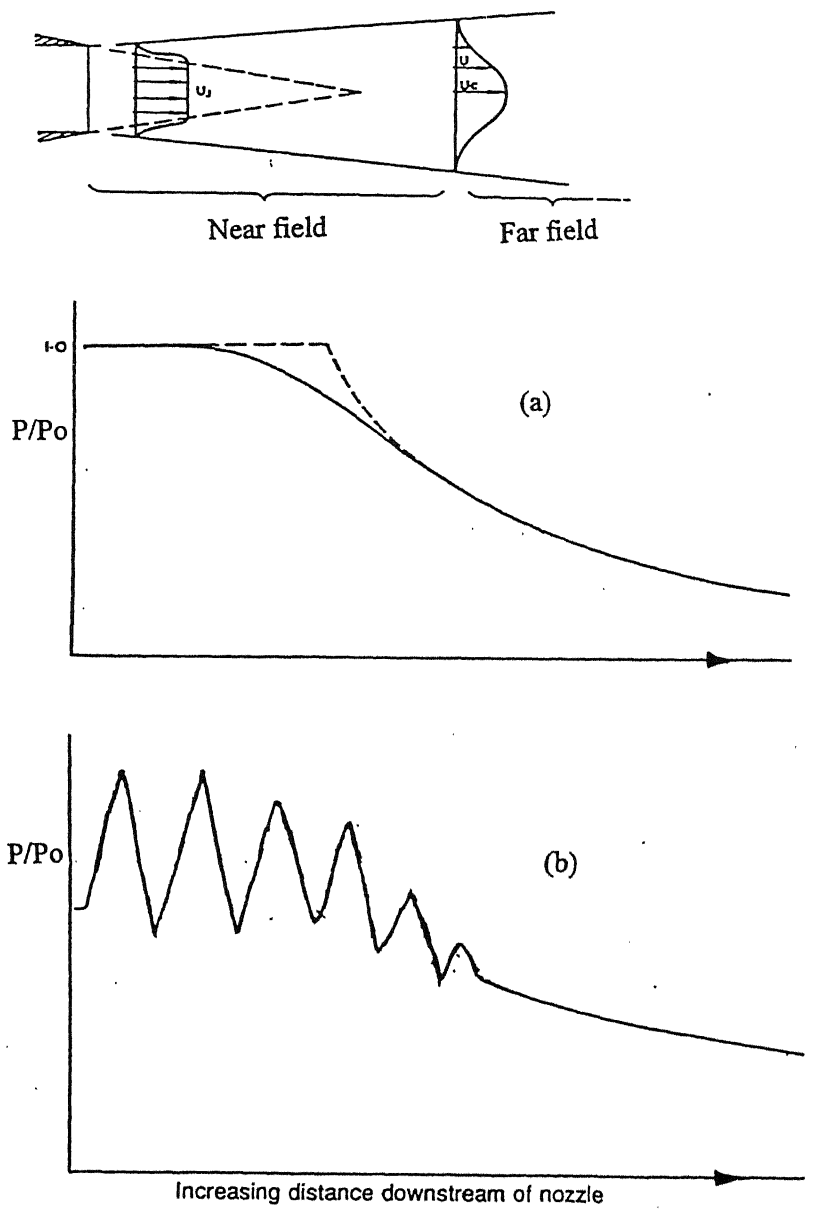

Fig. 1.1. Velocity decay rate in (a) correctly expanded and (b) underexpanded jets.

1.1.2 Jet Noise and its Control

The expression "jet noise" has become part of the international language, and is usually taken to mean the noise of jet-powered aircraft. However, strictly speaking, it covers only those sources associated with the mixing process between the exhaust flow of the engine and atmosphere, and those components associated with the shock system in an incorrectly expanded jet of supercritical velocity.

The origins and spectral characteristics of the jet mixing and shock associated noise are illustrated in Fig. 1.2. For jets operating in the sub critical regime (i.e. with an exhaust velocity less than the local speed of the sound), the mixing noise is the only component of noise. In the case of supercritical jets, shock-associated noise appears as a superimposed secondary source of a largely broadband nature. However, so-called screech tones have been observed in engine exhaust tests and are often a common feature of experimental work on cold model jets. The mechanisms that generate both screech and broadband shock-associated noise have to do with the shock-cells in the jet core.

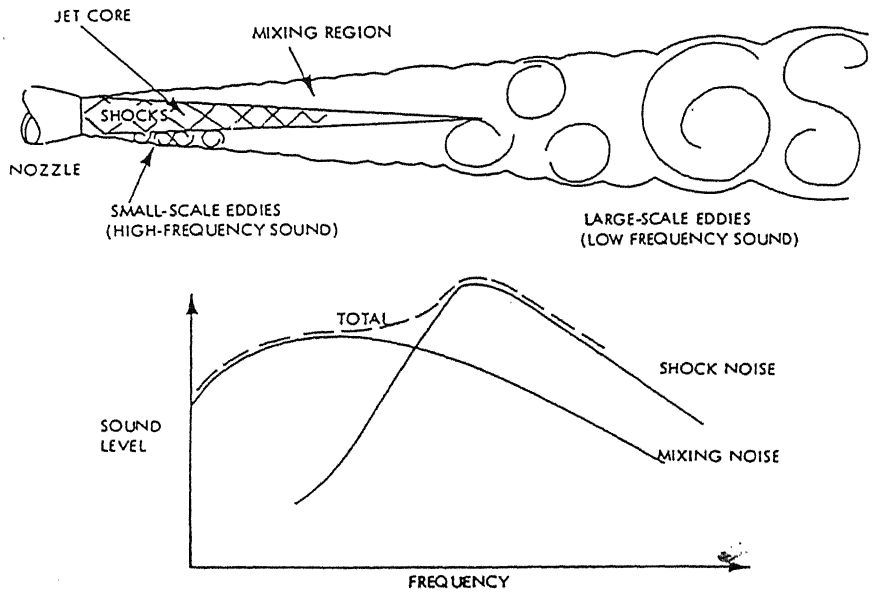

Fig. 1.2. Origin of shock and mixing noise components of jet noise spectrum.

The first generation of pure jets and, to a large extent, the low-bypass-ratio engines that succeeded them, all had extremely high exhaust velocities, which caused high levels of jet noise. The jet velocity could not be reduced, since it was controlled by the thrust requirement via the available total airflow, and jet noise had to be reduced by other approaches. These took the form of mechanical devices aimed at modifying the aerodynamic structure of the mixing process and controlling the energy dissipated as noise.

1.2 Practical Relevance

As it has been already pointed out that the primary motivating factor in jet flow studies is the desire to achieve enhancement of mixing and attenuation of noise. Such studies assume greater importance when the jet velocities involved are in the high compressible range. The problem becomes all the more complicated when the nozzles are operated under off-design conditions, i.e., when the static pressure at the nozzle exit is different from the ambient pressure. The complicated shock and rarefaction pattern existing in imperfectly expanded sonic and supersonic jets have been of fundamental interest in the study of Gas Dynamics. It is well understood that an underexpanded jet leads to expansion waves at the exit of the nozzle which extend to the free pressure jet boundary and reflect as weak compression waves. These compression waves coalesce to form the intercepting shock in the interior of the jet. When the degree of underexpansion is high, the oblique shocks are terminated with a normal shock which is called as Mach disk. The flow behind the Mach disk is clearly subsonic, whereas the flow behind the shock that reflects from the intersection of the intercepting (barrel) shock and Mach disk is still supersonic. The case of underexpanded jet is as shown in Fig.1.3. The shock strength is a function of how far off the design condition the nozzle is operated. These shocks result in additional noise. This shock associated noise is divided into two categories; a narrow band high amplitude tone referred to as jet screech and a broad band tone referred to as broad band shock-associated noise. Underexpanded jets occur in exhaust plumes of aircraft and rocket propulsion systems. They also find use for various industrial applications like metal cutting , swarf clearance, cooling, paint spreading, etc,.

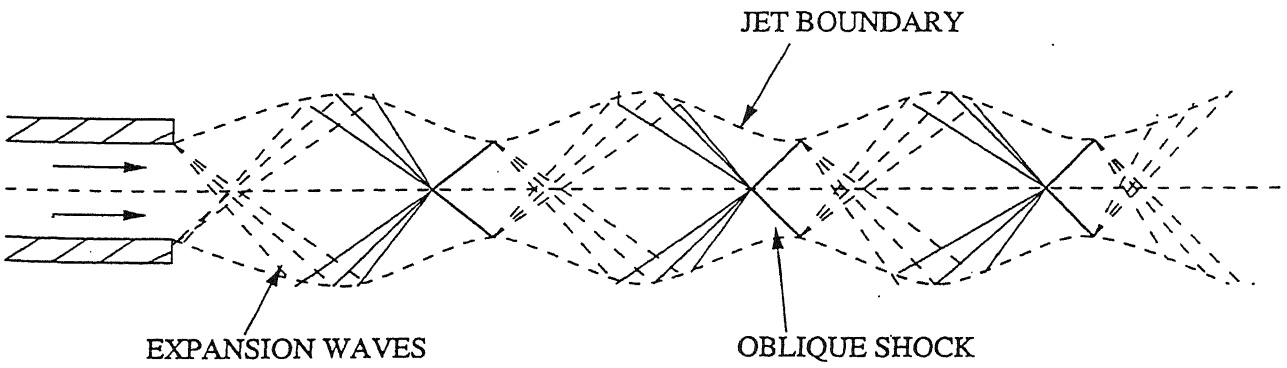

Fig. 1.3. Structure of the underexpanded jet.

When the jet exit pressure is less than the ambient pressure the jet is said to be overexpanded. The flow tries to attain the ambient pressure; this takes place across an oblique shock attached to the nozzle exit outside the duct, as shown in the Fig. 1.4. These days overexpanded jets has assumed greater importance as more and more launch vehicles are using overexpanded jet for their mission. India's very own GSLV is going to use overexpanded jets.

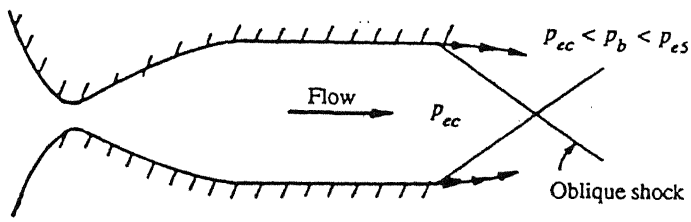

Fig. 1.4. Oblique shock at the exit of an overexpanded jet.

Within the past few years, engineers and scientists have faced two major challenges in which high speed flow mixing is important. The first challenge is to reduce supersonic jet noise, particularly suppressing the screech, in the high speed civil aircraft, and the second challenge is designing an efficient propulsion system for a hypersonic air-breathing vehicle which can ensure enhancement of mixing. The complexities in the shock-shear layer interaction make theoretical studies on underexpanded jet flow fields very difficult. Hence, for proper understanding of such flow fields experimental studies have become indispensable.

1.3 Passive Control of Jets

Among the two main types of jet control, passive controls are mostly desired not only because no external power source is required, but since in some cases the engineer is left with no other option. Passive control methods use geometrical modifications, which alter the flow structure. Some commonly used passive control methods are shown in Fig. 1.5. These methods mostly aim at disturbing the boundary layer at nozzle exit to achieve the desired flow behavior. Particularly, the grooves or tabs at the jet exit trip the boundary layer developing inside the nozzle. This drastically influences the shear layer growth, and the flow behavior, thus providing lot of scope for passive control effectiveness in promoting jet mixing. Some of the popularly employed passive controls are described in the following sections.

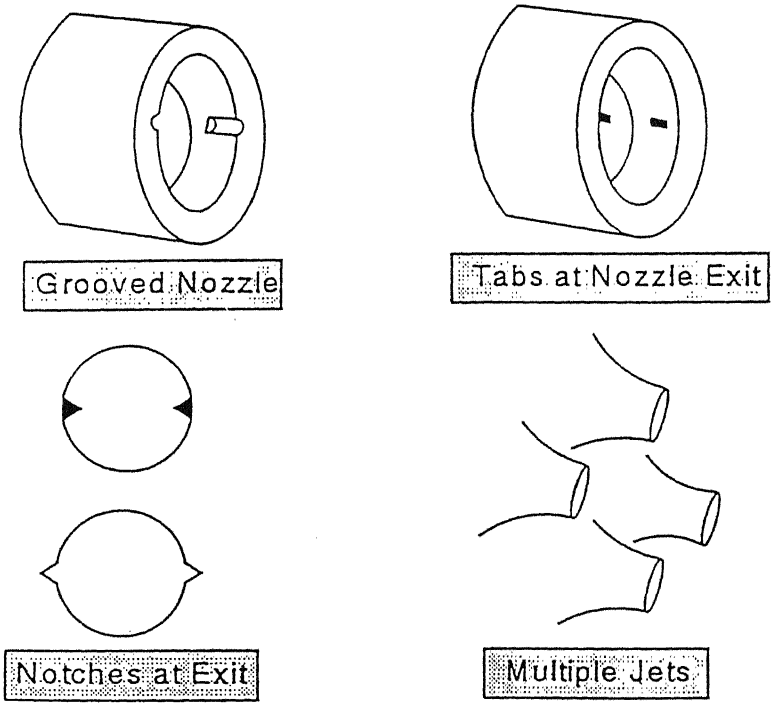

Fig. 1.5. Some commonly used passive control methods for jets.

1.3.1 Twin / Multiple Jets

For the same exit momentum flux, multijets have the following advantages over an equivalent single jet .

The increase in circumferential area when a single jet is split into multiple jets, in turn, increases the interaction of jets with the ambient fluid leading to increased entrainment. But proper choice of the inter-jet spacing is very important as very close spacing may lead to early merging of the jets resulting in reduction of effective area of interaction. This has been interpreted in terms of the reduction of the overall 'mixing surface' available.

Also, multiple jets have been found to attenuate jet noise. It is well known that acoustic power emitted from the jet is proportional to the 8^{th} power of the jet peak velocity for subsonic jets and 3^{rd} power for supersonic jets. Noise reduction in multijets is primarily due to the enhancement of mixing close to the exit leading to the rapid deceleration of the jet peak velocity. Moreover, the layer of slower moving ambient fluid between two adjacent jets causes acoustic refraction and reflection resulting in the shielding of the jet noise sources. Thus, inter-jet spacing plays a crucial role in the problem of noise reduction also. With this idea in mind, a part of the thesis is devoted to the investigation of the microjets at different radial locations.

1.3.2 Jets from Axisymmetric Nozzles with Notches,Tabs and Cut-outs

Another concept that has been proposed for mixing enhancement and jet noise reduction involves the introduction of notches at the nozzle exit. Streamwise vortices generated by the notches cut at the nozzle exit have been demonstrated to be effective in jet noise reduction. These vortices provide the necessary secondary instabilities which aid the faster amplification of the primary instabilities and hence the growth of coherent structures (coherent structures). Thus the evolution of the large-scale structures gets altered by the notches which in turn, alter the mixing and acoustic characteristics of the jet.

The use of small tabs or protrusions at the exit also has been employed effectively for mixing enhancement. It is more likely that the tab acts as a 'winglet' and produces a pair

of trailing vortices which have the same sense of rotation as the trailing vortices originating from the sides of a wing. It should be recognized that for the trailing vortices to form, the wing should be at an angle of attack producing a resultant lift. It is plausible that the boundary layer immediately upstream of the tabs is lifted away from the nozzle wall over a small recirculating zone, so that the streamlines are at an angle of attack with respect to the tab, producing a resultant force acting radially and away from the jet axis, leading to the generation of counter-rotating streamwise vortices. Thus, tripping or disturbing the boundary layer growing along the inner walls of the nozzle using tabs modifies the mixing characteristics of the flow field.

1.4 Active Flow Control

Active flow control (AFC) has the potential to enhance mixing, reduce broadband and discrete tone noise, delay separation, reduce drag, and augment lift. The design of an active flow control system requires knowledge of flow phenomenon and selection of appropriate actuators, sensors, and a control algorithm.

1.4.1 Actuators

The role of an actuator is to inject perturbations at a prescribed frequency into the flow at locations where the flow is most receptive to these inputs. The actuator leverages or disrupts the flow to bring about a desired effect. For example, the conventional excitation methods have relied on exciting instability modes with their most amplified frequency band to bring about jet mixing enhancement. For jet excitation the conventional philosophy has been to energize the large scale coherent structures or bring about vortex interactions that result in the engulfment of surrounding fluid (entrainment). The result is jet mixing enhancement. An example of disrupting a flow phenomena to bring about a desired effect is the suppression of cavity or jet impingement tones. In this case, the excitation destroys the spanwise coherence or disrupts organized structures in the initial region and prevents the sustenance of flow induced resonance.

In an ideal actuator the following characteristics are desired :

(i) controllability in frequency, amplitude and phase

(ii) High bandwidth

(iii) High dynamic range

(iv) No moving parts

(v) Low power requirements

(vi) Fast response

(vii) Ease of integration

(viii) Ease of miniaturization

(ix) Low cost

(x) Insensitive to temperature

(xi) Insensitive to Electro-Magnetic Interference (EMI)

Various types of actuators known are :

(a) Electro-magnetic acoustic drivers, voice coil actuators and ultrasonic actuators

(b) Electro pneumatic drivers

(c) Fluidic actuators

(d) Piezoelectric actuators

(e) Powered resonance tubes

Flow control actuators are designed to inject hydrodynamic perturbations at prescribed frequencies and amplitudes into a carefully selected region of the flow. While it is reasonably straightforward to characterize the output frequency of an actuator the characterization of effective amplitude (dynamic range) can be very challenging. Many actuators have dynamic range output that is significant only over a narrow band of frequencies thus creating a low-bandwidth problem. AFC applications need high bandwidth actuators that can be very effective over a wide range of fluid dynamic and geometric parameters. Some of the most effective actuators that have produced dramatic flow control can function only over a very narrow band of frequencies (e.g., piezoelectric) observed (saturation) and no further increase in jet mixing is observed. Electro-pneumatic drivers require compressed air for their operation and use a modulating valve to obtain pulsed flow at various frequencies. These drivers are capable of producing low frequency (<1000 Hz) excitation with a power of up to 4000 Watts. Fluidic actuators are potentially attractive for shear flow control for several reasons: they

have no moving parts, they can produce excitation that is controllable in frequency, amplitude and phase, they can operate in harsh thermal environments, are not susceptible to electromagnetic interference, and finally they are easy to integrate into a functioning device.

1.4.2 Microjets

A unique active control was attempted which was used to disrupt the feedback loop and thereby reducing the lift loss and the associated unsteady loads. Flow control was implemented by placing multiple supersonic microjets around the periphery of the main jet. The use of such microjets has many potential advantages over conventional systems. First, their extremely small size allow them to be used in places where traditional systems cannot work due to space limitation. Secondly, much faster system response of the microjets will allow the flow through these microjets to be dynamically manipulated. Also, their extremely small size results in minimal mass flow rates and will result in negligible, if any, thrust loss of the primary jet. These properties make them very attractive from a practical perspective. The presence of these supersonic micro-flow streams can also be important for the interception of the upstream propagating acoustic disturbances. Furthermore, these high momentum jets can provide spatial/temporal distortions to the coherent shear-layer instabilities thus disrupting their interactions with the acoustic field.

1.5 Aim of the present Investigation

It is interesting to note that even though the present control is active, it is employed without an additional energy source. The energy required is drawn from the main settling chamber which drives the jet being investigated.

Although some passive controls like tabs, notches, grooves and cut-outs are reported to enhance mixing characteristics. But controls like tabs lead to significant thrust loss, notches, grooves and cut-outs make the flow coming out of the orifice unclean. Therefore an attempt has been made in the present study to investigate the effect of microjets as active control to enhance jet mixing at a supersonic Mach number. Also,

since it has been proved that position of multijets affect the jet mixing characteristics, a part of thesis also investigates the effect of microjets operated at various radial positions.

Chapter 2

Review of Literature

In this chapter, an exhaustive survey on literature of various types of control techniques has been presented which includes both active and passive. Since not enough literature is reported for microjets, hence multiple parallel jets and multiple impinging jets have also been studied. In addition to this, effectiveness of actuators as active controls is also studied below.

2.1 Free Jets

Free jet can be defined as a pressure driven unrestricted flow of a fluid into a quiescent ambience. Since a fluid boundary cannot sustain a pressure difference across it, the jet boundary is a free shear layer in which static pressure is constant throughout. The boundary layer at the exit of a nozzle develops as a free shear layer, mixing with the ambient fluid thereby entraining the ambient fluid into the jet stream. Thus, the mass flow at any cross section of the jet progressively increases along the downstream direction.

2.2 Jets from Nozzles with Tabs

A tab is a small protrusion into the flow, which produces a counter-rotating streamwise vortex pair that can affect the jet flow development significantly. The streamwise vortices usually have a long life and, once introduced in the flow, tend to persist over tens of nozzle exit diameters downstream. This is in contrast to azimuthal vortical structures that are more energetic but have a shorter life span. The generation mechanism of the streamwise vortex pairs by the tabs and their effect on the entrainment and spreading of free jets have been discussed in [1]

In a continuing effort to increase mixing in free shear flows, several researchers have investigated vortex generators in the form of tabs in recent years. Bradbury and Khadam [2] were the first to study in detail the effect of tabs on axisymmetric jet flows. They found that the tabs or small protrusion in the jet flow at the nozzle exit can significantly increase the jet spread. They reported reduction in jet core length from 6De

to 3De, where De is the nozzle exit diameter. Zaman et. al. [3] and Ahuja et. al. [4] carried out a systematic study of jet mixing enhancement with tabs and found that the tabs can increase the jet mixing not only at low speed condition but enhance the mixing at high speed and high temperature conditions also. Ahuja [4] studied a round jet flow at Mach number 1.12 and total temperature 684 K. He found that the potential core length of the jet can be reduced from 6De to less than 2De by using two diametrically opposite tabs. He also concluded that, the tabs can reduce low-frequency noise up to 5 to 6 dB. Most of the investigators have focused their attention on the application of tabs to the overall mixing enhancement performance of tabs and jet noise reduction. However, it was in 1993 that, Zaman et. al. [3] carried out an extensive flow visualization study using laser sheet and cigar smoke illumination and pressure measurements to understand the physics of vortex generation by tabs. They conjectured that the jet distortion introduced by a tab is due to the generation of streamwise vortices. They postulated the generation of these vortices to the presence of two types of sources, the details of which can be found in their paper [3]. Recent study by Navin Kumar Singh and Rathakrishnan [5] have shown that the argument that the projection of tabs beyond the boundary layer thickness is ineffective, presented by Zaman at al [1], is not true and the tabs can extend upto the radius in the case of circular nozzle.

2.3 Jets from Nozzles with Notches

The passive control scheme investigated in this study is based on the modification of the boundary layer growing along the nozzle inner walls achieved through partial notches. Streamwise vortices generated by the notches cut at the nozzle exit have been demonstrated to be effective in jet noise reduction [6]. These vortices provide the necessary secondary instabilities which aid the faster amplification of the primary instabilities and hence the growth of the coherent structures. In effect, the streamwise vortices bring in three-dimensionality to the otherwise, basically, two-dimensional spanwise organized vortical structures (coherent structures). Thus the evolution of the large-scale structures gets altered by the notches which in turn, alter the mixing and acoustic characteristics of the jet. Similar studies have been conducted by many researchers([6], [7], [8]). Pannu and Johannesen [6] investigated underexpanded jets

issuing from notched nozzles. The centerline pitot pressure data indicated that the shock cell structure was modified and the jet decayed faster than the unnotched nozzle flow beyond the core region. They demonstrated that the dominant feature of the flow which determined the structure far downstream was the trailing vortices shed from the swept edges of the notches. They concluded that the notches were effective silencers mainly because they caused the noise sources to be surrounded by a broad region of low speed turbulent flow.

Smith and Hughes [7] presented experimental results obtained in jets from notched nozzles in a co-flowing freestream. The results showed that even at low jet velocities and with slowly tapering nozzles the notches produced quite distinct vortices which persisted well downstream. It was also observed that the introduction of a free stream had little effect on the development in the region of the vortices, though it reduced the rate of decay of the centreline velocity in the main part of the jet. Norum [8] tested a variety of asymmetric nozzles and had some success in alleviating the screech feedback loop. Varying lip thickness of the tube and introducing external tabs were found to decrease screech amplitude for certain modes. Long slots made on the tube yielded extensive suppression for all screech modes. Miller and Seel [9] studied jets issuing from underexpanded nozzles fitted with castellations around their exit and compared them with those leaving plain nozzles. They observed significant improvement in jet entrainment rates in the case of nozzles with castellations.

Krothapalli et al [10] investigated the effect of slotting on the noise of an axisymmetric supersonic jet. They observed that the addition of fingers or slots to a converging axisymmetric nozzle contributed to significant noise reduction. They concluded that slots weakened the shock cell structure near the nozzle exit and thereby reduced the shock-associated noise. Wishart et al [11] reported the experimental results on supersonic jet control using point disturbances inside the nozzle instead of at the exit of the nozzle. They observed significant changes in shear layer development.

Yu et al [12] experimentally studied supersonic flow mixing and combustion using a supersonic nozzle that featured notches and ramps on its expansion side interior wall. The ramp nozzles were found to have a stronger effect on the supersonic flow mixing as compared to the notched ones.

Verma and Rathakrishnan [13] carried out experimental investigation to study the effects of notches on the flow characteristics of elliptic-slot free jets. They observed that the angle of the sharp corner in the notch geometry plays a dominant role in the development of elliptic jets. They also reported that at underexpanded conditions the shock structure in the jet core is weakened considerably, close to the exit, as the angle of the sharp corner is increased from 60^0 to 90^0, resulting in significant reductions in far-field OASPL.

2.4 Jets from Nozzles with Cut-Outs

Conventional plane and axisymmetric nozzles offer limited scope for control of jet mixing and acoustic characteristics. Hence, studies both theoretical and experimental, have been made on jetsfrom nozzles of unconventional exit geometries. Wlezien and Kibens [14] studied the influence of nozzle asymmetry on supersonic jets. The asymmetric nozzles were constant-diameter tubes with various cutout exit shapes. They observed that the introduction of cutouts had a strong effect on the mixing and noise characteristics of the jet flow field. Nozzles with multiple cutouts were found to release internal pressure before the jet reached the ends of the cutouts. The jet plume spread faster than the reference jet, had a lower core-flow Mach number, and did not support screech. Rice and Raman [15] experimentally studied the influence of nozzle exit geometry on jet mixing and noise production in the case of beveled rectangular nozzles. All beveled geometries were found to provide screech noise reduction for underexpanded jets and an upstream mixing noise directivity shift which could be beneficial for improving acoustic treatment performance of a shroded system. Morris et al [16] made a generalized analytical study on single supersonic non-ideally expanded jets with arbitrary exit geometry. They used the boundary element method to predict the shock-spacing and screech tone in a vortex sheet model of a single jet. Both these models could predict with reasonable accuracy the shock-cell spacing and screech tone frequency. The use of orifices instead of nozzles is further justified by Gutmark and Schadow [17] who have shown that an elliptic orifice jet of AR = 3.1 has features similar to an elliptic jet with a well designed contraction. Elangovan and Rathakrishnan [18] studied jets from plain and rectangular orifices with semi-circular cut-outs for both sonic and underexpanded

conditions. The rectangular orifice with cut-outs at the minor axis ends shoed more effective mixing with shorter core lengths and faster near field jet decay when compared with the plain rectangular and the rectangular orifice with the cut-outs at the major axis ends.

Elangovan and Rathakrishnan [19, 20] evaluated the effect of vortex generators in the form of grooves on the penetration and spreading of jets from circular nozzles. In their experiments they found that the grooves weakened the shock cell structure of the underexpanded jets. The jet flow field was found to be strongly influenced by the groove length. Rathakrishnan et al [21] made measurements of sound pressure level on twin elliptic slot jets at close spacings to study their noise characteristics. Results pointed out that spacing is a more crucial parameter than aspect ratio and that twin elliptic slot jets fall in between slotted and plain nozzles in noise suppression.

2.5 Multiple Free Jets

Twin, triple and four jet configurations with Laval nozzles at supersonic Mach numbers have been studied by Rathakrishnan [22]. In this investigation, the analysis was carried out by varying the internozzle spacing between the jets. The entrainment characteristics and the jet decay for different configurations were studied. Moustafa and Rathakrishnan [23] studied the flow field of multijet with square configuration issuing from axisymmetric Laval nozzles. The results show a strong influence of pressure ratio on jet decay, but the inter-nozzle spacing had a little effect on centreline decay. Disimile et al [24] studied the mixing characteristics of twin impinging circular jets, at angles of nozzle configuration. The rates of decay of centreline total pressure were found to be similar for both 30 and 45 Ahmed et al [25] investigated the measurements in a free jet. Time mean velocity measurements show how the development of a free jet may be influenced by subjecting it to the pulsations transmitted from a surrounding annular jet. Wlezien [26] studied the nozzle geometry effects on supersonic jet interaction .It was observed that the nodal amplitudes are strongly dependent on nozzle spacing. For closely spaced nozzles, coupling occurs at low Mach numbers and is suppressed at high Mach numbers. The converse is true for large spacing.

Krothapalli et al [27] had presented the results of experiments with a multiple jet configuration. They concentrated on the development of a single jet in an array of rectangular jets. They observed that the individual jets acted quite independently of each other near the nozzle exit. The mutual interaction between the jets resulted in a lower turbulence level when compared to a single jet at corresponding locations. Marsters [28] studied experimentally the flow field from an array of rectangular jets. He observed that the velocity profiles across individual jets showed self preservation prior to merging suggesting that the jets decayed independently upstream of merging. It was concluded that when the nozzles were closely spaced, the rate of decay was greatly retarded, which indicated the reduction in mixing and momentum transfer from the jet.

Raghunath and Reid [29] made a study on the flow field and noise level of multiple jets. The effect of number of jets (5,7 and 9) on the momentum of the combined jet was also investigated. They observed substantial reduction in noise level for the five-jet case. It was also found that that the reduction in noise level by increasing the number of jets above five was rather small. They concluded that a multiple jet nozzle with five jets (equispaced and arranged along the circumference of the circle) offered an advantage in terms of noise reduction without significant reduction in the momentum of the jet. Scheweizer [30] investigated the mixing process in the near field of a triple rectangular jet. The mixing process was dominated by rolling-up mechanism of the free shear layer into rectangular vortices. The vortex shedding frequency was found to be a function of Reynolds number, slit width and velocity ratio between the inner and outer jets. Raman and Cornelius [31] studied the jet mixing control using excitation from miniature oscillating jets. They observed that the jet velocity decays more rapidly for the forced than the unforced jet. The normalized mass flux ratio was higher for the forced jet than for the unforced one.

Krothapalli et al [32] experimentally studied the structure and development of partially confined multiple jets (jets issuing from an array of rectangular nozzles). Measurements of mean velocity and Reynold stress were made. They observed that for downstream distances greater than 60 widths, the flow field was nearly homogeneous and the turbulence appeared to be quite similar to that of a grid generated turbulence.

2.6 Twin Parallel Free Jets

Miller and Comings [33] studied the subsonic flow field generated by identical twin jets of air issuing from parallel slot nozzles in a common wall. The entrainment of ambient air by individual jets close to the nozzle exit was found to create a sub-atmospheric region between the two jets. For this reason, the two jets attracted each other and finally merged together to form a single jet. A free stagnation point was observed on the plane of symmetry. The flow characteristics of the combined jet exhibited all characteristics of a single jet flow. Upstream of the merging region of the jets, two stable symmetrical; counter-rotating vortices which recycled air into the inner layers of the jets were observed. Tanaka [34] studied the flow field created by twin parallel two-dimensional jets using a single wire probe. A vane probe was used to determine the flow direction. He observed that even though the velocity profiles of the combined flow were similar and agreed well with the theoretical profile of the single jet, the distributions of the turbulence intensities showed a different property from those of the single jet in the initial region by requiring that the internal stream tube undergo sufficient compressive turning to cancel the local pressure gradient due to area expansion. A method was proposed to calculate Mach disk position.

Yuu et al [35] studied the turbulence characteristics of twin plane parallel jets. They observed a high negative shear stress in the merging region. Marsters [36] studied analytically and experimentally the flow field of the two plane parallel jets issuing from free-standing nozzles. In this case, interjet air entrainment was allowed and the formation of vortices upstream of the merging region was not observed. His works included measurements of static pressure and mean velocities and was not concerned with turbulent intensities. Elbana et al [37] reported results of an experimental study on the interaction of two identical two-dimensional turbulent jets issuing from parallel free-standing nozzles. The results showed that the velocity profiles of the combined flow were similar and in agreement with that of the single jet. They observed that the distributions of the three components of turbulent velocity fluctuations showed different behaviour than that for the single jet, but the maximum shear stress had nearly the same value as that in the single jet. Okamato et al [38] presented an experimental study on the interaction of two turbulent circular ventilated jets. They observed that the twin jet

interacted and joined in the form of an ellipse at a downstream distance becoming close to a circular jet at a far downstream distance. Rathakrishnan et al [39] carried out an experimental investigation on mean flow field of two jets issuing from two circular nozzles set on a common end wall. They observed that for the range of nozzle spacings studied, the twin jet combined completely into a single jet at a downstream distance of around 30 nozzle diameters.

2.7 Twin / Multiple Impinging Jets

The presence of a solid wall (kept at an angle or normal to the jet axes) could drastically alter the flow and acoustic characteristics of a twin/ multi jet flow field. Such configurations occur in the impingement cooling, rocket launching, propulsion of V/ STOL aircrafts etc. The resulting flow field id characterized by the impingement tone that influences the initial flow development and hence the mixing and noise characteristics of the flow field, and the fountain flow or the reverse flow resulting from the collision of the radial wall jet that develops after impingement. Sherrieb [40] conducted experimental studies to measure propulsion-induced ground effects on a generalized V/ STOL aircraft model with two-, three-, and four-jet configuration. The four-jet configuration was shown to be an attractive arrangement because the flow field caused buoyancy close to the ground, situates the fountain (reverse flow) near the aircraft center of gravity (reducing induced moments), and carried the exhaust gases along the paths that limited reingestion. Deflecting the jets towards each other and away from each other was found to reduce reingestion of hot gases into the engine intake. Savory and Toy [41] reported results of an experimental investigation of the interaction between twin side-by-side circular jets issuing into a cross flow, utilizing a real-time video digitization system to obtain quantitative data from the visualized flow fields. They observed that the nozzle spacing was not a suitable scaling parameter since the development of widely spaced jets was fundamentally different from that of closely spaced jets where there was no cross flow penetration between jets. Siclari et al [42] studied theoretically and experimentally the flow field of two impinging jets. They proposed a single analytical momentum model, which could adequately predict the characteristics of the stagnation lines generated by

unequal strength vertical jets. But some discrepancies were observed in case of obliquely impinging jets.

Elbanna and Sabbagh [43] presented the results of an experimental study of the flow field characteristics of the interaction of two-dimensional jets impinging against a normal ground plane. It was found that, in a two-impinging-jet flow, the rate of decay was higher than that for a single jet. Miller and Wilson [44] experimentally investigated the wall jets created by single and twin high-pressure jet impingement. They observed that twin jet flows were dominated by a reinforced region on the symmetry flow compared to a single jet flow. Nozzle spacing and height were found to have a strong influence on the acoustic properties of the impinging jet flows.

Knowels and Bray [45] studied experimentally, the flow fields associated with single and twin jets impinging in cross flows. The results showed that the ground vortex penetration increased with height for twin jets and it seemed to be associated with jet merging. At a particular nozzle height, the twin nozzle toe-in angle had a strong effect on vortex penetration as a consequence of jet merging. Miller [46] conducted an experimental investigation into the wall jets created by single, twin and four inclined impinging jets. He observed that the splay angle (both inward and outward toe-in / toe-out) had a strong effect on the flow field. Outward splay cases tended to produce a more azimuthally uniform flow field, whereas the inward splay behavior was strongly dependent on height, spacing and splay angle.

A model for characterization of the impingement region was proposed by Giralt et al [47] in which the velocity and the jet width at the location above the wall surface where the jet deflects have been chosen as the velocity and length scales, respectively. These results were found to agree closely to inviscid solutions. Donaldson and Snedeker [48] conducted parametric study of the wall pressure distribution, choosing various shapes such as concave, convex hemispheres, cylindrical cup and flat pate. They considered wall pressure distribution due to three types of jets from a convergent nozzle, namely, subsonic, moderately and highly underexpanded. The pressure distributions are used to compute the radial velocity gradient at the impingement stagnation point. It was found that for normal impingement, this gradient correlates with the freejet centerline velocity and half-radius at the same axial location. They reported a fall-off in the radial

velocity gradient at the impingement stagnation point for oblique impingement as compared to normal impingement.

In addition to complexities such as fine scale coherent and incoherent structures, impinging jets are associated with vortex rebounding phenomenon, reversal of axial velocity and unsteady separation at the wall resulting in the formation of secondary vortex structures which have vorticity of opposite sense as compared to the primary vortices of the free jet. A physical model on the formation of the secondary vortex as a result of impingement of the primary vortex was proposed and investigated by Harvey and Perry [49]. The surface pressures on the wall are divided into two distinct zones, the positive pressures and the periodic pressure variations. Knowels [50] reported that minimum pressure point corresponds to ground vortex core position, while the maximum pressure point corresponds to the ground vortex penetration point, and the zero pressure corresponds to the ground vortex separation point. Ignatius and Rathakrishnan [51] experimentally investigated the normal and oblique, subsonic and underexpanded impingement. The shadowgraph pictures of normal and oblique impingement show that the stand-off shock remains parallel to the nozzle exit plane when the wall is moved away from the nozzle exit. The jet spread was found to be strongly influenced by obliqueness of the wall, whereas the wall pressure similarity is independent of obliqueness. The positive pressure zone at the center of impingement planes disappears for a wall at $10D_e$ for subsonic impingement, whereas for underexpanded it disappears as as early as $4D_e$.

2.8 Actuators as active flow control

For actuators that produce sound (acoustic excitation) one could measure the Sound Pressure Level (SPL) dB, or corresponding p' (rms) levels. Alternate metrics of active actuation include fluctuating velocity (u'(rms)) levels measured at the point of injection in flows that we were trying to control. Raman et al [52] made it possible to relate the measured SPLs (p', rms) and fluctuating velocity (u',rms) perturbation levels. The connection between the u' and p' fluctuations will be made for the plane excitation using acoustic drivers connected to plenum chamber. A hot wire and microphone were placed simultaneously 0.125 D on either side of the jet exit plane. The data showed that higher sound pressure levels are required at higher frequencies to produce the same u'fe

(velocity perturbation levels at frequency f). Raman et al [53] and Stanek et al [54] used piezoelectric actuators which consisted of a piezo ceramic element that is bonded to the surface of a wedge shaped cantilevered aluminium element. The peizo ceramic element outputs oscillatory motion that is amplified by exploiting the resonant structural vibration of the wedge shaped amplifier. In the work of Raman et al [52] two frequency excitation was successful and the two frequency excitation signal was produced using a complex waveform generator. The signal is represented as: $u = A \sin(2\omega t + \varphi) + B \sin \omega t$, where 2ω is the fundamental and ω represents the sub harmonic. The initial phase difference is the angle by which the fundamental coherent velocity the coherent sub harmonic velocity. Raman et al [52] used Ling electro-pneumatic actuators in conjunction with a complex waveform generator to produce the controlled multi-frequency signal. Electro-pneumatic drivers are capable of producing low frequency (<1000 Hz) excitation with a power of upto 4000 Watts.

Recent work done at the NASA Glenn Research Center provides examples of the application of the fluidic devices for jet mixing enhancement and cavity resonance suppression. Two examples of applications are provided in this paper. In the first application, Raman [55] two bi-stable fluidic nozzles were located on either side of a larger scale primary rectangular nozzle. The two fluidic nozzles were interconnected through their feedback tubes and then operated either in- or out-of-phase with respect to each other. Excitation in the in-phase (sinuous) mode resulted in a 35% enhancement of the mass flux of the primary jet. In the second application, Raman et al [56] used miniaturized (1 mm i.d.) fluidic nozzles developed by Bowles Fluidic Corporation to suppress cavity tone resonance. It was seen that with the upstream excitation the cavity tone is suppressed by 10 dB with only a 0.12%(of the main flow) mass injection. Downstream excitation had no effect on the cavity tone. In addition, steady mass injection at the same levels had no effect on the cavity tones.

It is seen from the above discussions that even though a vast quantum of literature on jet control is reported, almost all of them are passive in nature. Further, controls like tab will result in significant thrust loss and controls like notches, grooves and cutouts will make the flow coming out of the nozzle orifice unclean. Actuators although do not alter the nozzle geometry, but they occupy a lot of space and are very cumbersome to handle.

Therefore, it is desirable to have control, which will improve the jet mixing characteristics without any adverse effects as above.

Rathakrishnan et al [57] investigated experimentally with four microjets of 1mm orifice diameter located at 90^0 interval along the middle pcd of base region. The Mach numbers of suddenly expanded flows were 1.87, 2.2 and 2.58. the jets were operated with nozzle pressure ratio (NPR) from 3 to 11. it was found that microjets can serve as active controllers for base pressure. Also, the wall pressure was not significantly influenced by microjets.

Although microjets were used as active control for base pressure in suddenly expanded axi-symmetric flows by Rathakrishnan et al [57], there is perhaps no work done in investigating the behavior of microjets for jet control. With this aim an attempt is made in the present study to investigate the effect of microjets as active control to enhance jet mixing at a supersonic Mach number. The microjets employed were 0.5 mm in diameter with four microjets located at orthogonal diametrical positions. Investigation was carried out with two microjets operating at one time and all the four microjets operating at the other. To investigate the behavior of microjets at different radial locations, a part of thesis deals with microjets positioned at different pcd's i.e. at 22, 24 and 26 mm respectively.

Chapter 3

Experimental Setup and Procedure

This chapter gives an overview of the test facility, describes the experimental arrangements, the measurement carried out and the various tools developed for the same. The uncertainty in the measurement is mentioned for all the measurements carried out.

3.1 The Test Facility

The experiments were conducted in the jet test facility at the High Speed Aerodynamics Laboratory, Indian Institute of Technology Kanpur, India. The layout of the laboratory is shown in Fig 3.1. The test facility consists of (1) compressor, (2) storage tanks and (3) jet test facility.

A two-stage reciprocating compressor, capable of delivering 360 cfm of air at a pressure of 500 psig is being used in this laboratory. The compressor is driven by a 150 hp 3-Ph induction motor. A cooling water circuit, driven by an independent pump, cools the compressed air through an inter-cooler. The compressed air is then passed through a pre-filter consisting of porous stone candles; to remove solid contaminates like rust particles and oil droplets. An activated carbon filter is further used for finer filtering. The compressed air is dried in a dual-tower semi-automatic silica gel dryer. While one tower is in use, a portion of the dried air is heated and used to reactivate the other. A diaphragm type back pressure valve operated by pressure relief pilot, permits the dryer to operate at 500 psig, while the pressure in the storage tanks builds up from atmospheric to storage pressure. The compressed dry air is stored in three tanks, having a total capacity of 3000 ft^3 at 300 psig.

The air enters the settling chamber through a tunnel section with a gate valve followed by a pressure regulating valve (PRV), and a mixing length. The settling chamber is connected to the mixing length by a wide-angle diffuser. The flow is further conditioned inside the settling chamber by closely meshed grids meant for minimizing

turbulence. The settling chamber is a constant area circular section of 300 mm inner diameter and 600 mm length. The test model is fixed at the end of the settling chamber with O-ring sealing to avoid leakage. A photograph of the test facility along with the traversing system and instruments is shown in Fig 3.2.

3.2 Instrumentation for Pressure Measurements

The pitot pressure sensed by the probe was measured using a PSI model 9010 16-channel pressure transducer (interfaced with a PC386). The model 9010 transducer is capable of measuring pressures up to 300 psig, which is approximately 20 atm. The software provided by the manufacturer was used to interface the transducer with a computer. The user-friendly menu-driven software acquires data, and shows the pressure readings from all the 16 channels simultaneously in a window type display on the computer screen. The software can be used to choose the units of pressure from a list of available units, perform a rezero/full calibration, etc. The transducer also has a facility to choose the number of samples to be averaged, by means of dip-switch settings. The accuracy of the transducer (after rezero calibration) is specified to be ± 0.15% full scale. A view of the pressure transducer and computer is shown in figure 3.3. The settling chamber pressure was similarly displayed on the computer display using one of the 16 channels of the PSI 9010 transducer. The pressure measurements are accurate within ± 1.8%. The stagnation pressure was maintained with an accuracy of ± 0.1%. The maximum uncertainty in the pitot pressure data was estimated to be ± 3.5% [58].

3.3 Experimental Models and Measurement Procedure

A Mach 2 convergent-divergent nozzle was used in the present study. The nozzle had a 30° semi-convergent angle and 7° semi-divergent angle. The nozzle exit diameter was 11.4 mm. For generating microjets at three radial locations around the nozzle exit radius, 3 inserts as shown in Fig.3.4 were fabricated. The microjets distances studied were r/r_e = 1.93, 2.10, and 2.28, where r_e is the nozzle exit radius and r is the radial distance of the microjet. On each insert 4 microjets of diameter 0.5 mm each were located on two orthogonal diameters as shown in Fig.3.4. The microjets were operated by blowing air

from a separate settling chamber. The nozzle pressure ratios (NPR) for microjets and the main jet were the same in the present investigation. Measurements were made with NPR 4 to 10, in steps of one. Microjets were operated two at a time and four at a time depending on the requirement. For two microjets operation, only two jets on a diameter were activated.

The flow measurements include pitot pressure survey along the (geometric) centreline of the jet, at correct and incorrectly expanded flow conditions. For the spread and entrainment analysis, pitot pressure was measured at points on rectangular grids in the X-Y, X-Z and Y-Z planes. A typical grid consisted of 50 to 300 points depending on the axial location. For example, the jet width is small at the exit plane, and hence, lesser number of points are sufficient to obtain the cross-sectional structure. As the jet grows in size along the axial direction, the number of points required to get the cross-sectional structure would be more in number.

The pitot pressure probe is mounted on a three-dimensional traverse (see Fig.3.2), for the pitot pressure surveys conducted over the entire flow field. The traverse has six degrees of freedom, which also includes a probe-yawing mechanism. The traverse has a spatial resolution of 0.1 mm. in all the three dimensions. The pitot probe used had an inner diameter of 0.4 mm. and outer diameter of 0.6 mm. Pitot pressure measurements prove to be important in high speed supersonic jets, where the flow regime is shock dominated. As mentioned by Rice and Raman [15], supersonic flows pose considerable measurement problems in using hot-wire or hot-film anemometry. To avoid these difficulties one can measure the raw total pressure, i.e., the total pressure downstream of the bow-shock standing ahead of the pitot tube in supersonic flow.

3.4 The Shadowgraph System

In shadowgraph the positions of the image points on the view screen are affected by the deflections in the test section. The reflected rays are brought to focus in the focal plane, and the light beam uniformly illuminates the screen. The screen is placed at a position close to the test section so that the effect of ray deflection becomes visible. This effect, termed as shadow effect, is illustrated in Fig. 3.5. On the screen there are bright zones where the rays crowd closer and dark zones where the rays diverge away. At places

where the spacing between the rays is unchanged, the illumination is normal even though there has been refraction.

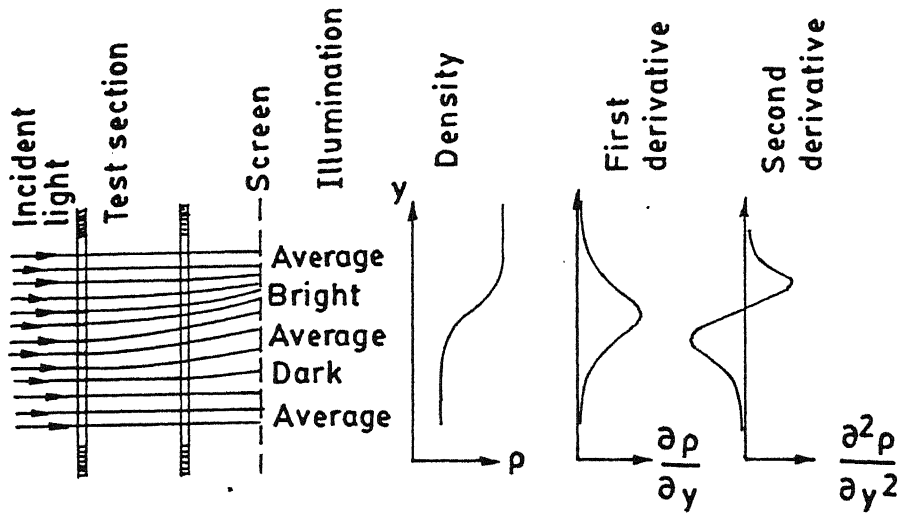

Fig. 3.5. The shadow effect

Thus, the shadow effect depends not on the absolute deflection but on the relative deflection of the light rays, that is, on the rate at which they converge or diverge on coming out of the test-section.

A shadowgraph.consists of a light source, a collimating lens, and viewing screen, as shown in Fig. 3.6.

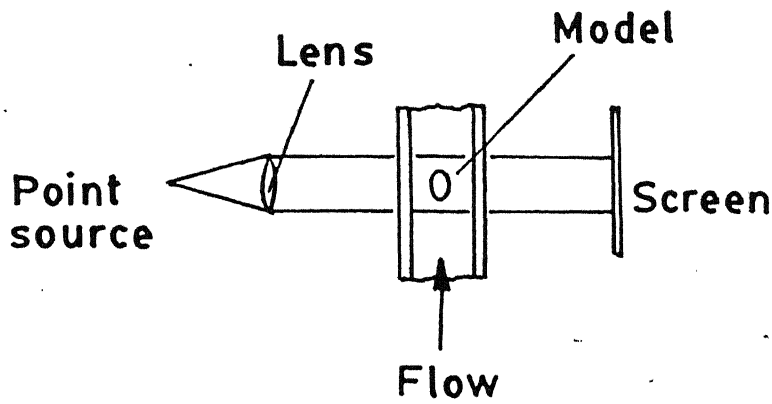

Fig. 3.6. The Shadowgraph System

Let us assume that the test-section has stagnant air in it and that the illumination on the screen is of uniform intensity. When flow takes place through the test-section the light beam will be refracted wherever there is a density gradient. However, if the density

gradient everywhere in the test-section is constant, all light rays would deflect by the same amount, and there would be no change in the illumination of the picture on the screen. Only when there is a gradient in density gradient there will be tendency for light rays to converge or diverge. In other words, the variations in illumination of the picture on the screen are proportional to the second derivative of the density. For a two-dimensional flow the increase of light intensity can be expressed as

$$\Delta I = k\,(\partial^2\rho/\partial x^2 + \partial^2\rho/\partial y^2)$$

where k is a constant and x and y are the coordinates in a plane normal to the light path.

Therefore, the shadowgraph is best suited only for flow fields with rapidly varying density gradients. A typical shadowgraph of a detached shock wave is shown in Fig. 3.7. We know from shock theory that density increases from upstream to downstream of such a shock in an S-shaped curve. Hence, the shock has positive and negative rate of change of density gradient across it. Therefore, the shock is made up of a dark line followed by a bright line in the shadow picture, in accordance with the shadow effect.

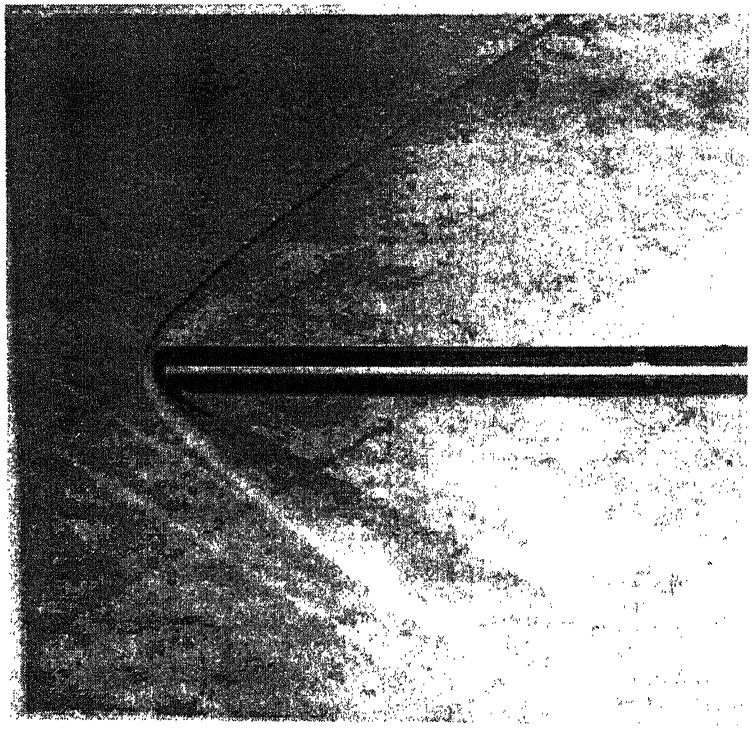

Fig. 3.7. Shadowgraph picture of a detached shock wave

3.5 Experimental Precautions

In addition to the measures taken to minimize errors, like linearity checks, rezero calibrations, etc., the following precautions were observed during the experiments.

- The vertical and horizontal alignment of the settling chamber was ensured.
- Care was exercised in the alignment of the models, to ensure proper positioning of the measurement planes.
- The nearest wall is 150 diameters. Hence, wall effects are negligible.
- The pressure lines and the settling chamber ports were ensured to be leak free.
- During the experiments, the stagnation pressure reading was constantly monitored.

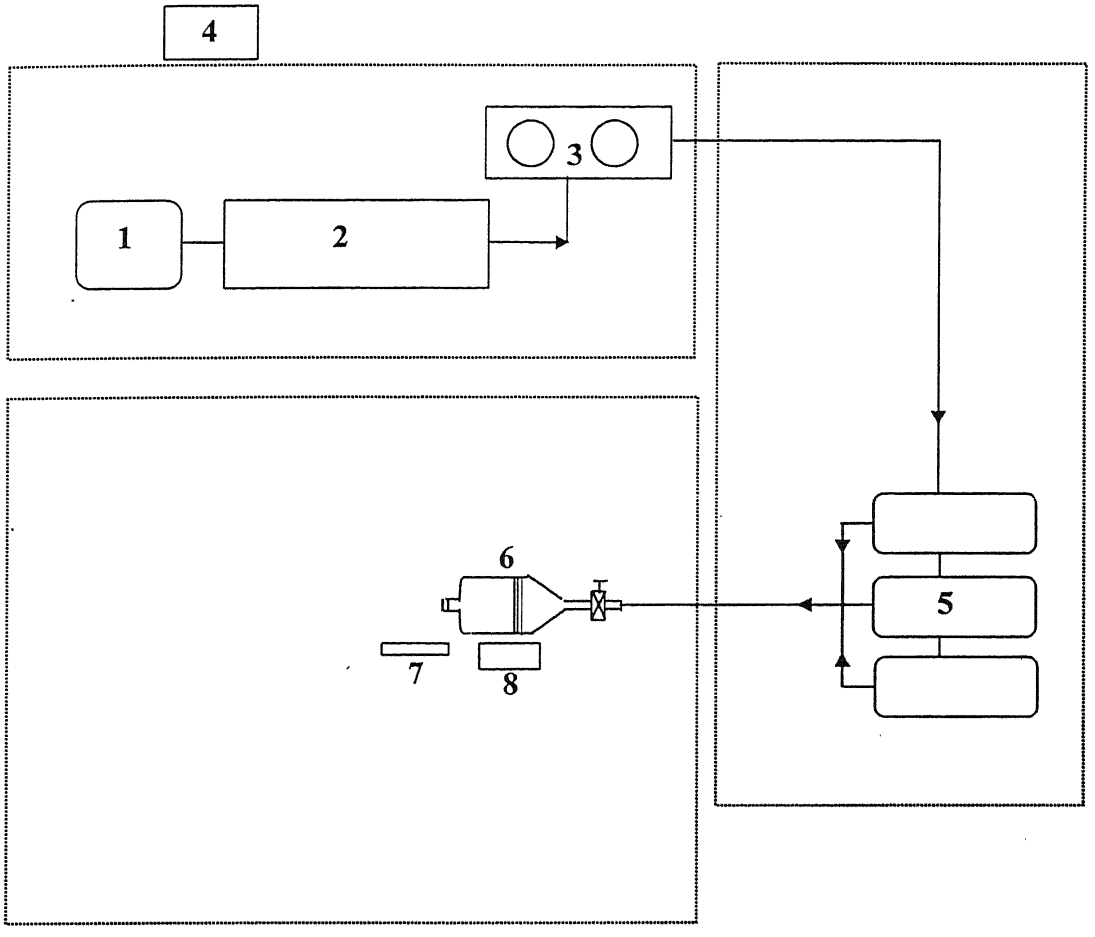

1. **150 hp induction motor**
2. **Ingersoll Rand two stage reciprocating compressor**
3. **Activated Charcoal Filter and Silica Gel dryer units**
4. **Water cooling unit**
5. **Storage tanks**
6. **Jet test facility**
7. **Manometer**
8. **Transducer and Computer desk**

Fig. 3.1. Layout of the Laboratory.

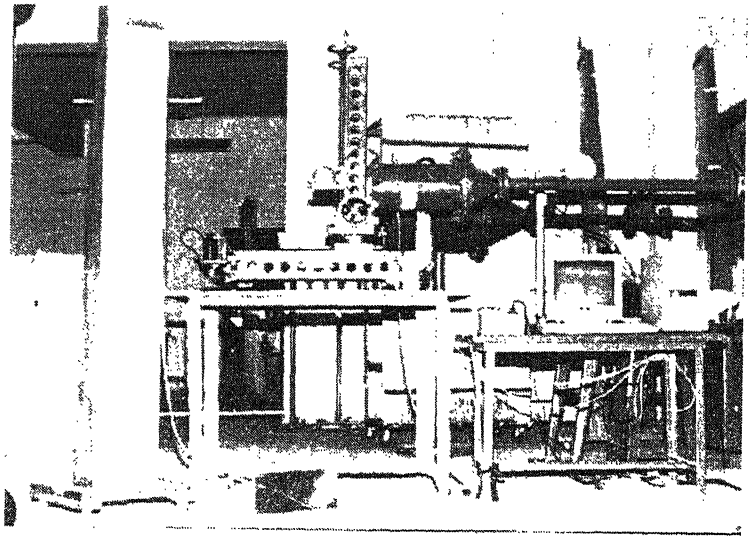

Figure 3.2 A view of the Jet Test Facility

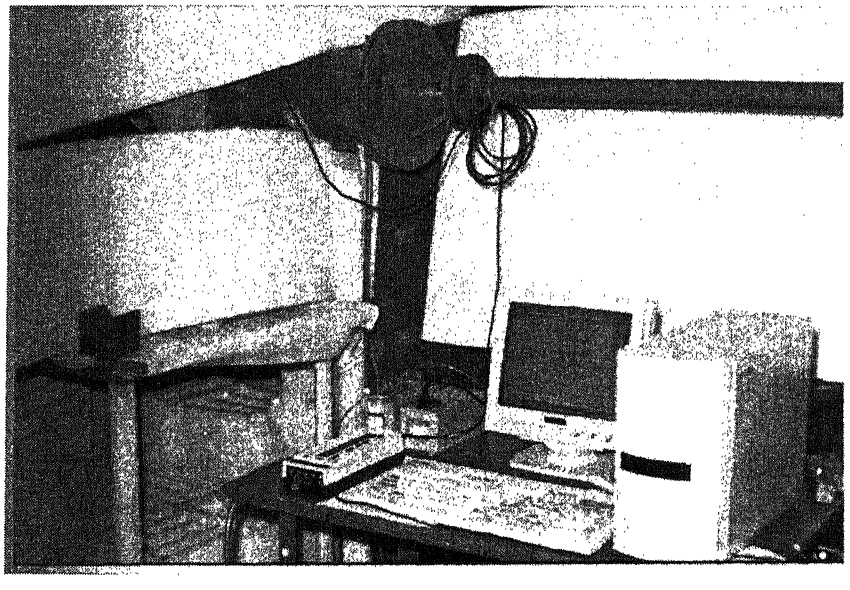

Figure 3.3 Pressure Measurement Setup

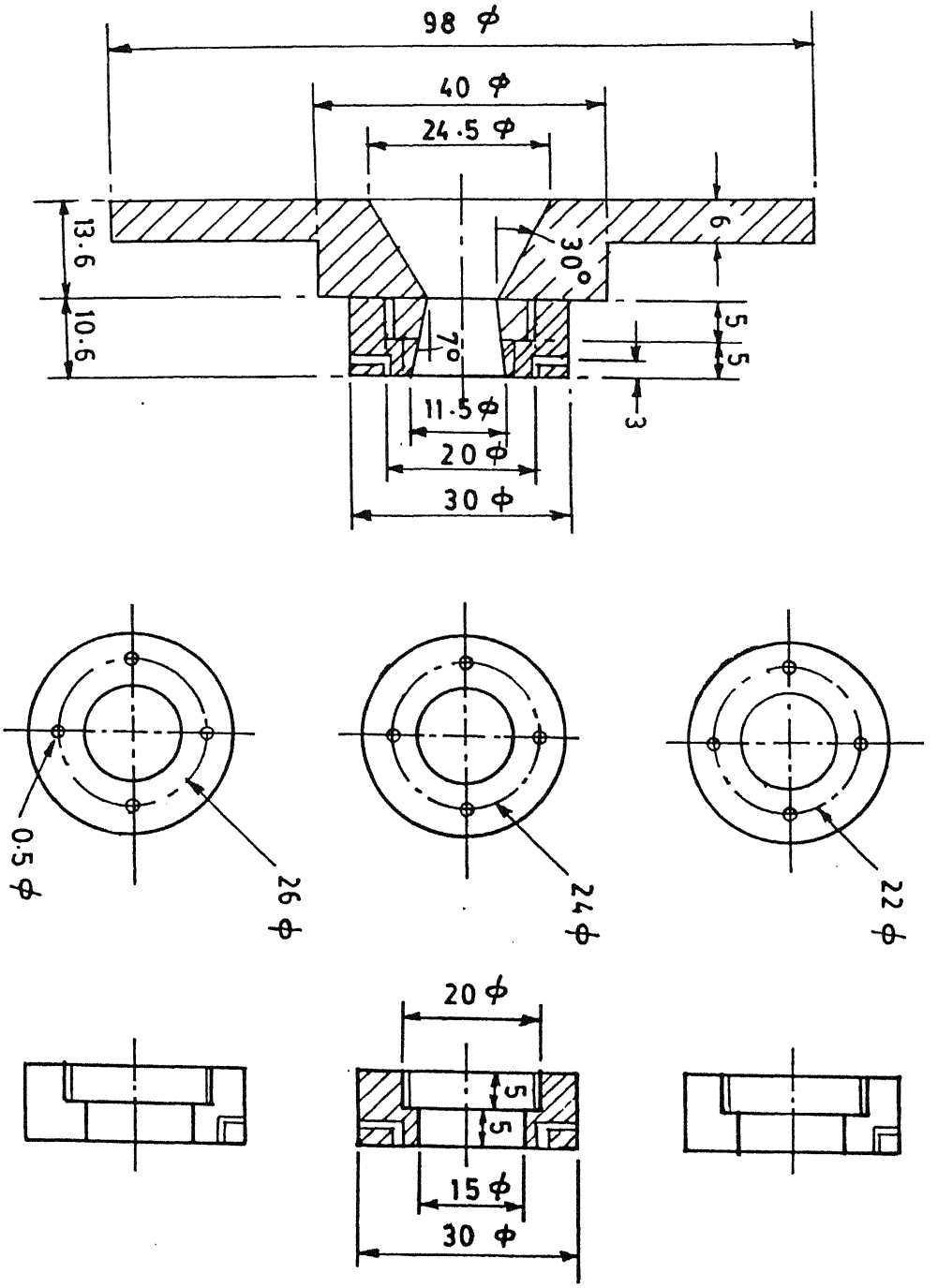

Fig. 3.4. Experimental Model.

Chapter 4

Results and Discussions

The measured data consists of pitot pressure along jet centreline at different axial locations from X/D_e = 0 to 30, where X is the axial distance and D_e the nozzle exit diameter. In supersonic flow the measured pitot pressure (P_t) is not the actual pressure but it is the pressure behind the bowshock positioned ahead of the pitot probe nose. In the present study no correction is made for this measured pressure since it is an impossible task to correct these pressures owing to wide variation of Mach numbers in the jet field. Nonetheless these measured pressures are good enough for analyzing the mixing characteristics of the jet and the shock cell length in the jet core. Hence the results presented, even though qualitative in nature, are good enough for analyzing the effectiveness of microjets on the jet mixing characteristics.

The measured pitot pressures are non-dimensionalised with the settling chamber pressure (P_o). The axial distance is non-dimensionalised with the nozzle exit diameter. In the present study, the nozzle pressure ratios tested were such that all the three levels of expansion namely over-, correctly and underexpanded conditions were covered.

4.1 Centreline Pressure Survey

The jet centreline decay for NPR 4 for the cases of 0, 2 and 4 microjets were presented in Figs. 4.1 to 4.3 for r/r_e = 1.93, 2.10 and 2.18, respectively. For Mach 2 jet this condition corresponds to overexpansion. It is seen from these results that, the microjets are extremely efficient in weakening the shocks in the jet core. This may be regarded as a definite advantage from jet acoustics point of view since, shock strength reduction results in reduction of shock associated noise and hence reduction in overall sound pressure level. The effect of microjets on core length is only marginal for this NPR. Also, influence of 2 and 4 microjets are almost identical. (The radial location of microjets seems to be a marginal influence on the jet control).

Centerline decay results for NPR 5 are present in Figs. 4.4 to 4.6. This NPR is also a case of overexpansion but with a reduction in adverse pressure gradient compared to NPR 4. The microjets were found to offer shielding to entrainment in the vicinity of nozzle exit. Shocks with microjets remain much stronger compared to plane nozzle. Because of this the core length comes down considerably, when the microjets are introduced. For plain nozzle, the core extends upto $8D_e$ whereas for the nozzle with microjets, the core extents only upto $5D_e$. Here again the radial locations is only of marginal effect on the jet control, but the number of jets for radial location $r/r_e = 1.93$ shows different influence between 2 and 4 microjets. The mixing enhancement offered by 4 microjets is much higher than that with 2 microjets. Whereas, for $r/r_e = 2.10$ and 2.18 there is no significant difference between the behaviours of 2 and 4 microjets.

For NPR 7 similar results as above are shown in Figs. 4.7 to 4.9. For Mach 2 jet, this NPR is close to the correct expansion NPR of 7.8. Therefore the adverse pressure gradient is only marginal. It is interesting to note that, even though the microjets do not offer any distinct advantage in terms of reducing the shock strength in the jet core, the core length has come down from nearly $18D_e$ for the plain nozzle to about $10D_e$ for the 2 and 4 microjets. This clearly indicates that the additional shear introduced by the microjets augments the micro level mixing of the main jet. To ensure the above behaviour, measurements were made with NPR 8, which is again nearly correct expansion for Mach 2 jet, are presented in Figs. 4.10 to 4.12. Here again it is seen that there is considerable reduction in core-length when the microjets are introduced.

The effect of microjets in the presence of favourable pressure gradient can be seen from the results presented in Figs. 4.12 to 4.15 for NPR 9. The shielding to jet mixing offered by the microjets is clearly seen from these results in the near field. However, beyond $12D_e$, the additional shear due to microjets results in significant advantage in terms of core length reduction. For the plain jet, the core extends as far as $18D_e$ whereas with microjets the core ends at about $12D_e$, for all the three radial locations tested. Here again 2 and 4 jets show only marginal difference in their influence for $r/r_e = 1.93$. However, the 4 jets showing better performance in terms of reducing the core length is evident for $r/r_e = 2.10$ and 2.18.

The effect of increase in the degree of favourable pressure gradient on jet mixing with microjets is shown in Figs. 4.16 to 4.18. These results are for NPR 10. Here again it is seen that, the shocks preserve their strength in the near field when the microjets are introduced. But beyond some axial distance for all the cases of radial locations of microjets it is seen that the mixing is significantly influenced by the microjets and core is reduced from nearly $18D_e$ of plain nozzle to about $12D_e$ for 4 microjets case and to about $16D_e$ for 2 microjets case.

From the above results, it is evident that the number of microjets is of only marginal consequence for overexpanded and correctly expanded jets. But for underexpanded jets, the 4 microjets appears to be a better mixing promoter compared to 2 microjets especially with increase in favourable pressure gradient.

4.2 Isobaric Contours

To understand the physics of the jet propagation in the presence of microjets, pressure measurement were made in grid points. Depending on the configurations (plain nozzle, nozzle with 2 and 4 microjets) the grid measurements were made over one-half of the jet cross-section and symmetry was exploited to analyze the jet. The measured pressures in the jet field have been non-dimensionalised with the corresponding stagnation pressure in the settling chamber. The non-dimensional pressure contours in the Y-Z plane at different axial locations from $X/D_e = 0$ to 15 are analyzed.

4.2.1. Overexpanded Jets

The isobaric contours for jets at NPR 5 for the cases of no, 2 and 4 microjets for microjet location $r/r_e = 1.93$ are presented in Figs. 4.19 to 4.29. In the discussions of centerline decay it was seen that at overexpansion, the microjets offer some kind of shielding to the jet core in the near field upto (approx.) $X/D_e = 5$. From the isobaric contours in Fig. 4.19 it is seen that, when there are no microjets, the pressure starts decreasing continuously from the jet centerline to jet boundary. The innermost isobaric lobes in the figure correspond to 70% of the stagnation pressure. When 2 microjets are operated, it is interesting to note that large portion of flow around jet axis in the plane normal to

microjets plane is unaffected by jet mixing at the periphery. Whereas, when 4 microjets are operated the portion of 70% isobar is much smaller compared to 2-microjet case. The reason of this behaviour is that when there are no microjets, mixing initiated at the jet boundaries could be able to penetrate the jet all around the periphery and progress towards the centerline. When 2 microjets are activated, the microjets have their own mixing process and thereby retard the penetration of mixing in the plane of microjets (Fig. 4.19). When 4 microjets are activated, all the 4 initiate mixing and move towards the centerline slightly faster than 2 jets case as seen in fig. 4.19. The retarded penetration of mixing with 2 and 4 microjets is seen as stronger shocks as compared to plane nozzle jet. The 2 microjets case exhibits the strongest shock followed by 4 and no microjet, as seen in Fig. 4.1. At $X/D_e = 1$, the mixing initiated by the microjets and the main jet shear layers interact and move towards the jet axis. This is seen as clustering of isobaric lines in Fig. 4.20. As the jet moves further, at $X/D_e = 2$, the 2 microjet case even though retains it's identity in the form of two kinks, has penetrated considerably towards the centerline and 4 microjet configuration has almost dominated the entire mixing process across the jet. At $X/D_e = 3$, the penetration of mixing almost approached the jet axis. For the plain nozzle jet, there are two distinct zones of mixing seen around jet axis. Whereas, for 2 and 4 microjets, the mixing is over a single zone around the jet axis, as seen in Fig. 4.22. At $X/D_e = 4$, it is seen that the high pressure zone around the jet axis is divided into a number of isobaric regions, indicating that the strong inertial region has been divided into local zones. Whereas, for 2 and 4 microjets, the high inertia zone at the jet axis retains it's identity over a single zone, as shown in Fig. 4.23. At $X/D_e = 5$, plain nozzle jet has high pressure zone around the jet axis. This prevails over a considerable area. Whereas, for 2 and 4 microjets, the high-pressure zone around the jet axis is getting influenced by the mixing process as seen in Fig. 4.24. The mixing dominance over jet axis progressively increases as seen in Fig. 4.25 to 4.29. For $X/D_e = 6$, 8, 10, 12 and 15, respectively. The high inertia zone over a considerable portion around jet axis for the plain nozzle is responsible for the mild shocks prevailing upto about $X/D_e = 8$, rendering the core longer than compared to 2 and 4 microjets. For X/D_e more than 15, the jet with and without microjets decay almost identically.

4.2.2 Correctly Expanded Jets

The isobaric contours for plain jet and jet with 2 and 4 microjets at NPR 7, which is nearly correctly expanded condition, are given in Figs. 4.30 to 4.40. for X/D_e = 0 to 15. For plain nozzle jet mixing activity has become very active at the periphery at NPR 7 as compared to NPR 5. This is in good agreement with the jet literature which states that in the absence of waves, the mixing initiated at the jet periphery can penetrate faster towards jet axis compared to wave dominated jets. When microjets are introduced, it is found that mixing process at the jet periphery is influenced only marginally. Further, the high inertia zone around the jet axis is of nearly equal size for the plain nozzle, 2 and 4 microjets, as seen in Fig. 4.30 for X/D_e = 0. This may be due to the expansion fan positioned at the nozzle lip which deflects the flow away from the centerline at X/D_e = 0. At X/D_e = 1, Fig. 4.31, it is seen that the mixing process is progressively moving towards the jet axis. Here again it is seen that there is not much difference between the plain and controlled jet. Similar isobaric contour patterns are observed at X/D_e =2, Fig. 4.32. But at X/D_e =3, the 2 microjets lost their identity but 4 microjets still have some identity. As the jet progresses, fragmentation of high inertia zone at the center exhibiting number of lobes of constant pressure around the jet axis is seen at X/D_e =6, Fig. 4.36. Also, a kind of elliptic shape of the jet cross-section is established at X/D_e = 5. For further downstream stations (X/D_e = 10, 12 and 15) the mixing has almost approached the centerline but, for plain nozzle jet there is significant portion of high inertia zone present at the central zone. From the above discussions it is evident that the additional shear activities introduced by the microjets could able to influence the jet mixing after X/D_e = 8. In the nearfield, because the flow is reflected away by the expansion fan at the nozzle exit, the microjets were not able to enhance the mixing process. This leads to almost identical shocks at the core upto X/D_e = 8. However, for X/D_e more than 8, the mild shocks present in the jet core for the plain nozzle have been almost neutralized by the microjet activity rendering the core to become shorter.

4.2.3 Underexpanded Jets

It is well established in jet literature that a control becomes effective when there is a favourable pressure gradient present, for passive control techniques. However, this influence was questioned by Sreejith and Rathakrishnan [59] and proved that there is no need of favourable pressure gradient for control to become most effective. Furthermore, it has been proved that for the case of passive control in the form of a tab extending upto nozzle center, the control was most effective at correctly expanded condition as compared to under- and overexpanded jet. Therefore, it is mandatory to look into control effectiveness considering all the parameters influencing the jet propagation. To have an insight into the control effectiveness of active control as in the present case, pressure measurements were made across the jet field, for NPR 9 and NPR 10, which correspond to underexpanded condition with favourable pressure gradient. The isobaric contours for axial locations $X/D_e = 0$ to 15 for NPR 9 are shown in Figs. 4.41 to 4.51. At $X/D_e = 0$, the additional mixing process initiated by microjets is clearly seen in Fig. 4.41. At $X/D_e = 1$, the activities of mixing has penetrated considerably and the high pressure zone at the center has started fragmenting. But there is no specific dominance of microjets on the mixing process (Fig. 4.42.). As the jet propagates, compared to lower NPRs' the mixing process has become faster for NPR 9 at $X/D_e = 2$ (Fig. 4.43.), $X/D_e = 3$ (Fig. 4.44.) and so on. The well-established elliptic cross-section of the jet at $X/D_e = 5$ at NPR 7 is observed as early as X/De = 2 for NPR 9. This clearly implies that controls perform better when a favourable pressure gradient is present. The size of ellipse grows as the jet moves further downstream. However, the shock strengths (high-pressure zones at the center) are not influenced much by the controls. But for $X/D_e = 12$, the microjets diffuse the weaker shocks present in the core of the plain nozzle jet. Because of this, the controlled jet has a significantly shorter core compared to the plain nozzle jet.

To authenticate the above observations of enhanced mixing experienced by the controlled jets under favourable pressure gradient, the favourable pressure gradient was enhanced by increasing the NPR from 9 to 10. The results for NPR 10 are presented in Figs. 4.52 to 4.62. It is interesting to note that as early as $X/D_e = 1$ the jet cross-section exhibits an elliptic nature. As we move further, it is seen that the mixing process is

enhanced, as seen as closely packed isobaric contours in Fig. 4.55 at $X/D_e = 3$ and so on. For this case also, the weak shock waves prevailing upto nearly $19D_e$ for the plain nozzle have been completely eliminated by the microjets at about $12D_e$. This can be taken as an advantage since one of the dreams of the jet researcher is to reduce the core-length and make the core as short as possible.

4.3 Flow Visualization

To gain an insight into the influence of the microjets on the wave structure in the jet core, flow visualization was carried out with shadowgraph technique for the cases of plain nozzle, 2 microjets and 4 microjets. Recording of the visualizations were done at NPR 10, 9, 7 and 5. In the discussions on centerline decay in section 4.1, it was seen that the expansion level of jet has a significant role to play on the wave structure in jet core. However, there it was not possible to exactly quantify the reduction of shock-cell length in the nearfield when the microjets were used. But from the flow visualization pictures, one can easily quantify the shock-cell lengths. The NPR covered in visualization is such that all the three expansions namely, over-, correct- and underexpanded jets were generated.

Wave Structure for NPR 10

The shocks and expansion waves in the core of jets with no controls, with 2 microjets and with 4 microjets are given in Fig. 4.63, for NPR 10. It is evident from these pictures that, the microjets act as effective controller in reducing the shock-cell length of first two cells. The first cell is the longest for the jet from plain nozzle (no controls). The length comes down compared to plain nozzle when 2 microjets are activated. Similar reduction in the cell length for second and third cells is also seen from these results. It is well known from Tam's theory that reduction in shock-cell length will result in shock associated noise reduction and hence reduction in OASPL for the jet.

Wave Structure for NPR 9

The visualization figures for NPR 9 for the three cases of jet without control, jet with 2 microjets control and jet with 4 microjets control are shown in Fig. 4.64. Here, again it is explicitly seen that the microjet control results in significant reduction in shock cell lengths for jets with 2 and 4 microjets compared to the jet without control. Further, the maximum width of first and second cells also show significant reduction.

Wave Structure for NPR 7

For the present case of Mach 2 jet, NPR 7 is closer to correctly expanded NPR namely 7.84 whereas, NPR 10 and 9 gave underexpanded jets with favourable pressure gradient. At NPR 7, which is slightly lower than the NPR required for correct expansion, therefore there is a mild adverse pressure gradient present at the nozzle exit. It is well known that the passive controls for jets work efficiently when there is favourable pressure gradient but, as discussed in section 4.1, for active controls in the form of microjets the existence of favourable pressure gradient does not seem to be mandatory for control effectiveness. The visualization pictures at NPR 7 authenticate the above point. It is explicit from these results that there is considerable reduction in the shock-cell length when the microjets are employed. Control with 4 microjets is found to be most effective in reducing the shock-cell length compared to 2 microjets.

Wave Structure for NPR 5

The jets at NPR 5 experience an increased adverse pressure gradient compared to NPR 7. It is interesting to note that the microjet control becomes more effective when the adverse pressure gradient is enhanced as evident by the reduction in the length of shock-cells for controlled jets compared to the plain jets. Here again 4 microjets reduce the core length more effectively than 2 microjets.

The above discussions reveal that the logic that the control becomes more effective in the presence of favourable pressure gradient does not seem to be valid for the active controls in the form of microjets.

Chapter 5

Conclusions

The microjets were found to be effective active controls for Mach 2 supersonic jet. For smaller radial locations, 4 microjets were found to be more effective than 2 microjets in enhancing mixing. The control effectiveness of microjets increases with decrease of adverse pressure gradient. The microjets were found to be most effective for almost correctly expanded jets. The jet core length reduced from $18D_e$ to $10D_e$ for correctly expanded jets. At correct expansion the number of microjets is only of marginal influence on jet mixing. The microjets were found to be effective mixing promoters at underexpanded conditions. Also, at this condition, the effect of 2 and 4 microjets on mixing promotion is distinctly different.

From isobaric contours, which were studied from X/De = 0 to 15, it is seen that the core length was shorter with 2 and 4 microjets. For correctly expanded jets from X/De = 0 to 8, microjets could significantly influence the jet mixing. From X/De = 10 to 15, the mixing almost approached the centerline but for plain nozzle jet there is significant portion of high inertia zone present at the centre.

To gain an insight into the influence of microjets, shadowgraph pictures were taken for various configurations. The shock-cell length was found to get decreased in the case of nozzle with 2 and 4 microjets. However, nozzle with 4 microjets led to larger reduction in shock-cell length for all the three cases namely, over-, correctly- and underexpanded jets.

Suggestions for Future Work

As for this case where a symmetrical configuration of only 2 and 4 microjets was employed, various different configurations with different number of microjets can be studied. Microjets applied at different angles to the main jet can be studied, care should be exercised to ensure that the angular microjets do not abate the thrust advantage. Microjets diameter can also be increased to a certain optimum value. Microjets pcd should be fully scanned so as to get a better view of the optimum placement of microjets. That is, one should experimentwith number of microjets and their location so as to get a better understanding of microjets as active controls.

Bibliography

[1] Zaman K B M Q, Reeder M F and Samimy M, 1994, "Control of an Axisymmetric Jet using Vortex Generators", *Physics of Fluids*, Vol. 6, No.2, pp. 778.

[2] Bradbury L J S and Khadem A H, 1975, "The distortion of a jet by tabs", *Journal of Fluid Mechanics,* Vol. 70, pp. 801-813.

[3] Zaman K B M Q, 1993, "Streamwise vorticity generation and mixing enhancement in free jet by Delta-Tabs", *AIAA Journal,* 93- 3253.

[4] Ahuja K K, 1993, "Mixing enhancement and jet noise reduction through tabs plus ejector", *AIAA Journal, 93-4347.*

[5] Singh N K and Rathakrishnan E, "Effect of Tab Geometry on Sonic Jet Characteristics" accepted in *22nd International Symposium on Space Technology and Science*, Morioka, Japan, May 28-June 3, 2000.

[6] Pannu S S and Johannesen N H, 1976, "The Structure of Jets from Notched Nozzles", *Journal of Fluid Mechanics*, Vol. 74, pp. 515-528 .

[7] Smith D J and Hughes T, 1984, "The Flow from Notched Nozzles in the presence of a Freestream", *Aeronautical Journal*, Vol. 88, pp. 77-85.

[8] Norum T D, 1983, "Screech Suppression in Supersonic Jets", *AIAA Journal*, Vol. 21, pp.235-240.

[9] Miller P and Seel M W R, 1991, "The Application of High Pressure Ejectors to Reaction Control Systems", *Aeronautical Journal*, Vol. 95, pp. 297-312.

[10] Krothapalli A, McDaniel J and Baganoff D, 1990, "Effect of Slotting on the noise of an axisymmetric supersonic jet", *AIAA Journal*, Vol. 28, pp. 2136-2138.

[11] Wishart D P, Prothapalli A and Mungal M G, 1993, "Supersonic Jet Control via Point Disturbances inside the Nozzle", *AIAA Journal*, Vol. 31, pp. 1340-1341.

[12] Yu K H, Schadow K C, Kraeutle K J and Gutmark E J, 1995, "Supersonic flow mixing and Combustion using Ramp Nozzles", *Journal of Propulsion and Power*, Vol. 11, pp. 1147-1153.

[13] Verma S B and Rathakrishnan E, 1998, "Mixing Enhancement and Noise Attenuation in Notched Elliptic-Slot Free Jets", *International Journal of Turbo and Jet Engines*, Vol. 5, pp. 7-25.

[14] Wlezien R W and Kibens V, 1988, "Influence of Nozzle Asymmetry on Supersonic Jets", *AIAA Journal*, Vol. 28, pp. 27-33.

[15] Rice E J and Raman G, 1993, "Supersonic Jets from Beveled Rectangular Nozzles", *ASME paper 93-WA/NCA-26.*

[16] Morris P J, Bhat T R S and Chen G, 1989, "A Linear Shock Cell Model for Jets of Arbitrary Exit Geometry", *Journal of Sound and Vibration*, Vol. 132, pp. 199-211.

[17] Gutmark E and Schadow K C, 1987, "Flow Characteristics of Orifice and Tapered Jets", *Physics of Fluids*, Vol. 30, pp. 885-891.

[18] Elangovan S and Rathakrishnan E, May 1998, "Effect of Cut-Outs on Underexpanded Rectangular Jets", *The Aeronautical Journal*, pp. 267-275.

[19] Elangovan S, 1996, "Studies on Passive-Controlled Sonic and Underexpanded Free Jeets", *Ph.D Thesis*, Indian Institute Of Technology, Kanpur, India.

[20] Elangovan S and Rathakrishnan E, 1998, "Passive Control Of Sonic and Supersonic Jets", *Proceedings of the 21st International Symposium on Space Technology and Science*, Vol. 1, Omiya.

[21] Srinivasan K, Elangovan S and Rathakrishnan E, 1997, " Twin Elliptic Jet as a Candidate for Attenuation of Jet Engine Exhaust Noise", *International Journal of Turbo and Jet Engines*, Vol. 14, pp. 99-104.

[22] Rathakrishnan E, 1995, "Studies on the Flow Field of Multiple Supersonic Jets", *ASME/JSME High Speed Jet Forum*, FED-Vol. 214, pp. 169-174.

[23] Rathakrishnan E and Moustafa H, 1993, "Studies on the Flow Field of Multijet with Square Configuration", *AIAA Journal*, Vol. 31, pp. 1189-1190.

[24] Disimile P J, Savory E and Toy P J, 1995, "Mixing Characteristics of Twin Impinging Circular Jets", *Journal of Propulsion and Power*, Vol. 11, pp. 1118-1124.

[25] Ahmed S and Turner T, Aug 1995, "Measurements in a Free Turbulent Jet", *ASME/EALA Conference on Laser Anemometry*, pp. 100-103.

[26] Wlezien R J, 1989, "Nozzle Geometry Effects on Supersonic Jet Interaction", *AIAA Journal*, Vol. 27, pp. 1361-1367.

[27] Krothapalli A, Baganoff Dand Karamcheti K, 1980, "Development and Structure of a Rectangular Jet in a Multiple Jet Configuration", *AIAA Journal*, Vol. 18, pp. 945-950.

[28] Marsters G F, 1980, "Measurements in the Flow Field of a Linear Array of Rectangular Nozzles", *Journal of Aircraft*, Vol. 17, pp. 42-46.

[29] Raghunathan S and Reid I M, 1981, "A Study of Multiple Jets", *AIAA Journal*, Vol. 19, pp. 124-127.

[30] Schweiger G, 1983, "Regular Structures in a Plane Triple Jet", *Journal of Fluid engineering*, Vol. 105, pp. 42-46.

[31] Raman G and Cornelius D, 1994, "jet mixing control using excitation from miniature oscillating jets", AIAA Journal, Vol. 33, pp. 365-368.

[32] Krothapalli A, Baganoff Dand Karamcheti K, 1980, "partially confined multiple jet mixing", *AIAA Journal*, Vol. 19, pp. 324-328.

[33] Miller D R and Comings E W, 1960, "Force-Momentum Fields in a Dual-Jet Flow", *Journal of Fluid Mechanics*, Vol. 7, pp. 237-256.

[34] Tanaka E, 1970, "The Interference of Two-Dimensional Parallel Jets (1st Report Experiments on Dual Jet)", *Bulletin of JSME*, Vol. 13, pp. 272-280.

[35] Yuu S, Shimoda F and Jotaki T, 1979, "Hot Wire Measurements in the Interacting Two-Plane Parallel Jets", *A I Ch E Journal*,Vol. 25, pp. 676-685.

[36] Marsters G F, 1977, "Interaction of Two Plane Parallel Jets", *AIAA Journal*, Vol. 15, pp. 1756-1762.

[37] Elbanna H, Gahin S and Rashed M I, 1983, "Investigation of Two Plane Parallel Jets", *AIAA Journal*, Vol. 21, pp. 986-991.

[38] Okamoto T, Yagita M, Watanabe A and Kawamura K, 1985, " Interaction of Twin Turbulent Circular Jet", *Bulletin of JSME*, Vol. 28, pp. 617-622.

[39] Rathakrishnan E, Reddy V and Padmanabhan K, 1989, "Some Studies on Twin Jet Propogation", *Mechanics Research Communications*, Vol. 16, pp. 279-287.

[40] Sherrieb H E, "Ground Effects Testing of Two-, Three-, and Four-Jet Configurations", 1979, *Journal of Aircraft*, Vol. 16, pp. 393-397.

[41] Savory E and Toy N, 1991, "Real Time Video Analysis of Twin Jets in a Crossflow", *Trans. ASME. Journal of Fluid Engineering*, Vol. 113, pp. 68-72.

[42] Siclari M J, Hill Jr. W J and Jenkins R C, "Stagnation Line and Upwash Formation of Two Impinging jets", 1981, *AIAA Journal*, Vol. 19, pp. 1286-1293.

[43] Elbanna H and Sabbagh J A, 1989, "Flow Visualization and Measurements in a Two- Dimensional Two-Iimpinging-Jet Flow." *AIAA Journal*, Vol. 27, pp. 420-426.

[44] Miller P and Wilson M, 1993, "Wall Jets Created by Single and Twin High Pressure Jet Impingement", *Aeronautical Journal*, Vol. 97, pp. 87-100.

[45] Knowels K and Bray D, 1993, "Ground Vortex Formed by Impinging Jets in Crossflow", *Journal of Aircraft*, Vol. 30, pp. 872-878.

[46] Miller P, 1995, "A Study of Wall Jets Resulting from Single and Multiple Inclined Jet Impingement", *Aeronautical Journal*, Vol. 99, pp. 201-216.

[47] Giral F, Chia C J and Trass O, 1977, "Characterization of the Impingement Region in an Axisymmetric Turbulent Jet", *Ind. Eng. Chem. Fundam.*, pp. 21-28.

[48] Donaldson C D and Snedeker R S, 1971, "A Study of Free Jet Impingement, Part1. Mean Properties of Free and Impinging jets", *Journal of Fluid Mechanics*, Vol. 45, pp. 281-319.

[49] Harvey J K and Perry F J, 1971, "Flow Field Produced by Trailing Vortices in the Vicinity of the Ground", *AIAA Journal*, Vol. 9, pp. 1659-1660.

[50] Knowels K, 1991, "Recent Research Iinto the Aerodynamics of ASTOVL Aircraft in Ground Environment", *IMECHE Part G: Journal of Aerospace Engg.*, pp 123-131.

[51] Ignatius T J and Rathakrishnan E, 1996, "Studies on Oblique Impinging Subsonic and Sonic Jets", *Fluids Dynamics Research*, Vol. 18, pp. 183-198.

[52] Raman G, Rice E J and Reshotko E, 1991, "An Experimental Study of Natural and Forced Modes in an Axisymmetric Jet", *NASA TM* 105225.

[53] Raman G, Kibens V, Cain A and Lepicovsky J, 2000, "Advanced Actuator Concepts for Active Aeroacoustic Control", *AIAA Paper* 2000-1930.

[54] Stanek M, Raman G, Kibens V and Ross J, 2000, "Cavity Tone Suppression Using High Frequency Excitation. *AIAA Paper* 2000-1905.

[55] Raman G, 1997, "Using Controlled Unsteady Fluid Mass Addition to Enhance Jet Mixing", *AIAA Journal*, Vol. 35, pp. 647-656.

[56] Raman G, Raghu S and Bencic T J, 1999, "Cavity Resonance Suppression Using Miniature Fluidic Oscillators", *AIAA Paper* 99-1900.

[57] Singh A K, Bansal M, Khan S A, Rathakrishnan E, "Base Pressure Control in Supersonic Regime Using Microjets", Proceedings of the International Symposium on "Recent Advances in Experimental Fluid Mechanics", December 2000, I.I.T Kanpur, pp. 121-131.

[58] Rathakrishnan E, "Instrumentation, Measurements and Experiments in Fluids". Book to be published.

[59] Sreejith R B and Rathakrishnan E, "Supersonic Jets from Nozzle with Cross-Wire", Proceedings of the International Symposium on "Recent Advances in Experimental Fluid Mechanics", December 2000, I.I.T Kanpur, pp. 219-228.

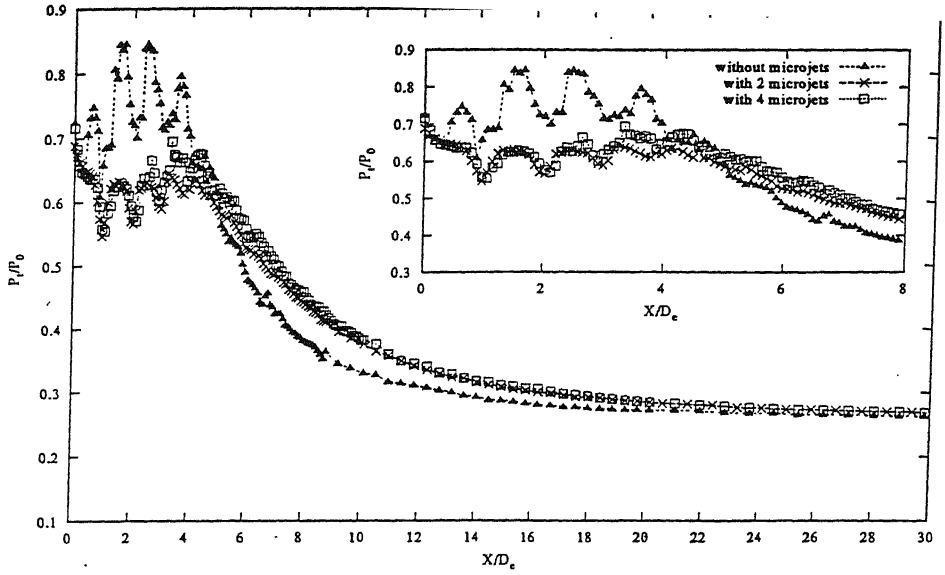

Fig. 4.1. Centreline Pressure Decay for NPR4 and $r/r_e = 1.93$.

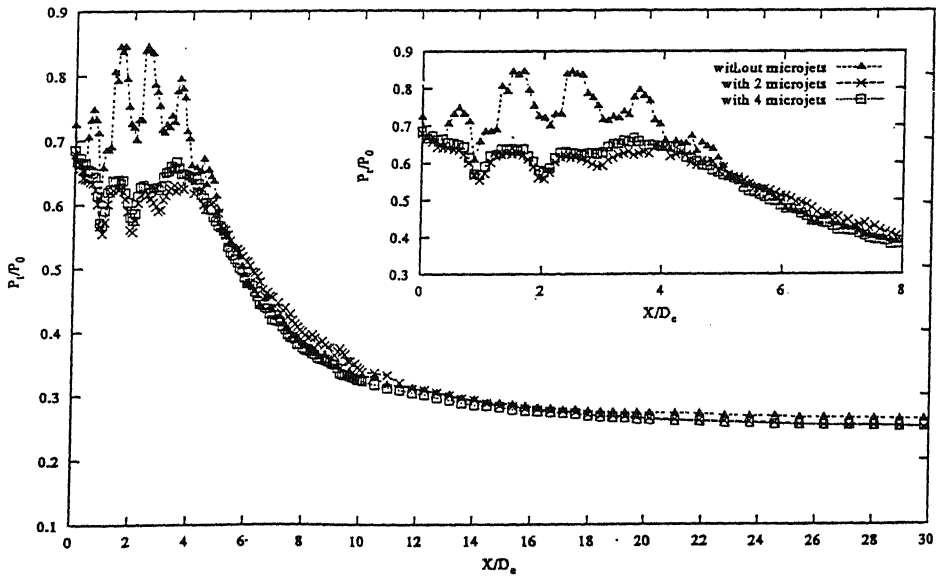

Fig. 4.2. Centreline Pressure Decay for NPR4 and $r/r_e = 2.10$

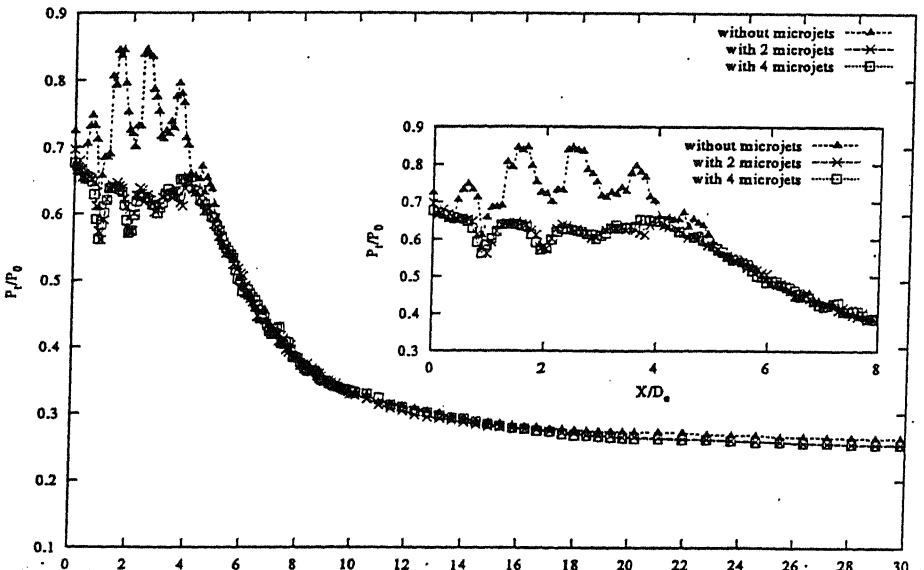

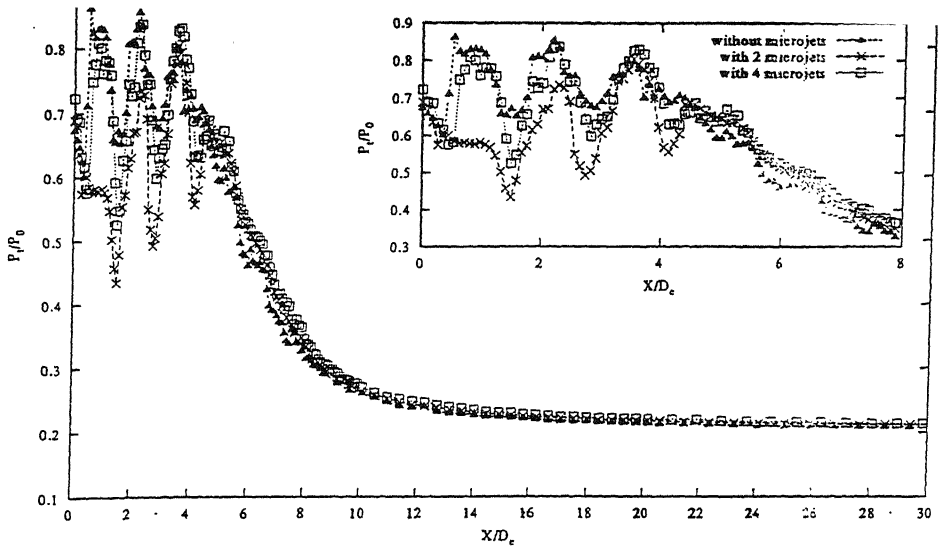

Fig. 4.4. Centreline Pressure Decay for NPR5 and $r/r_e = 1.93$.

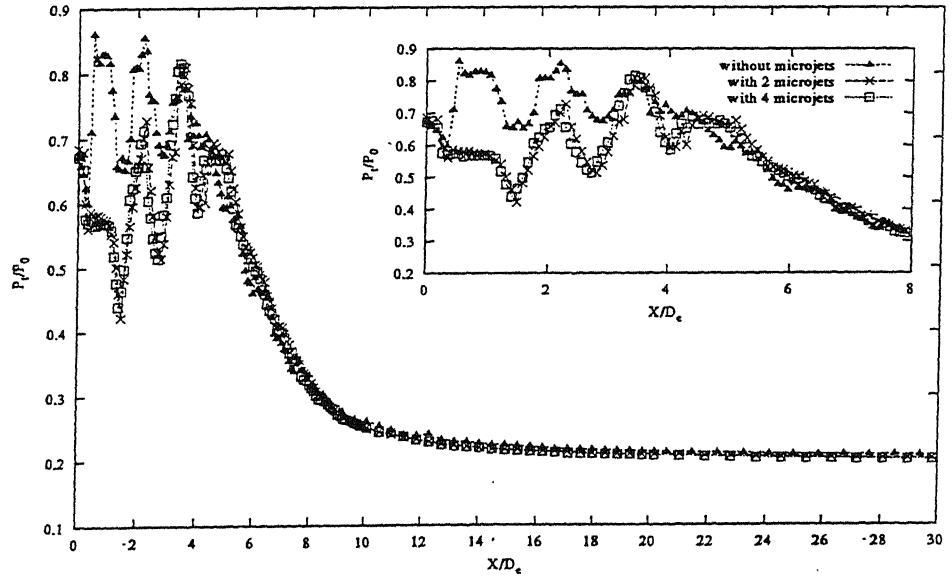

Fig. 4.5. Centreline Pressure Decay for NPR5 and $r/r_e = 2.10$.

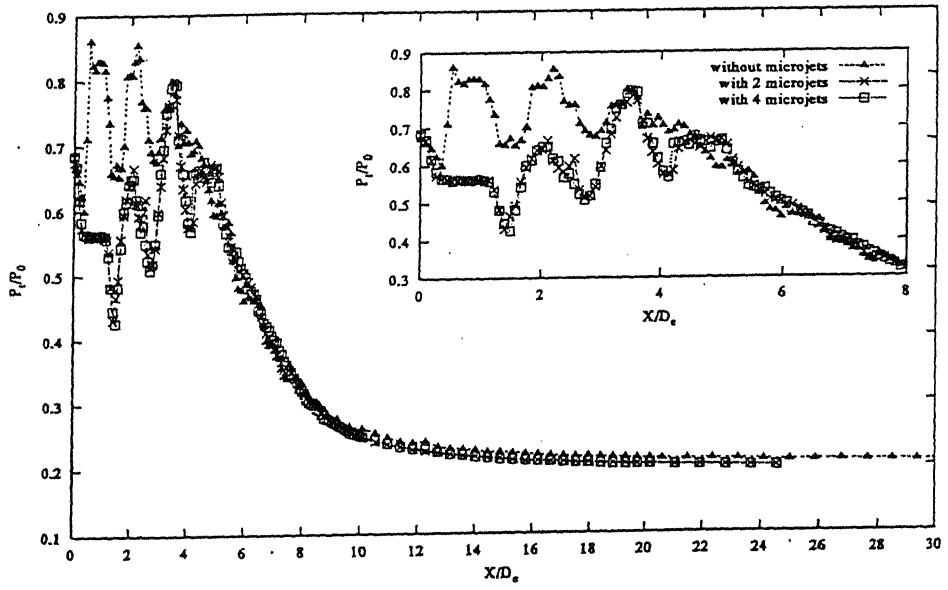

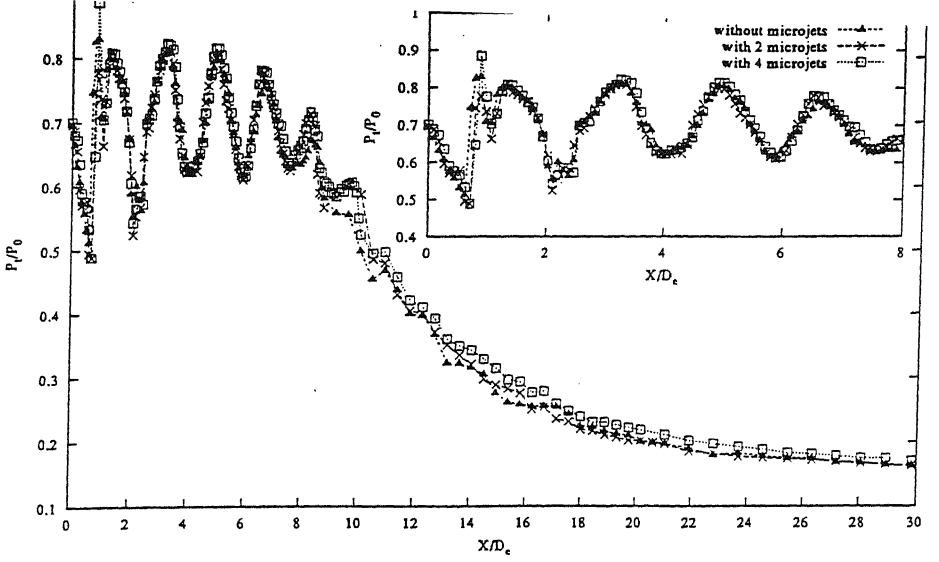

Fig. 4.7. Centreline Pressure Decay for NPR7 and $r/r_e = 1.93$.

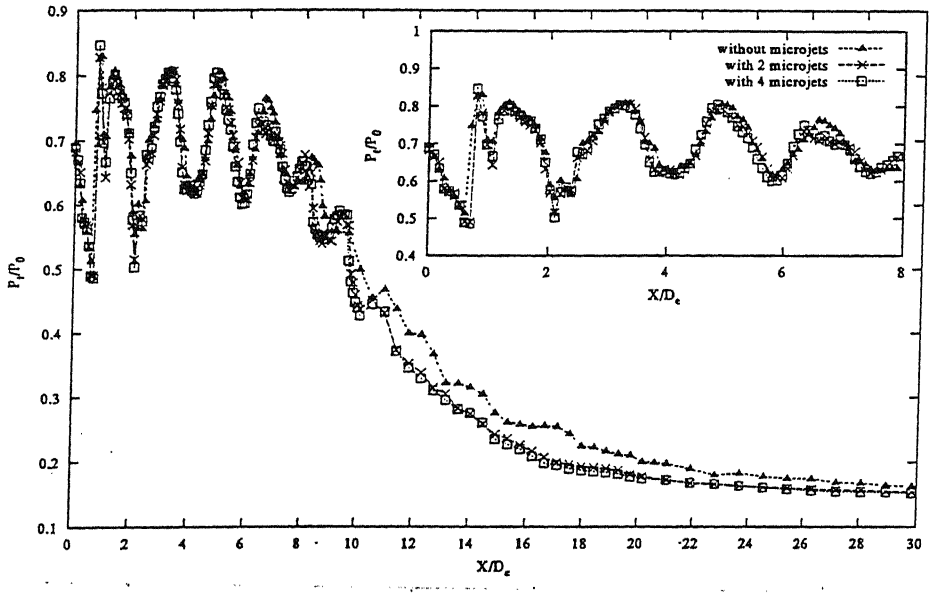

Fig. 4.8. Centreline Pressure Decay for NPR7 and $r/r_e = 2.10$.

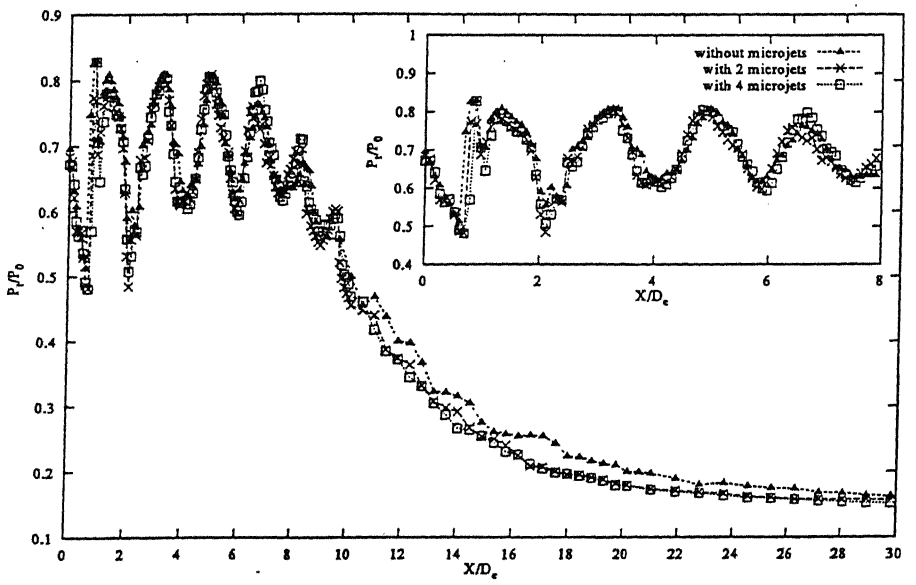

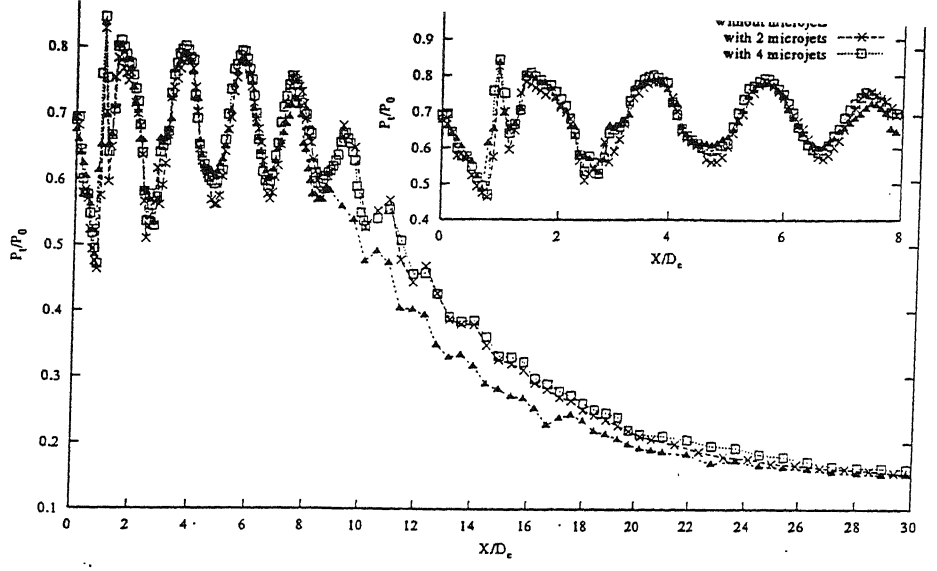

Fig. 4.10. Centreline Pressure Decay for NPR8 and $r/r_e = 1.93$.

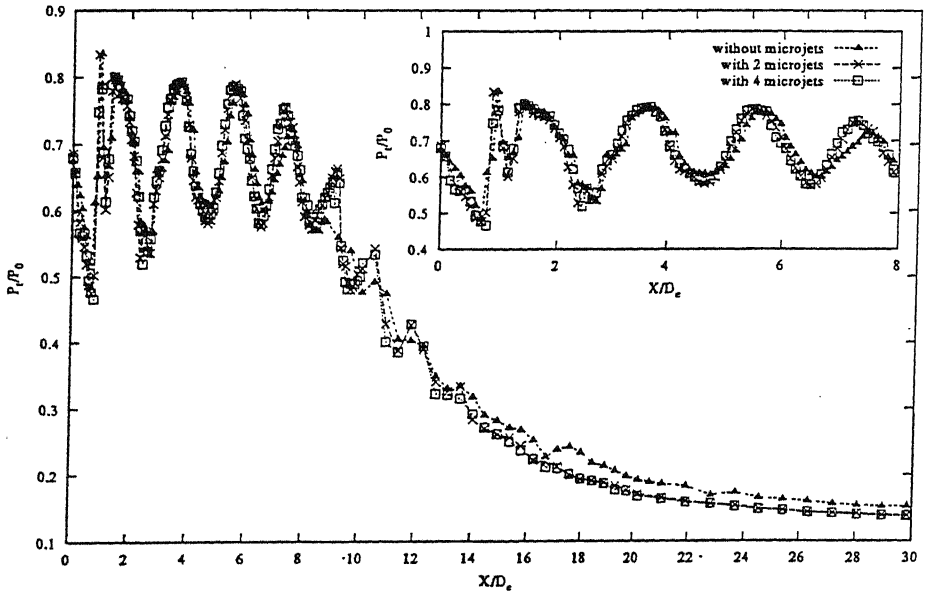

Fig. 4.11. Centreline Pressure Decay for NPR8 and $r/r_e = 2.10$.

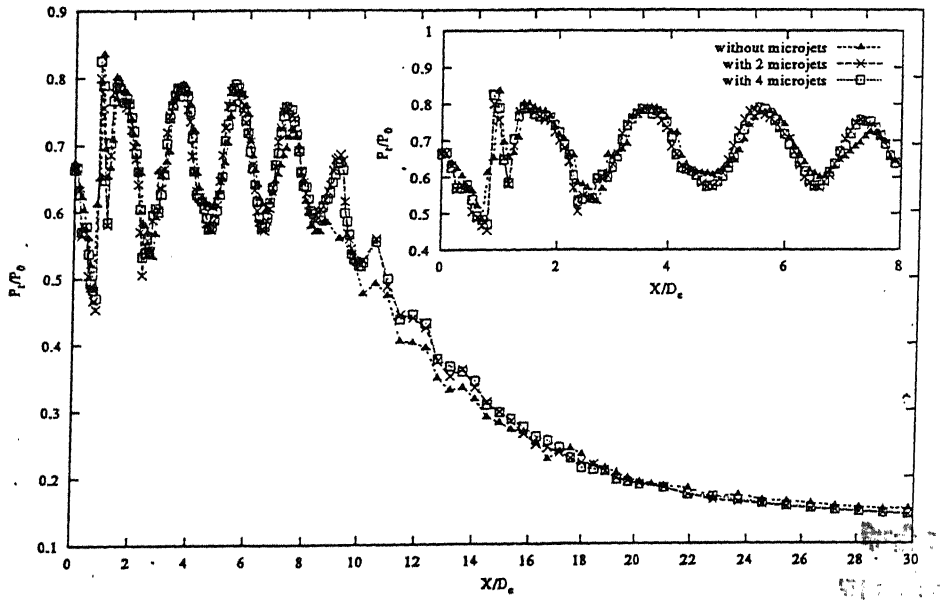

Fig. 4.12. Centreline Pressure Decay for NPR8 and

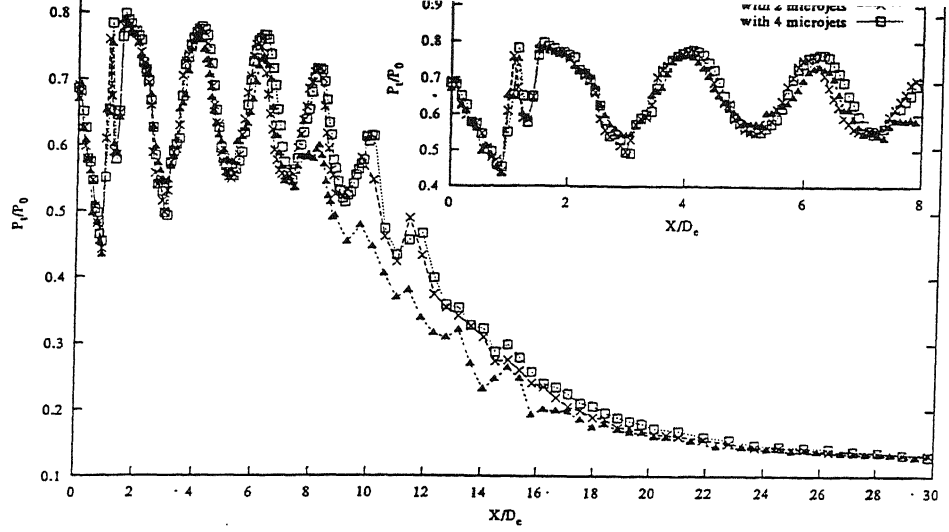

Fig. 4.13. Centreline Pressure Decay for NPR9 and $r/r_e = 1.93$.

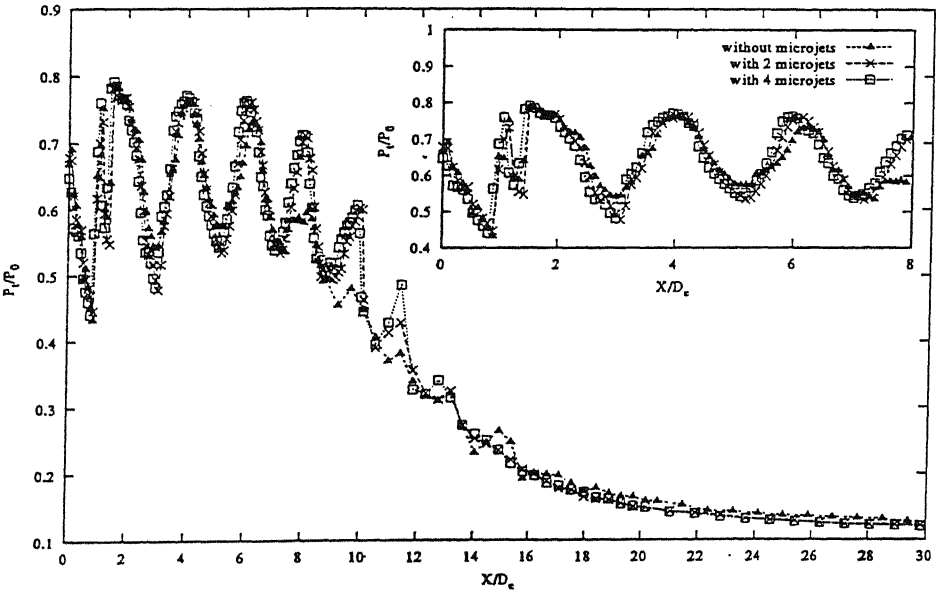

Fig. 4.14. Centreline Pressure Decay for NPR9 and $r/r_e = 2.10$.

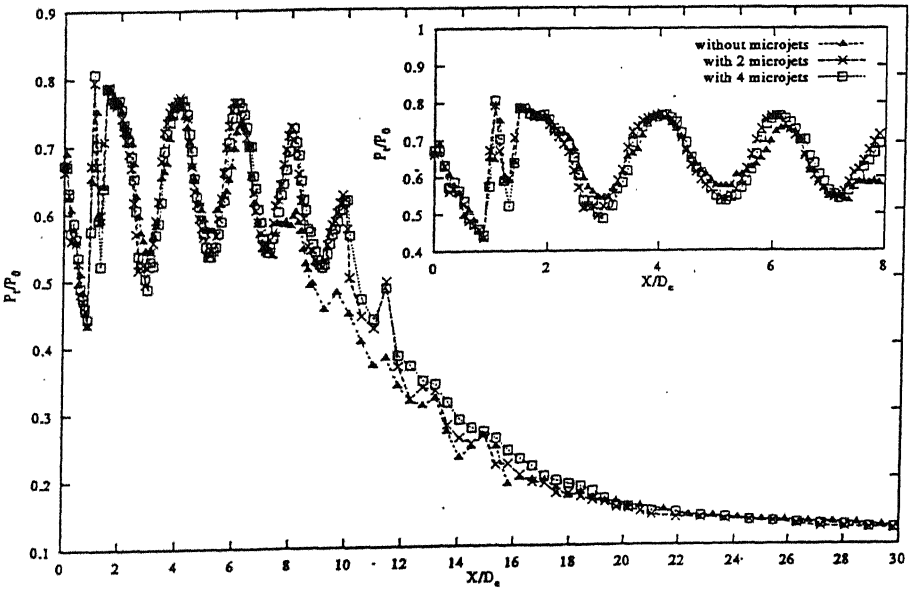

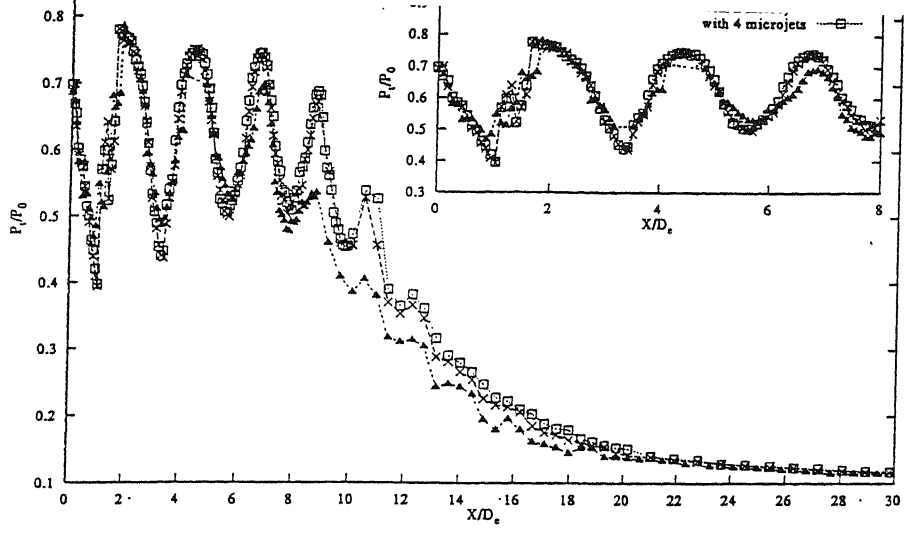

Fig. 4.16. Centreline Pressure Decay for NPR10 and $r/r_e = 1.93$.

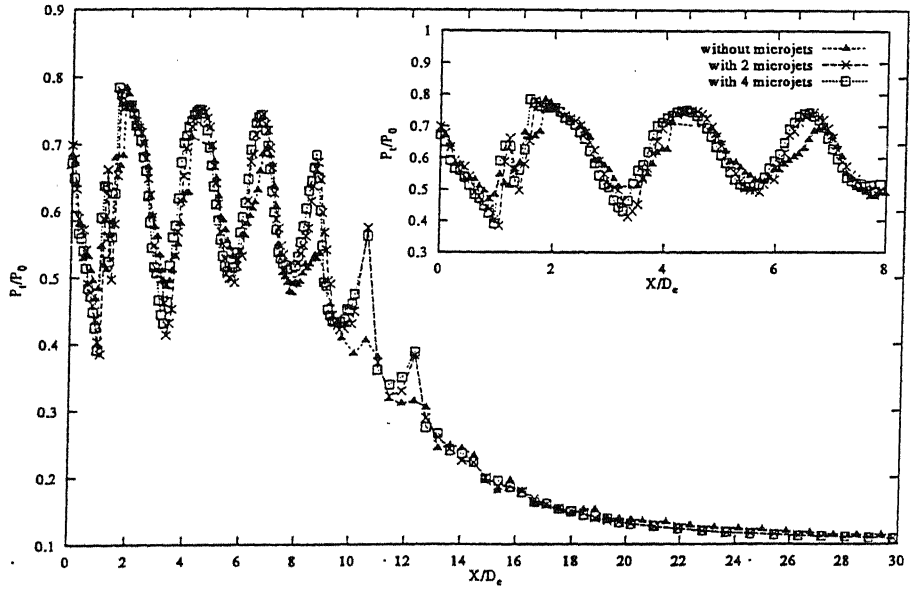

Fig. 4.17. Centreline Pressure Decay for NPR10 and $r/r_e = 2.10$.

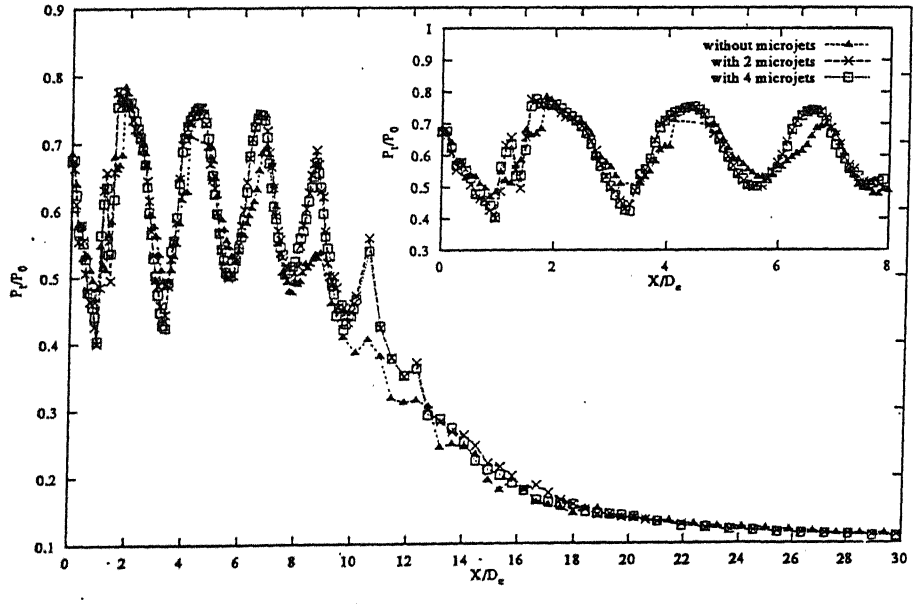

Fig. 4.18. Centreline Pressure Decay for NPR10 and $r/r_e = 2.18$.

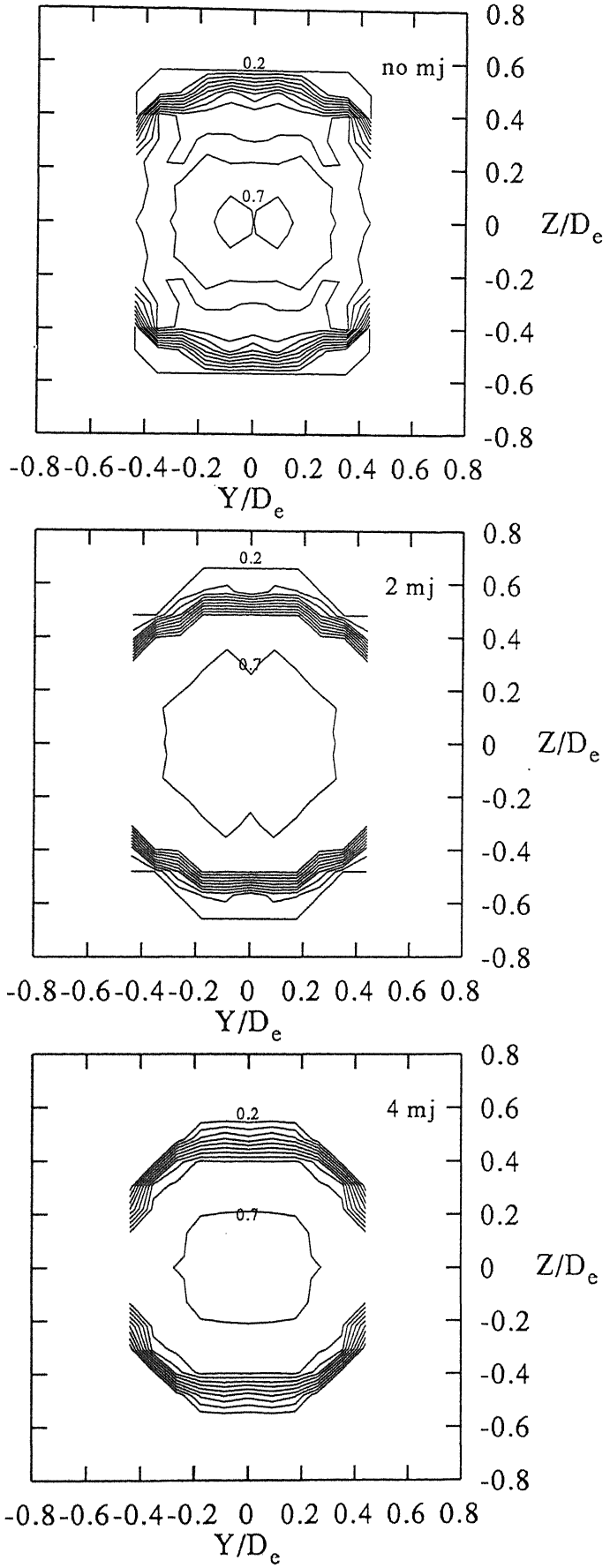

Fig 4.19. Contour Plots for NPR5, $X/D_e = 0$ and $r/r_e = 1.93$

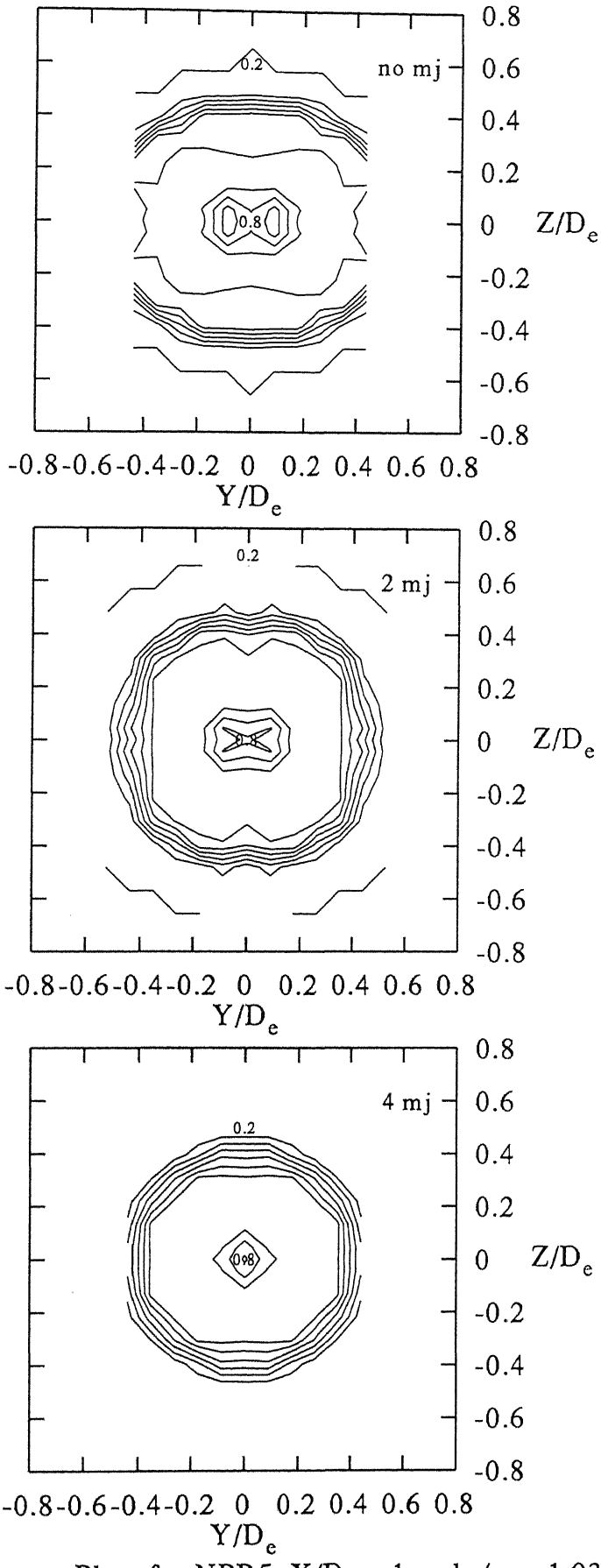

Fig 4.20. Contour Plots for NPR5, X/D_e = 1 and r/r_e = 1.93

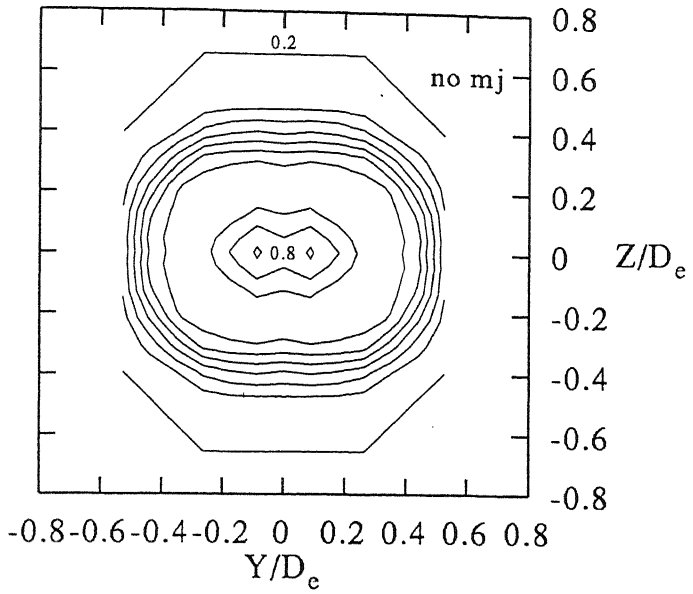

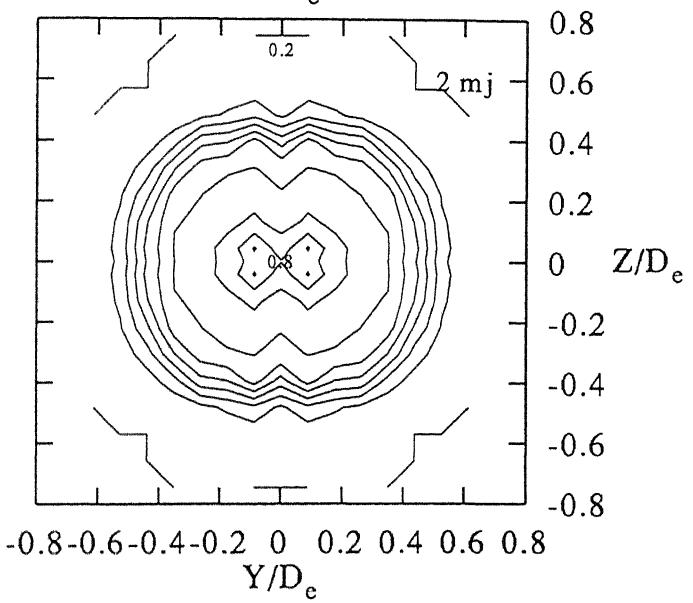

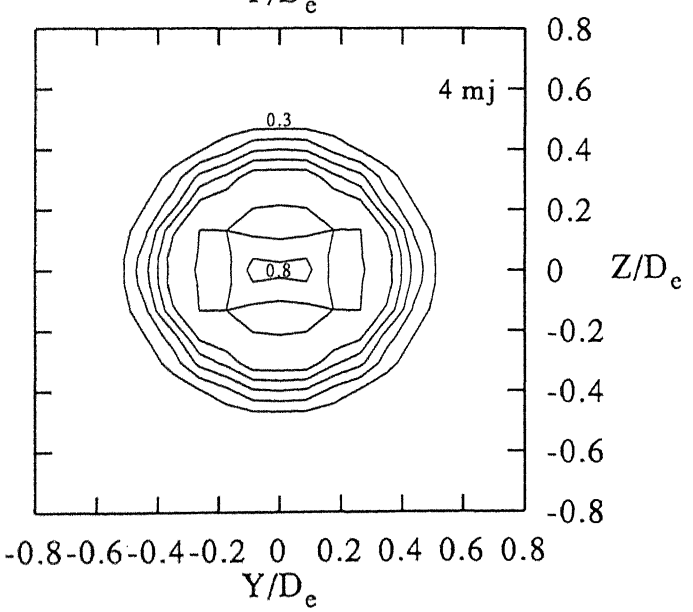

Fig 4.21. Contour Plots for NPR5, $X/D_e = 2$ and $r/r_e = 1.93$

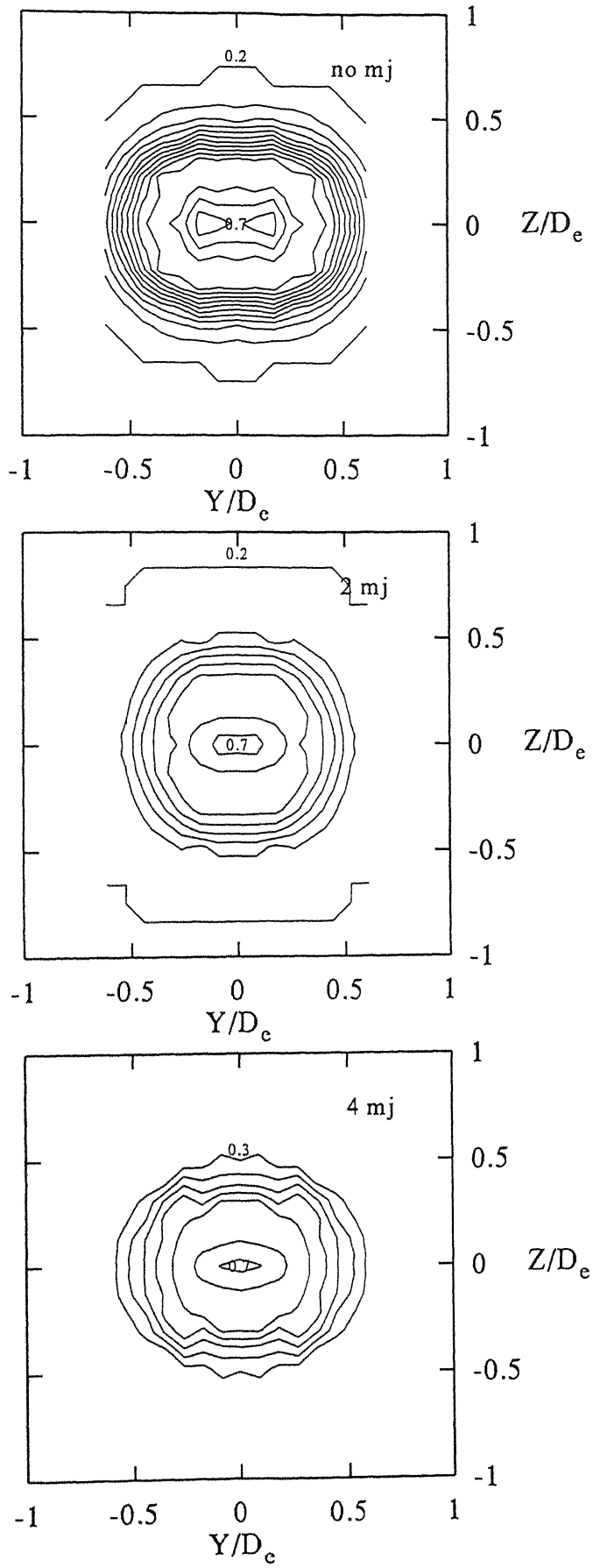

Fig 4.22. Contour Plots for NPR5, $X/D_e = 3$ and $r/r_e = 1.93$

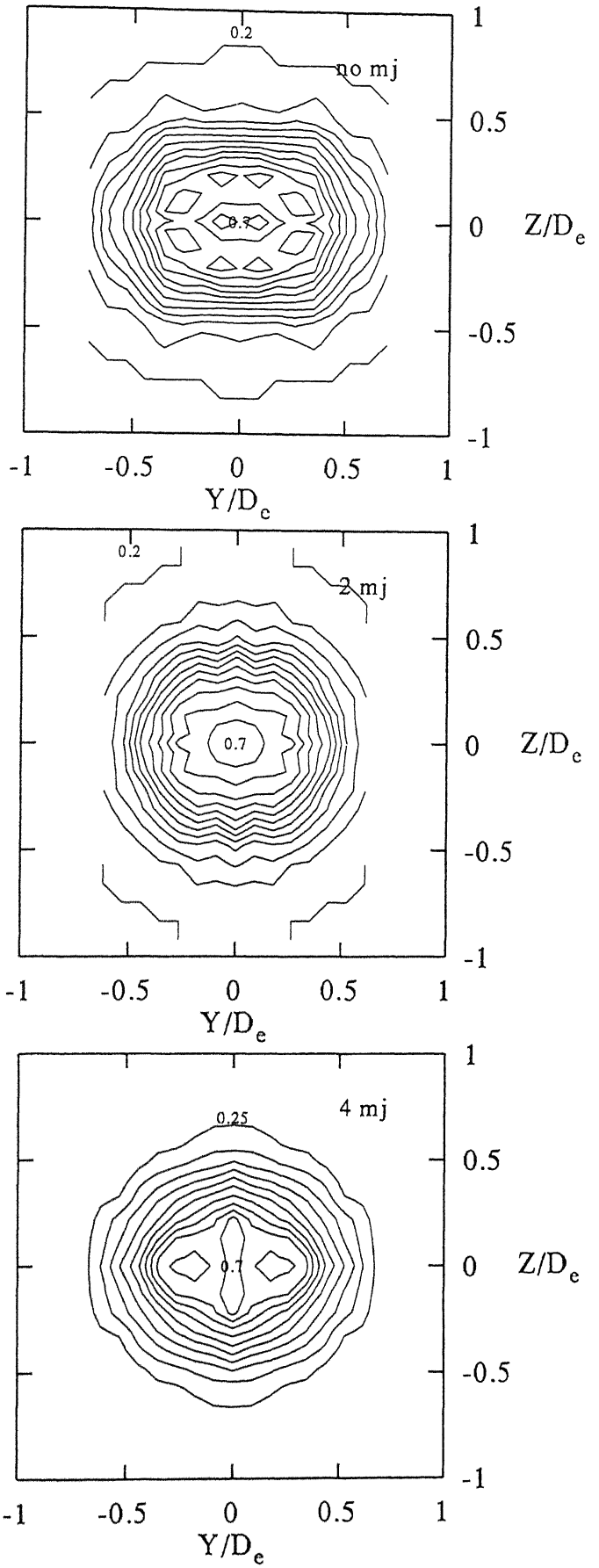

Fig 4.23. Contour Plots for NPR5, $X/D_e = 4$ and $r/r_e = 1.93$

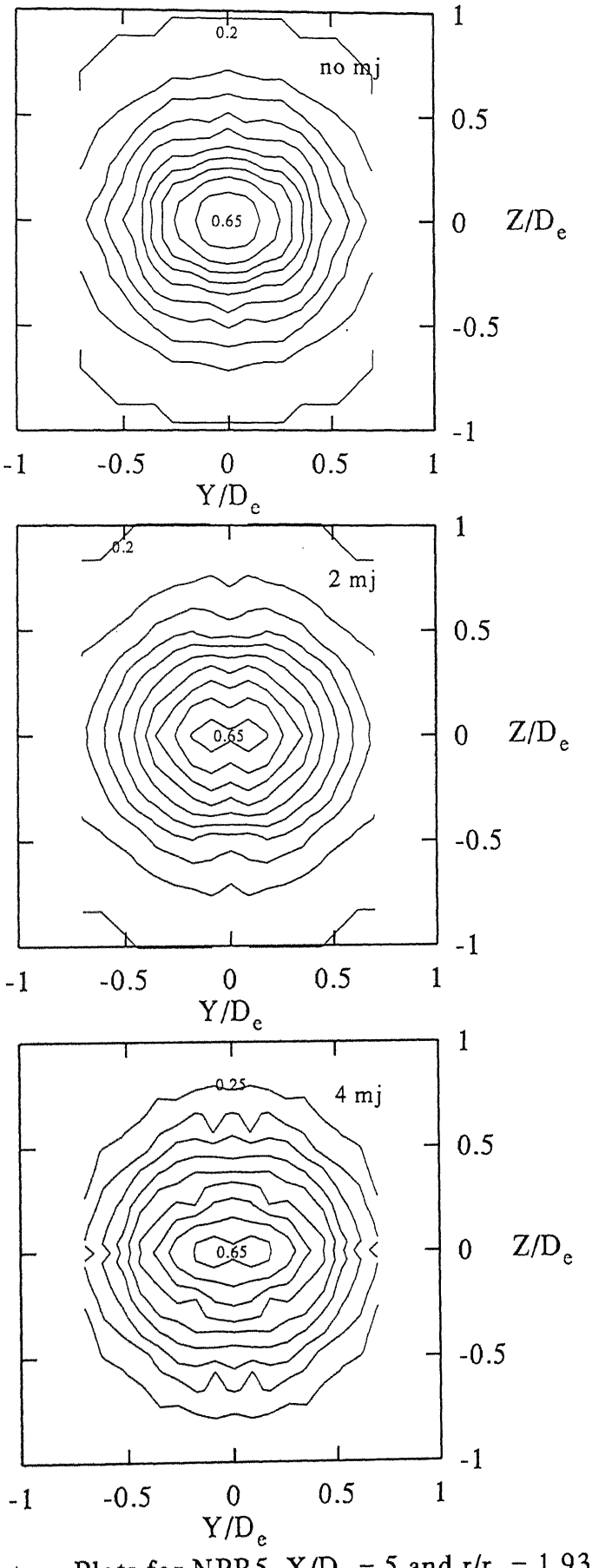

Fig 4.24. Contour Plots for NPR5, $X/D_e = 5$ and $r/r_e = 1.93$

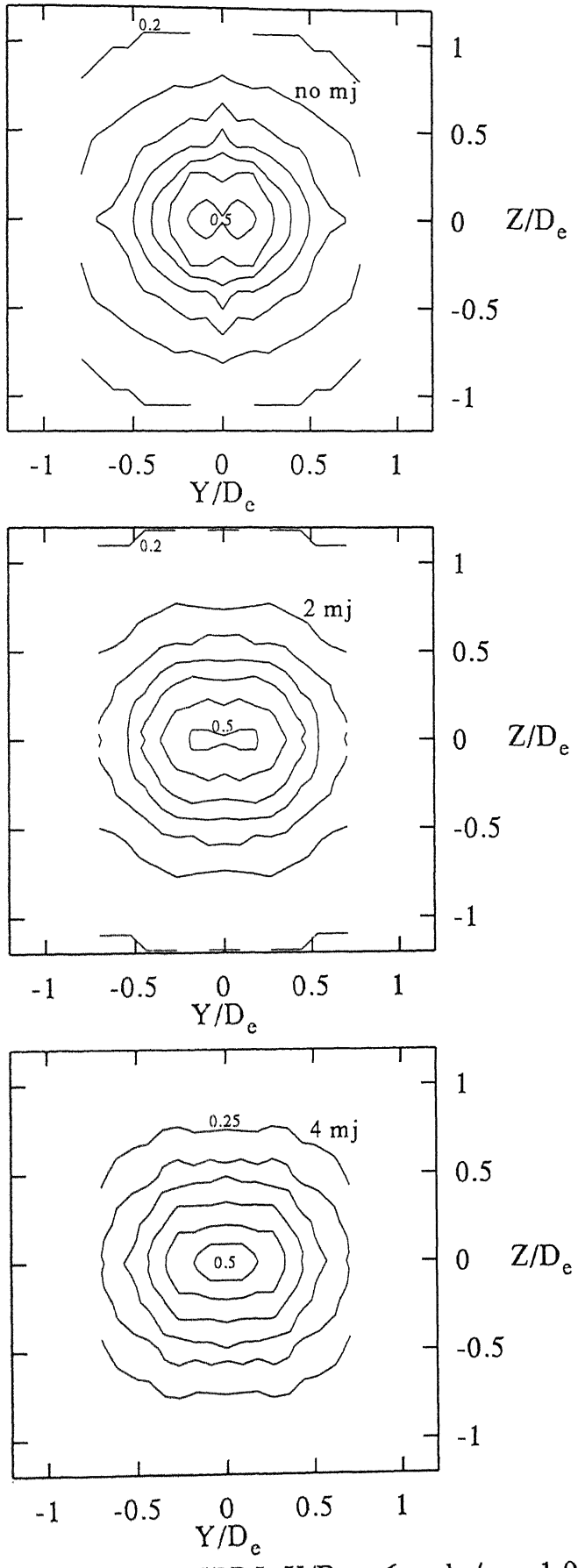

Fig 4.25. Contour Plots for NPR5, $X/D_e = 6$ and $r/r_e = 1.93$

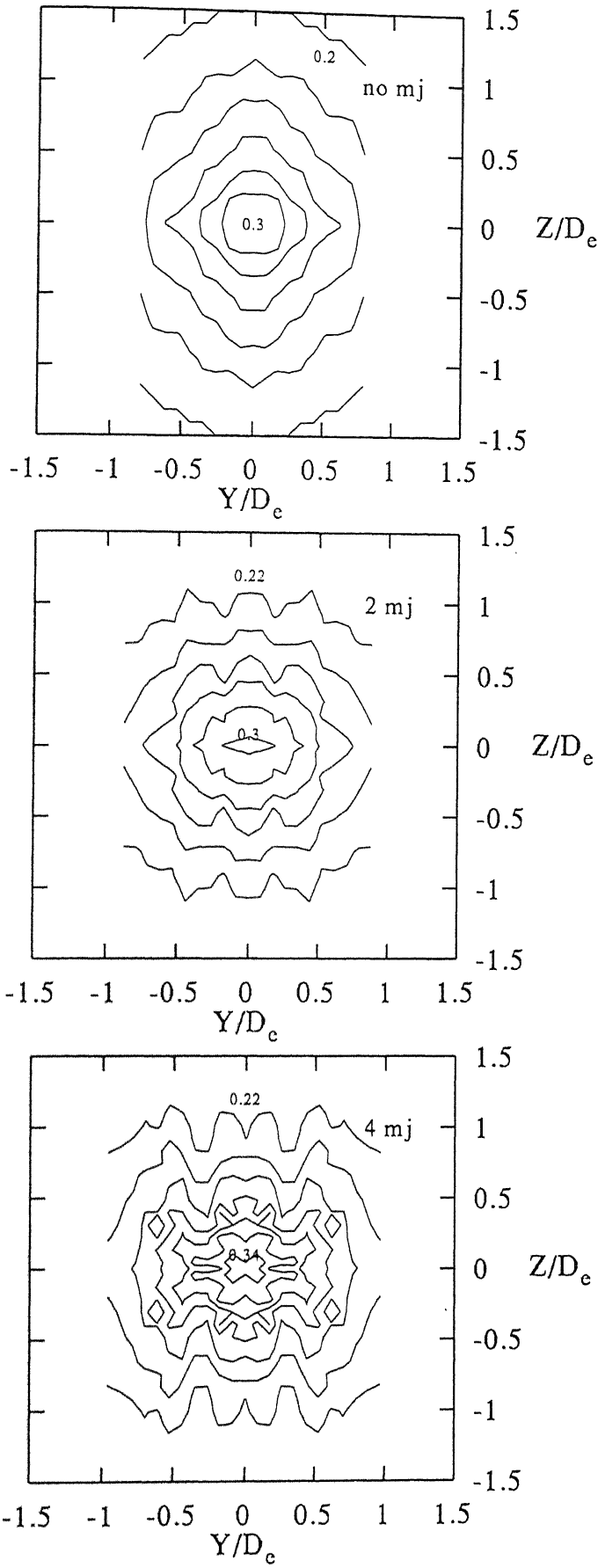

Fig 4.26. Contour Plots for NPR5, $X/D_e = 8$ and $r/r_e = 1.93$

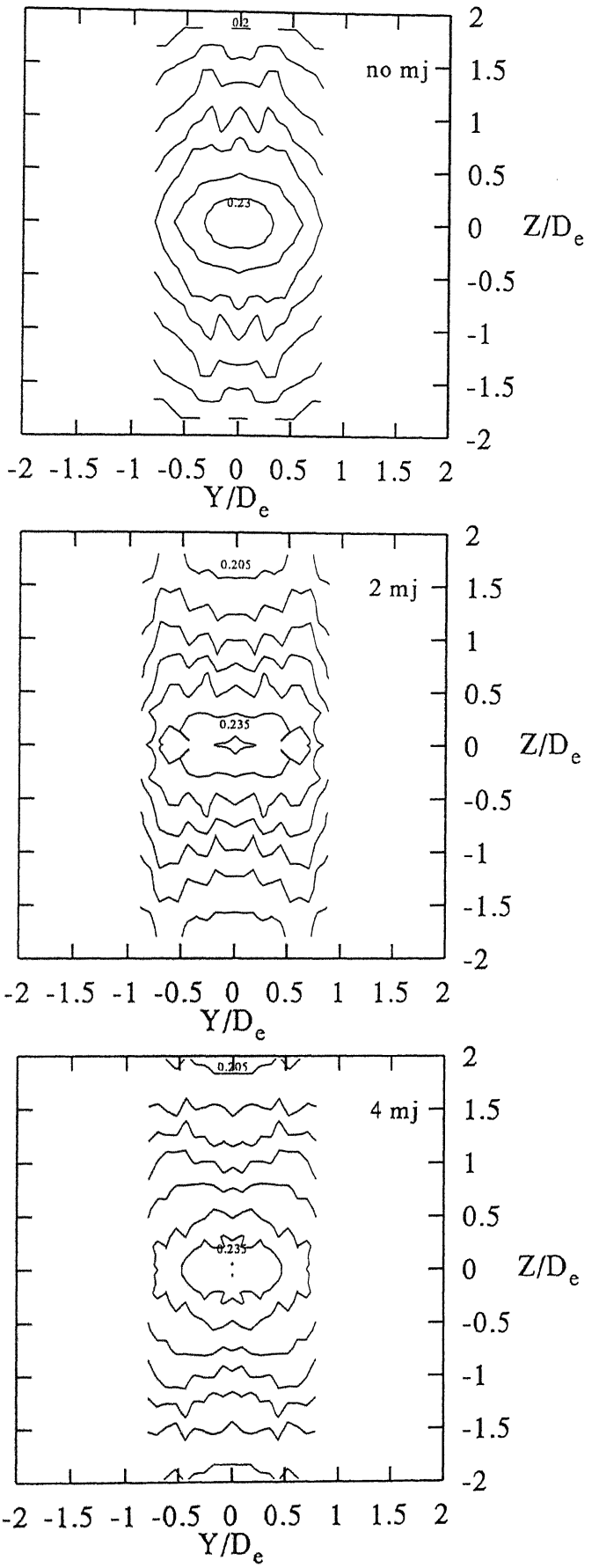

Fig 4.28. Contour Plots for NPR5, $X/D_e = 12$ and $r/r_e = 1.93$

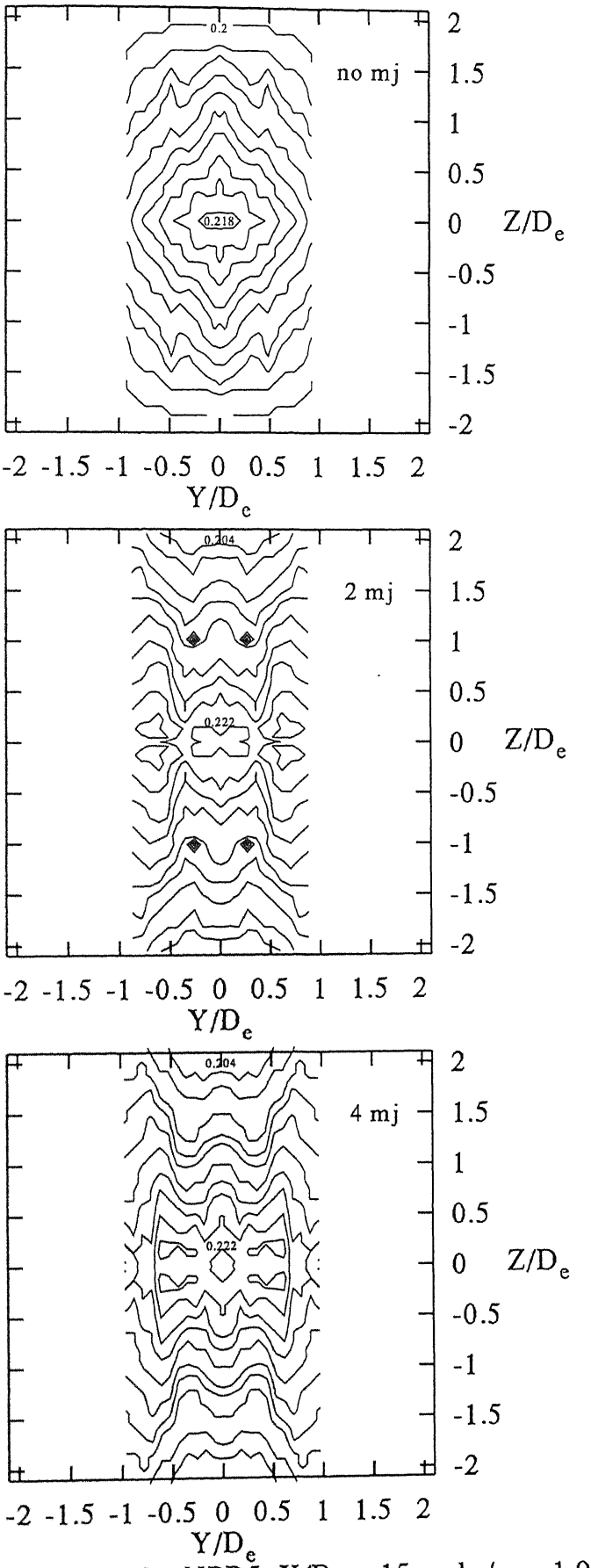

Fig 4.29. Contour Plots for NPR5, $X/D_e = 15$ and $r/r_e = 1.93$

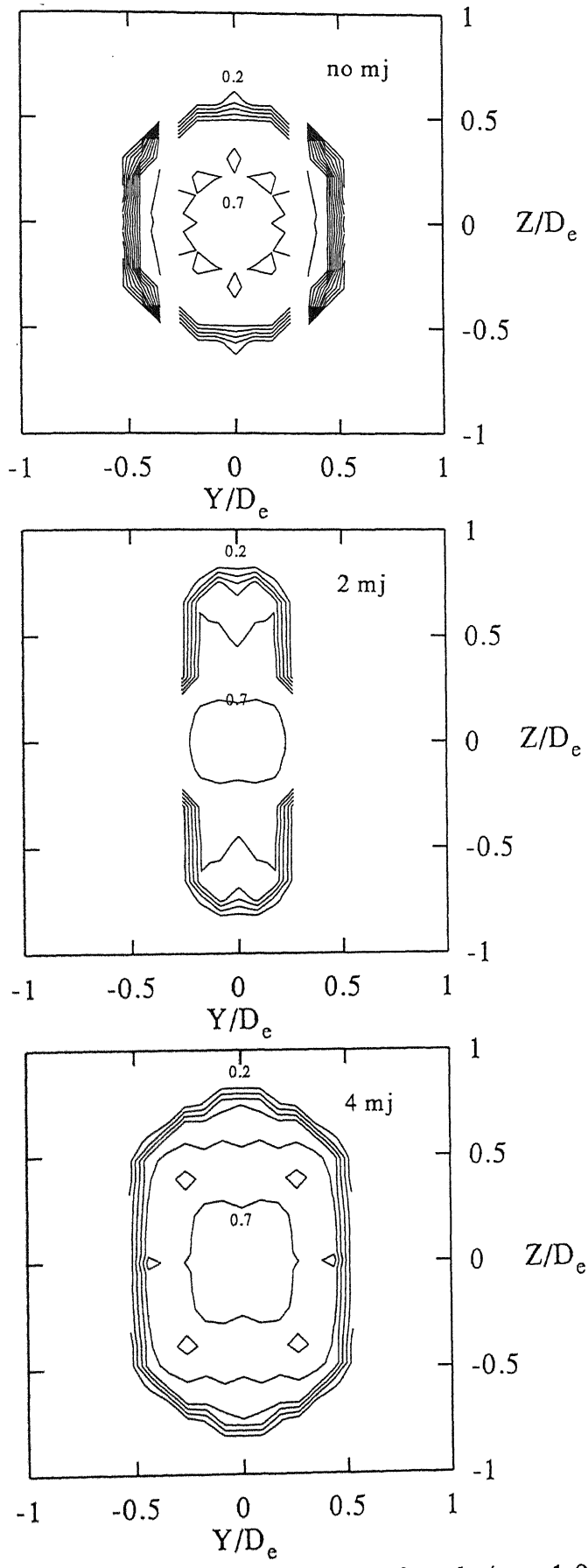

Fig 4.30. Contour Plots for NPR7, $X/D_e = 0$ and $r/r_e = 1.93$

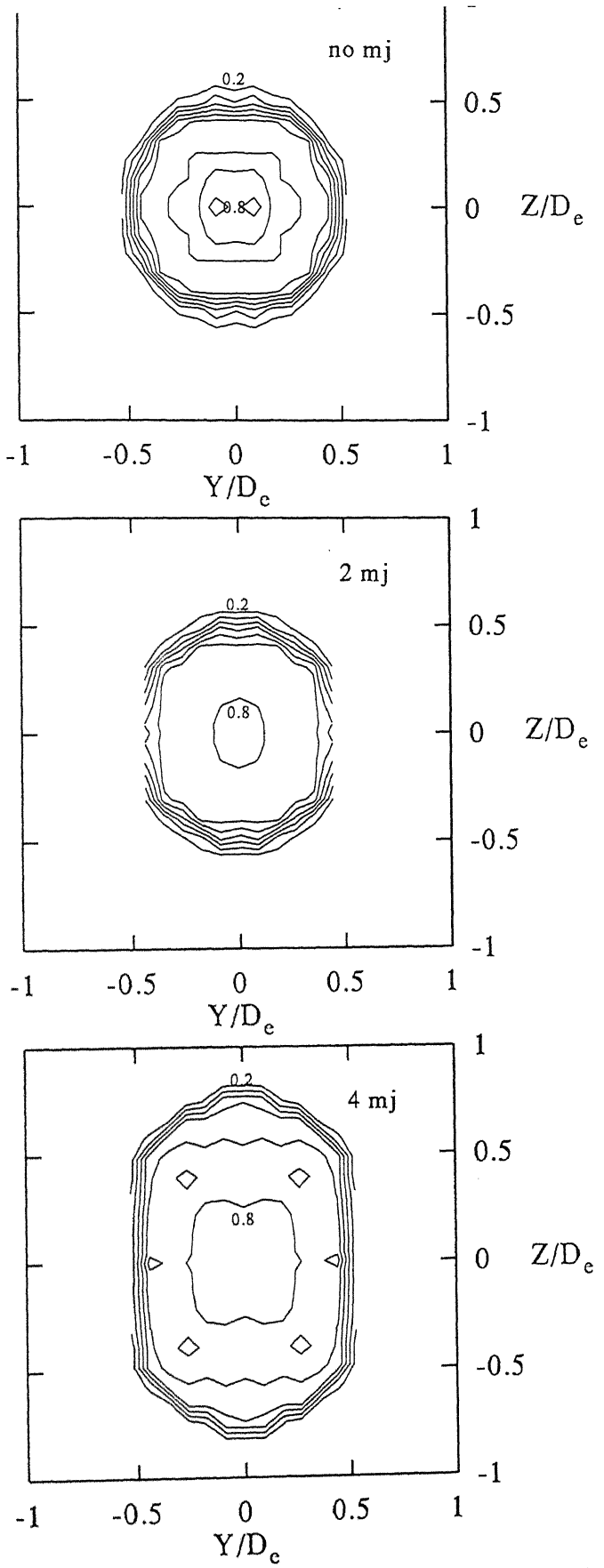

Fig 4.31. Contour Plots for NPR7, $X/D_e = 1$ and $r/r_e = 1.93$

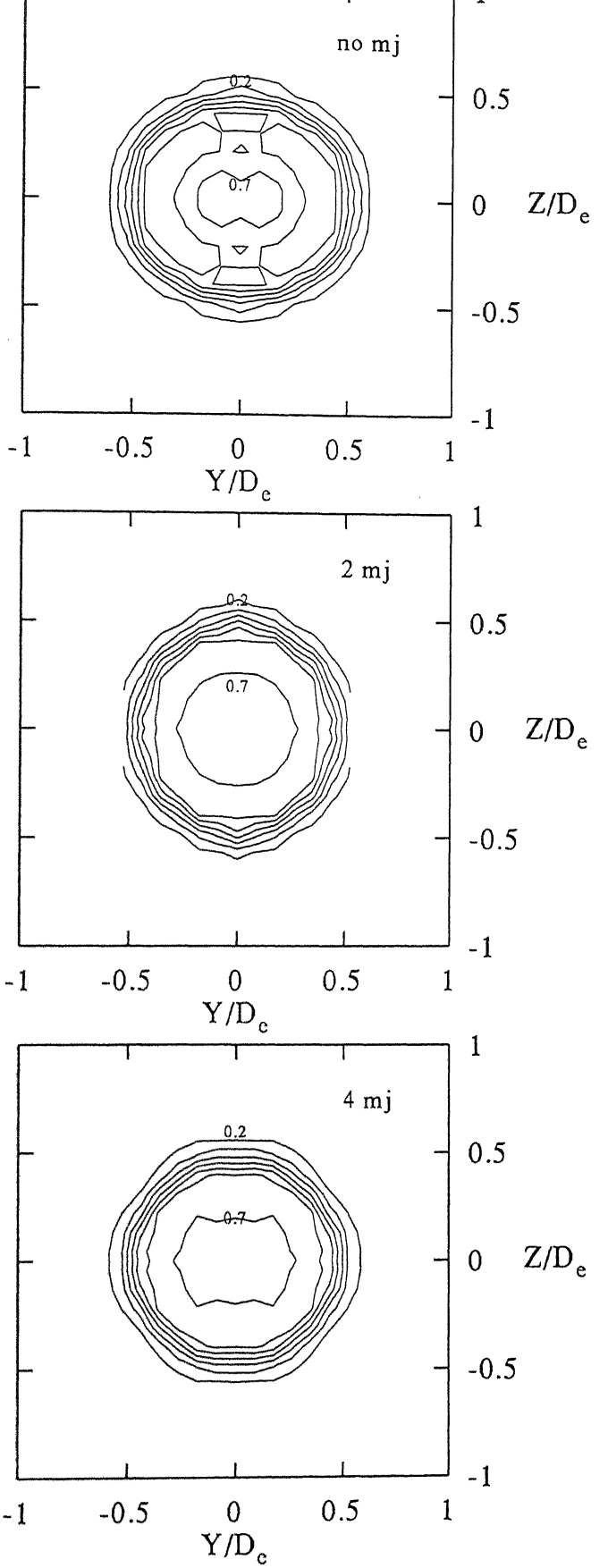

Fig 4.32. Contour Plots for NPR7, $X/D_e = 2$ and $r/r_e = 1.93$

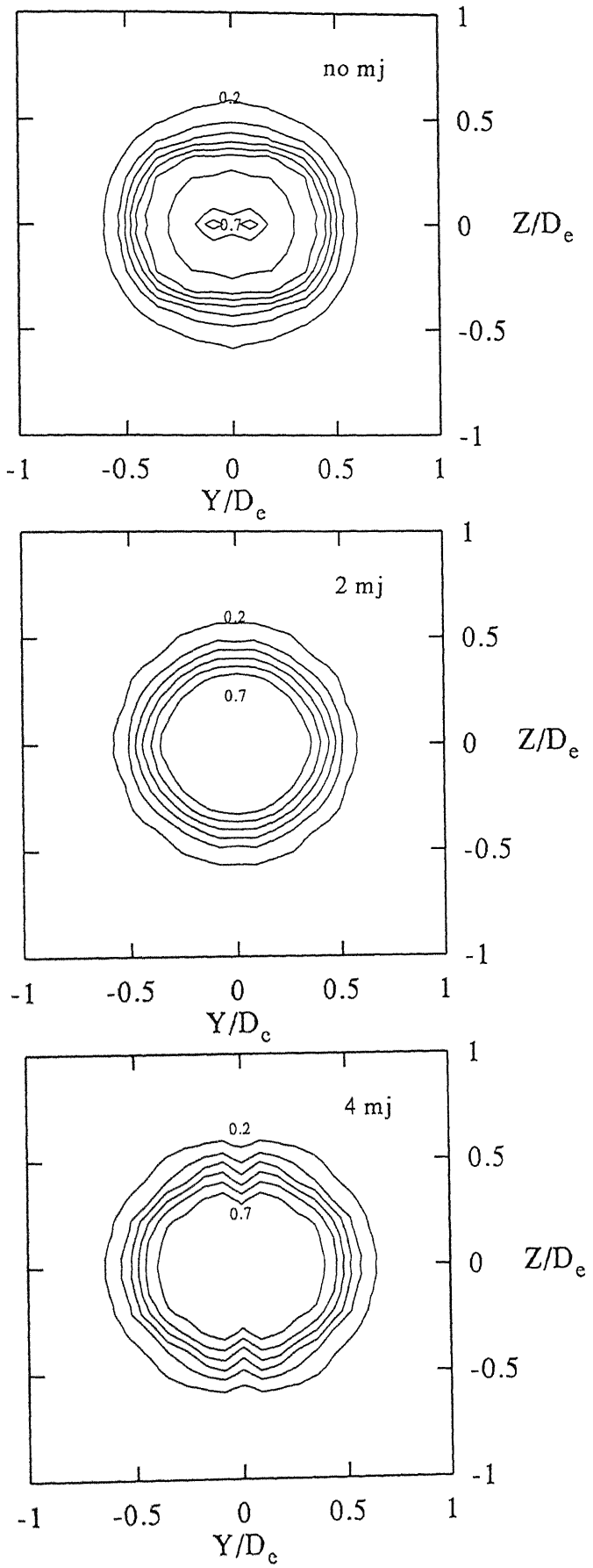

Fig 4.33. Contour Plots for NPR7, $X/D_e = 3$ and $r/r_e = 1.93$

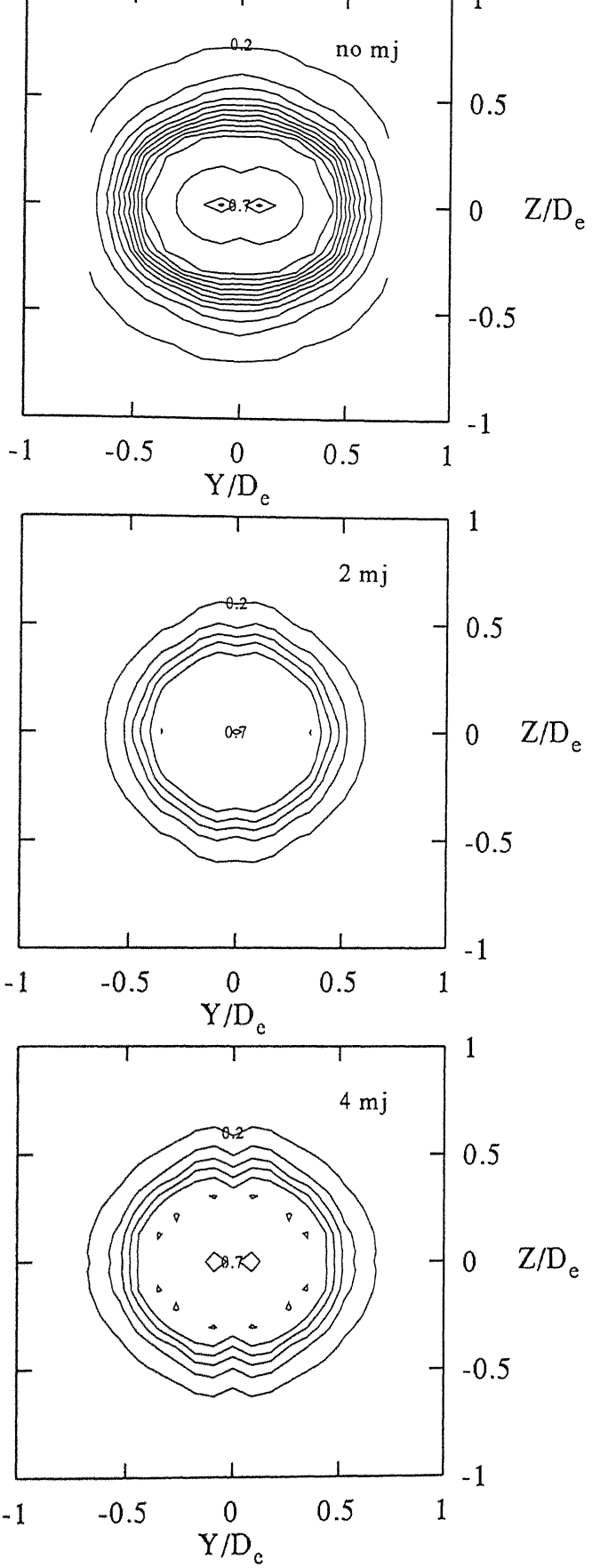

Fig 4.34. Contour Plots for NPR7, $X/D_e = 4$ and $r/r_e = 1.93$

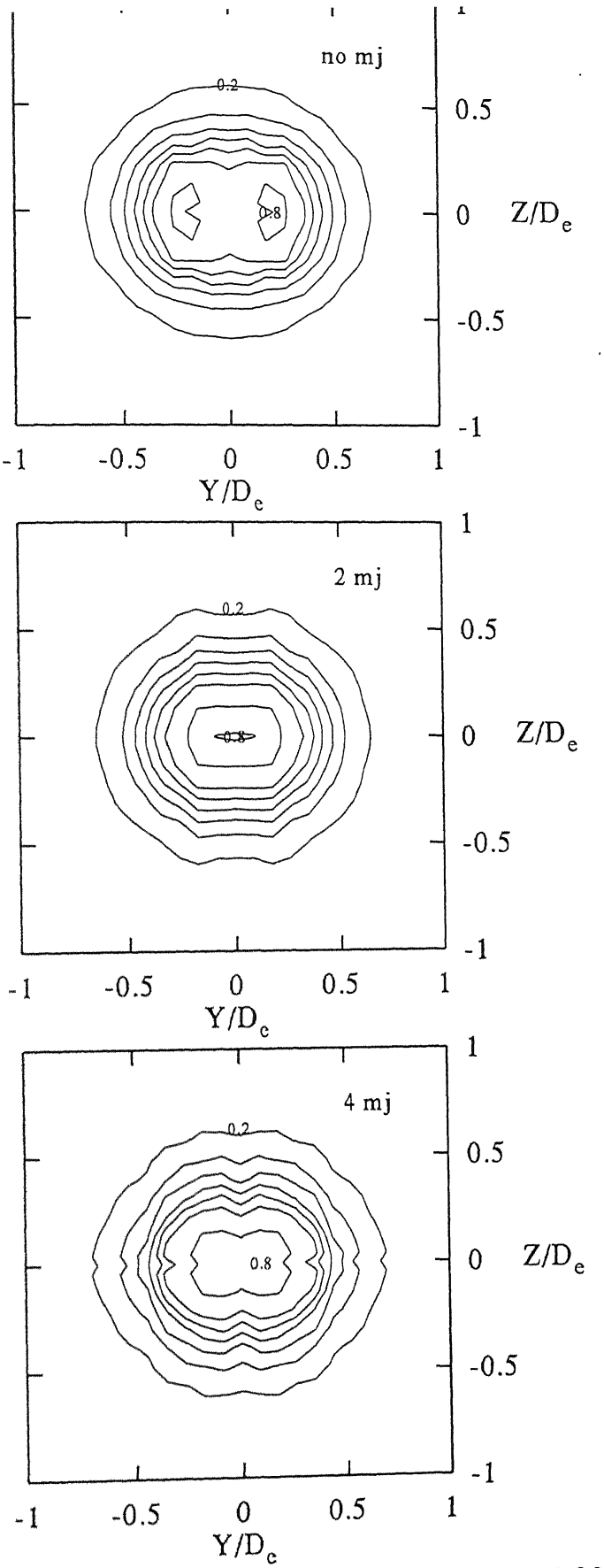

Fig 4.35. Contour Plots for NPR7, $X/D_e = 5$ and $r/r_e = 1.93$

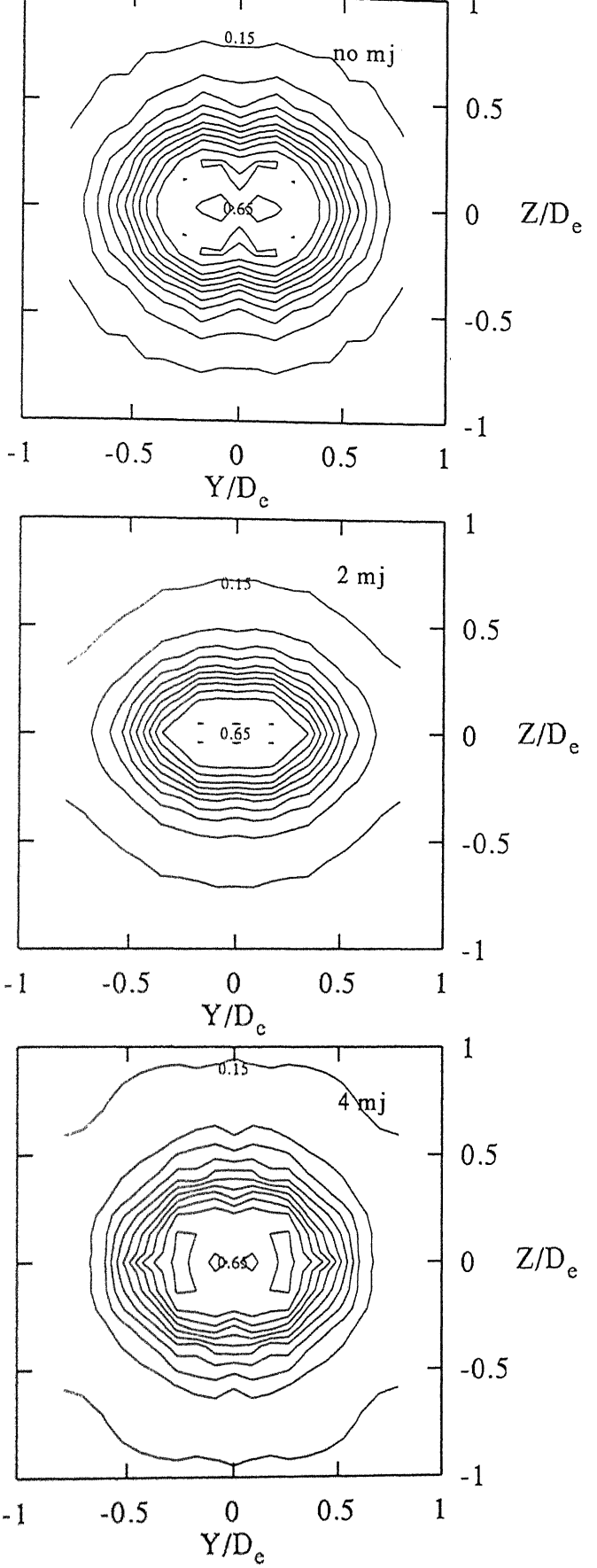

Fig 4.36. Contour Plots for NPR7, $X/D_e = 6$ and $r/r_e = 1.93$

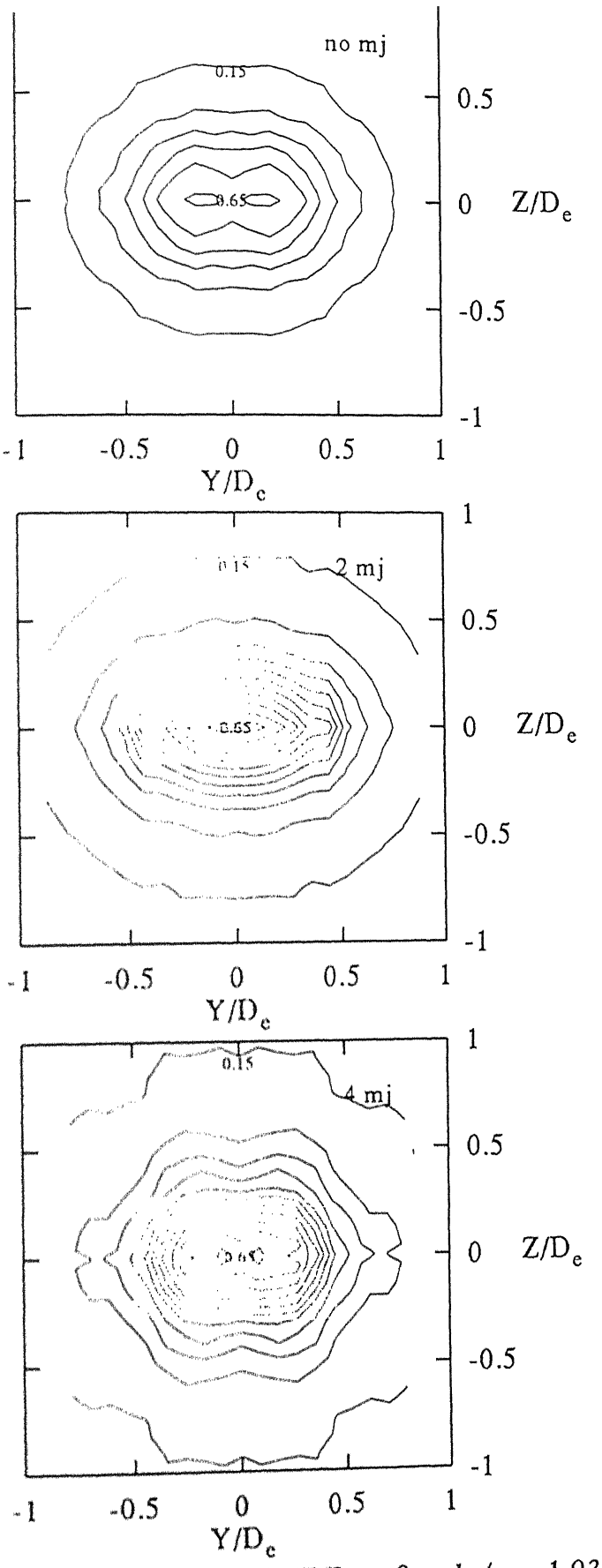

Fig 4.37. Contour Plots for NPR7, $X/D_e = 8$ and $r/r_e = 1.93$

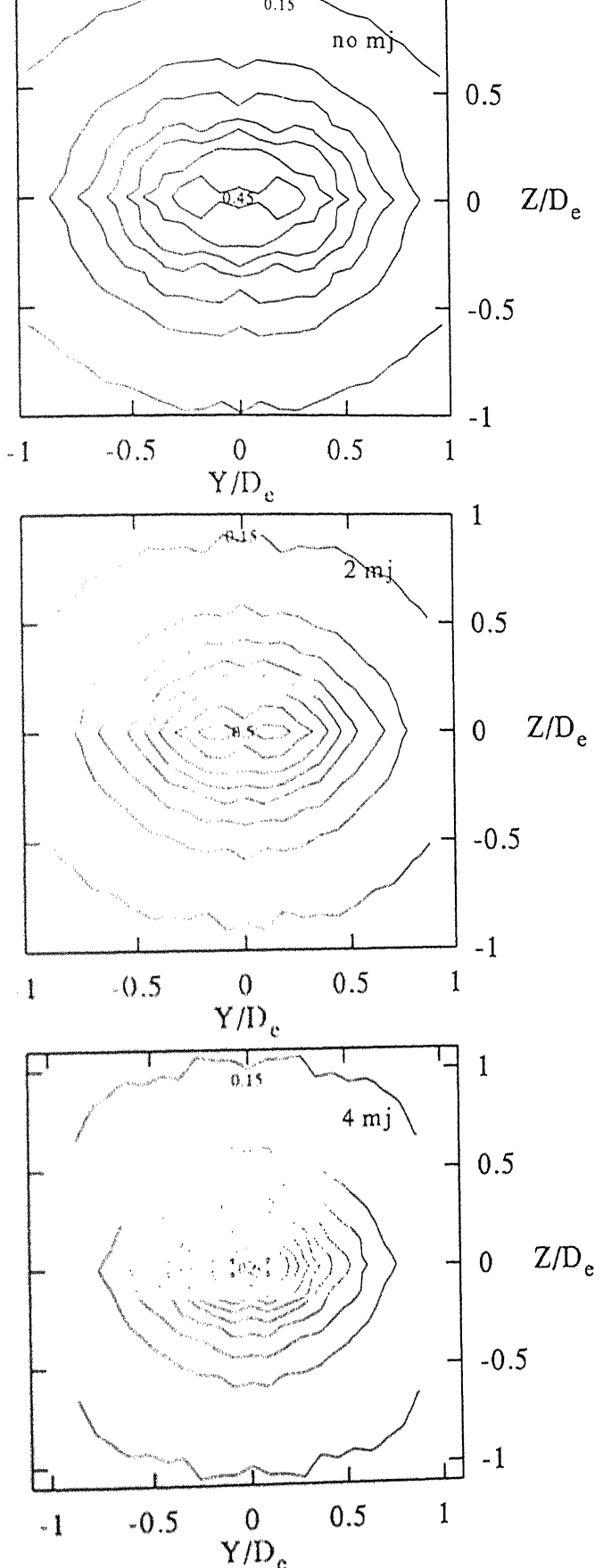

Fig 4.38. Contour Plots for NPR7, $X/D_e = 10$ and $r/r_e = 1.93$

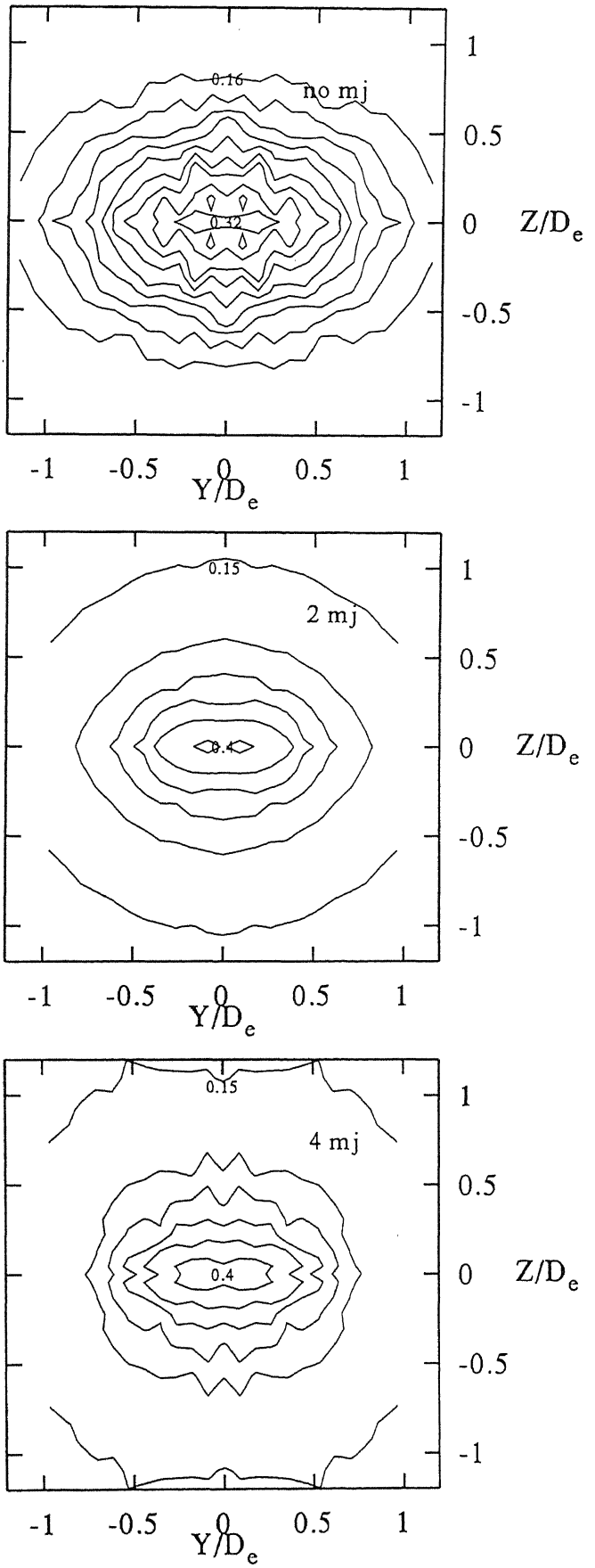

Fig 4.39. Contour Plots for NPR7, $X/D_e = 12$ and $r/r_e = 1.93$

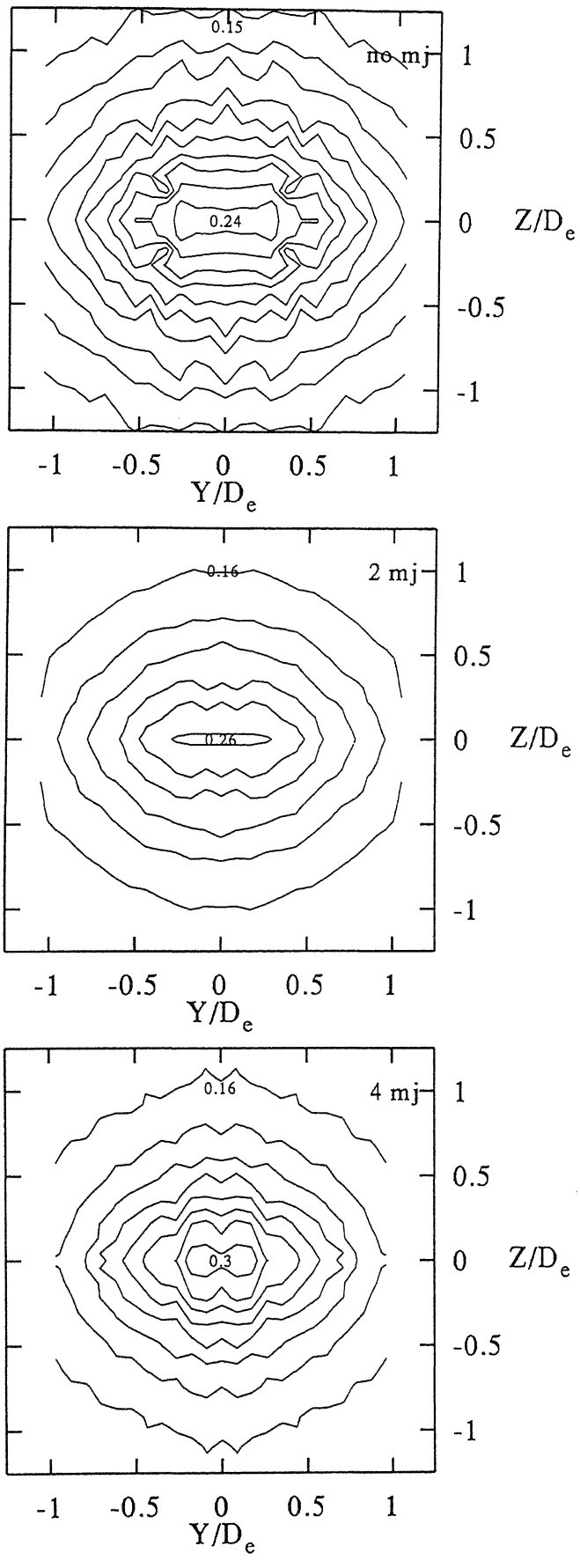

Fig 4.40. Contour Plots for NPR7, $X/D_e = 15$ and $r/r_e = 1.93$

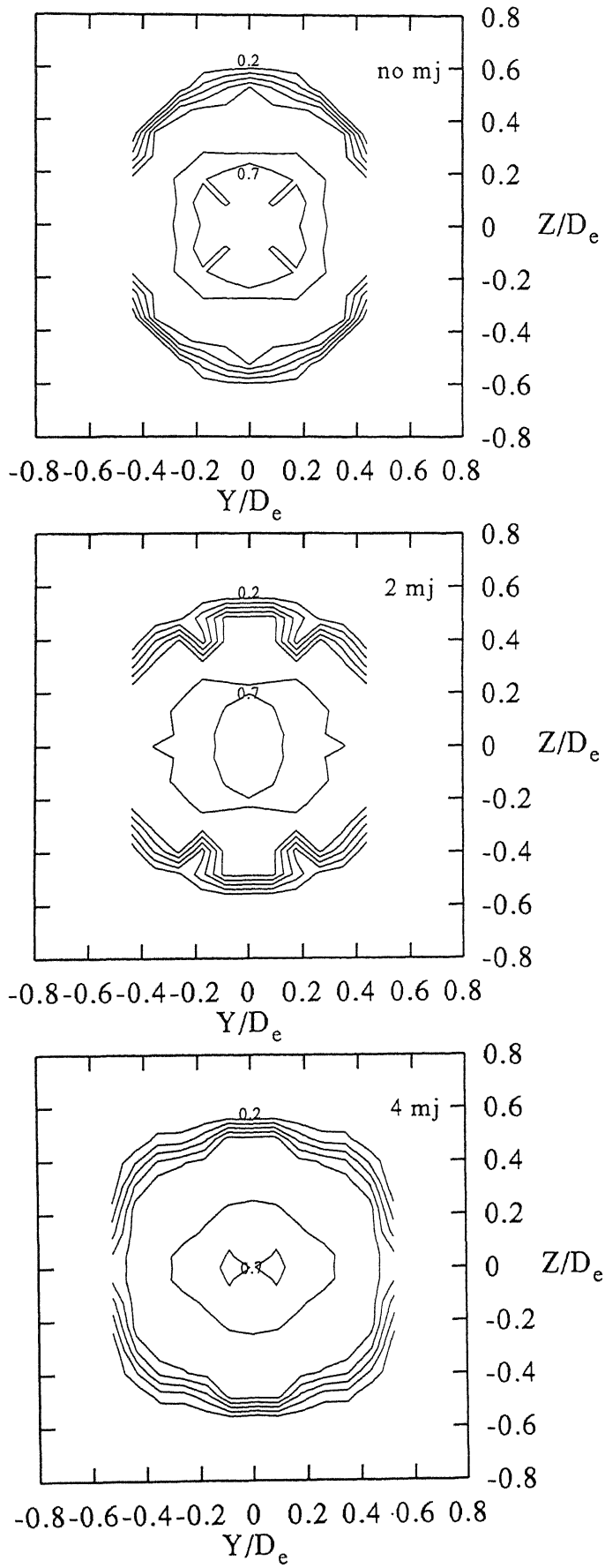

Fig 4.41. Contour Plots for NPR9, $X/D_e = 0$ and $r/r_e = 1.93$

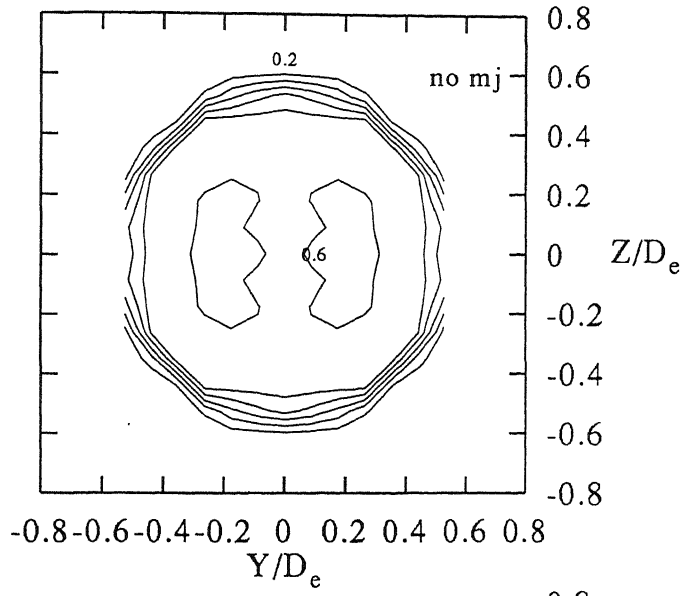

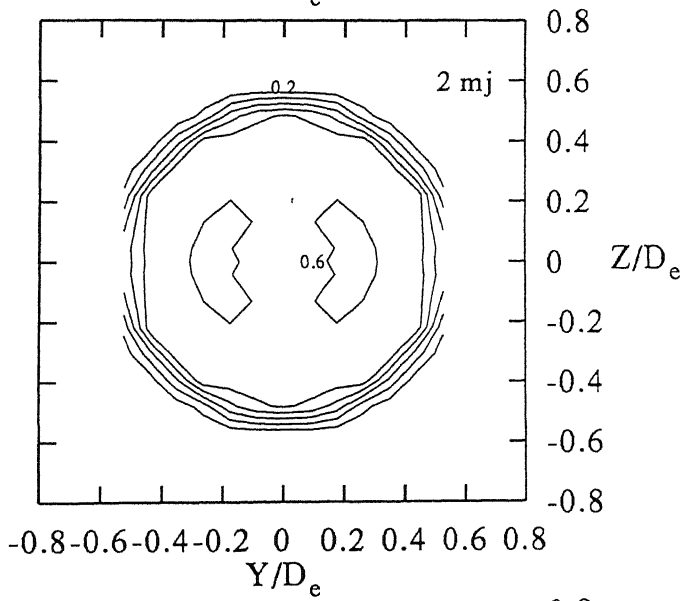

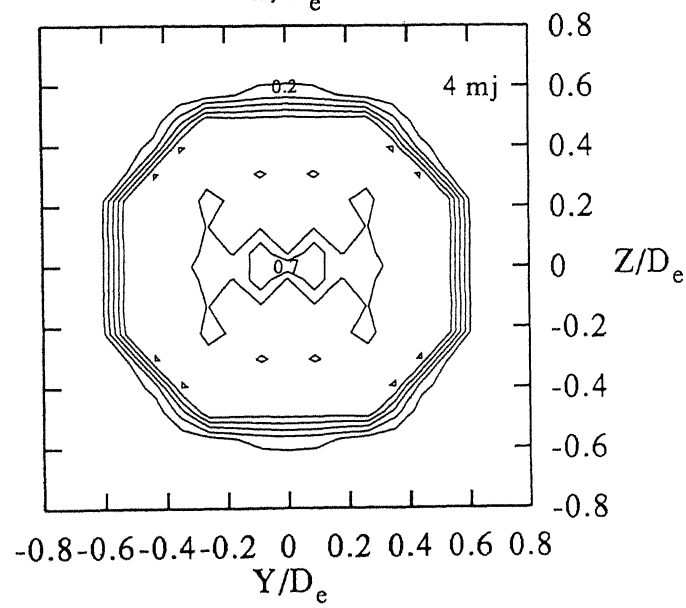

Fig 4.42. Contour Plots for NPR9, $X/D_e = 1$ and $r/r_e = 1.93$

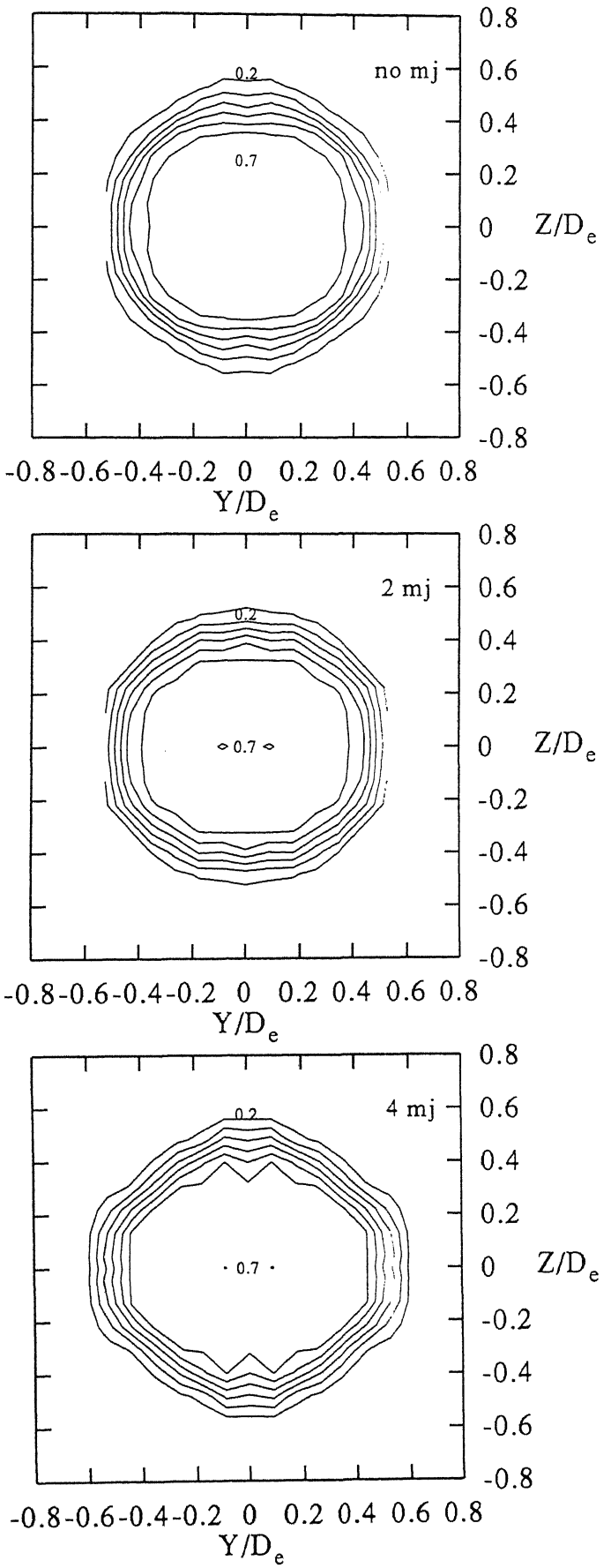

Fig 4.43. Contour Plots for NPR9, $X/D_e = 2$ and $r/r_e = 1.93$

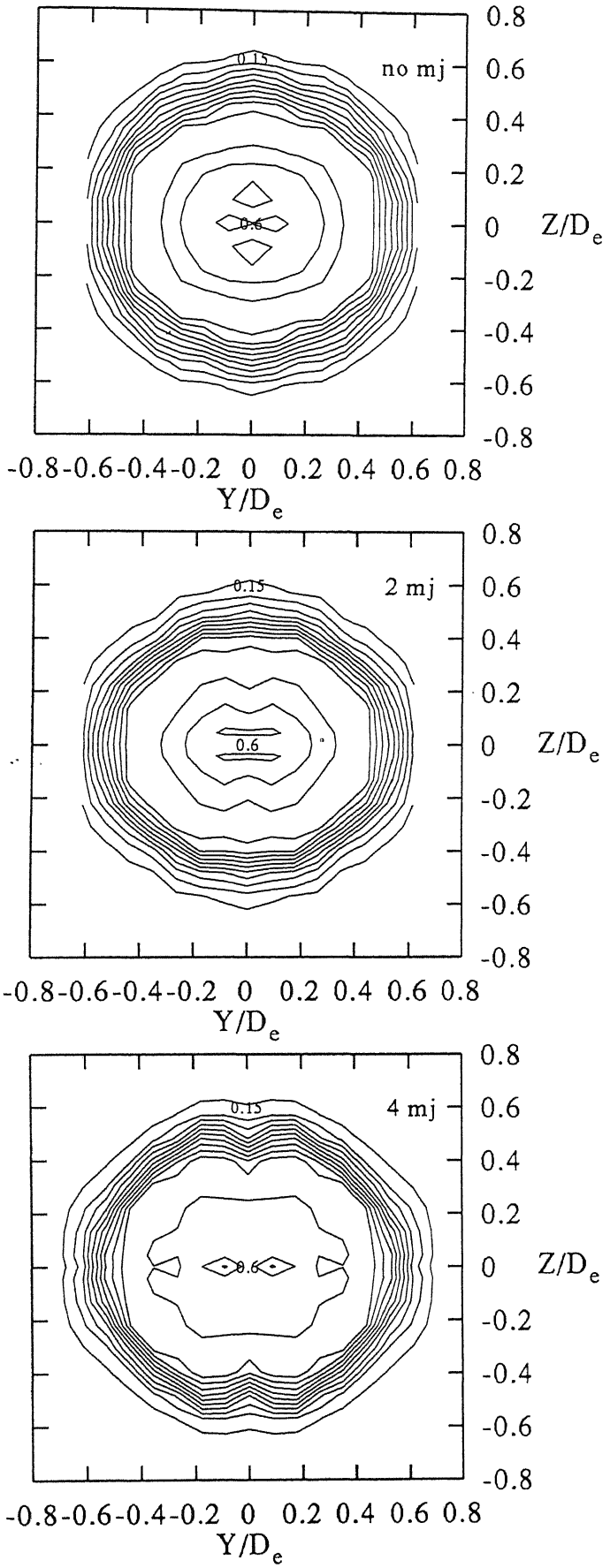

Fig 4.44. Contour Plots for NPR9, $X/D_e = 3$ and $r/r_e = 1.93$

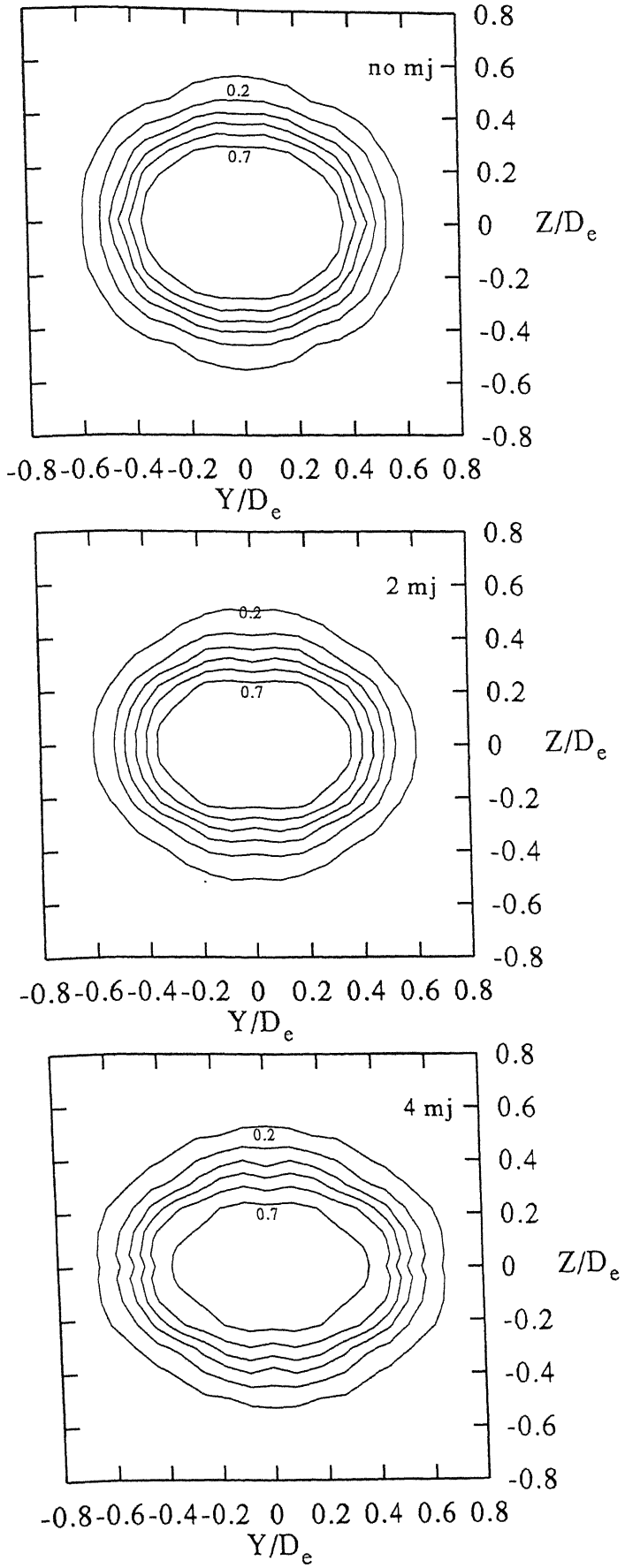

Fig 4.45. Contour Plots for NPR9, $X/D_e = 4$ and $r/r_e = 1.93$

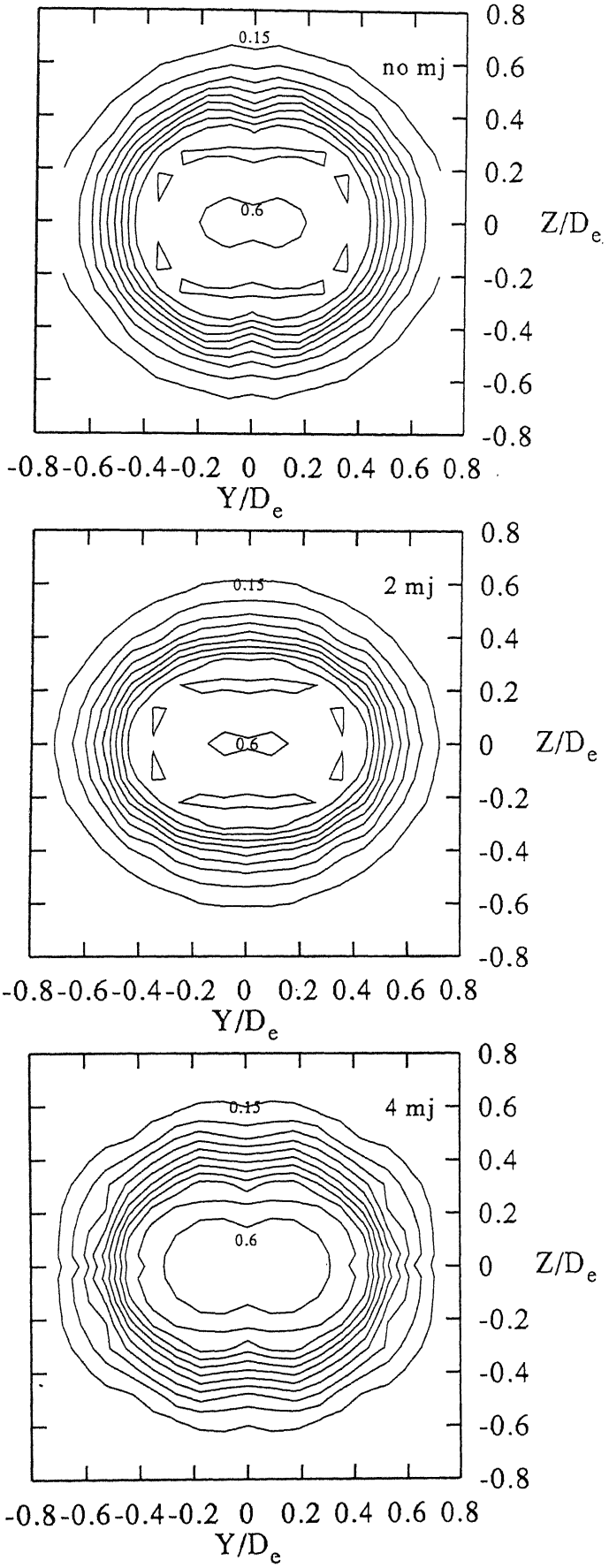

Fig 4.46. Contour Plots for NPR9, $X/D_e = 5$ and $r/r_e = 1.93$

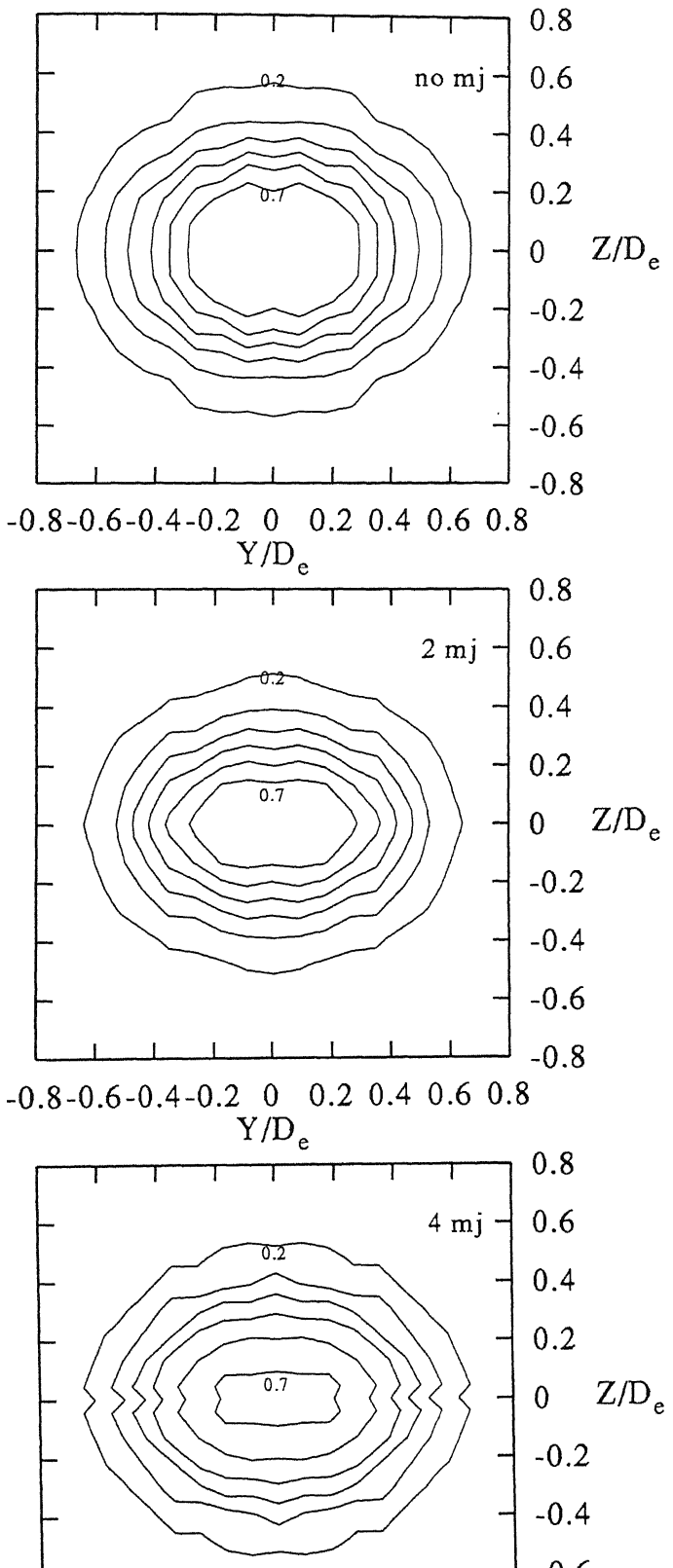

Fig 4.47. Contour Plots for NPR9, $X/D_e = 6$ and $r/r_e = 1.93$

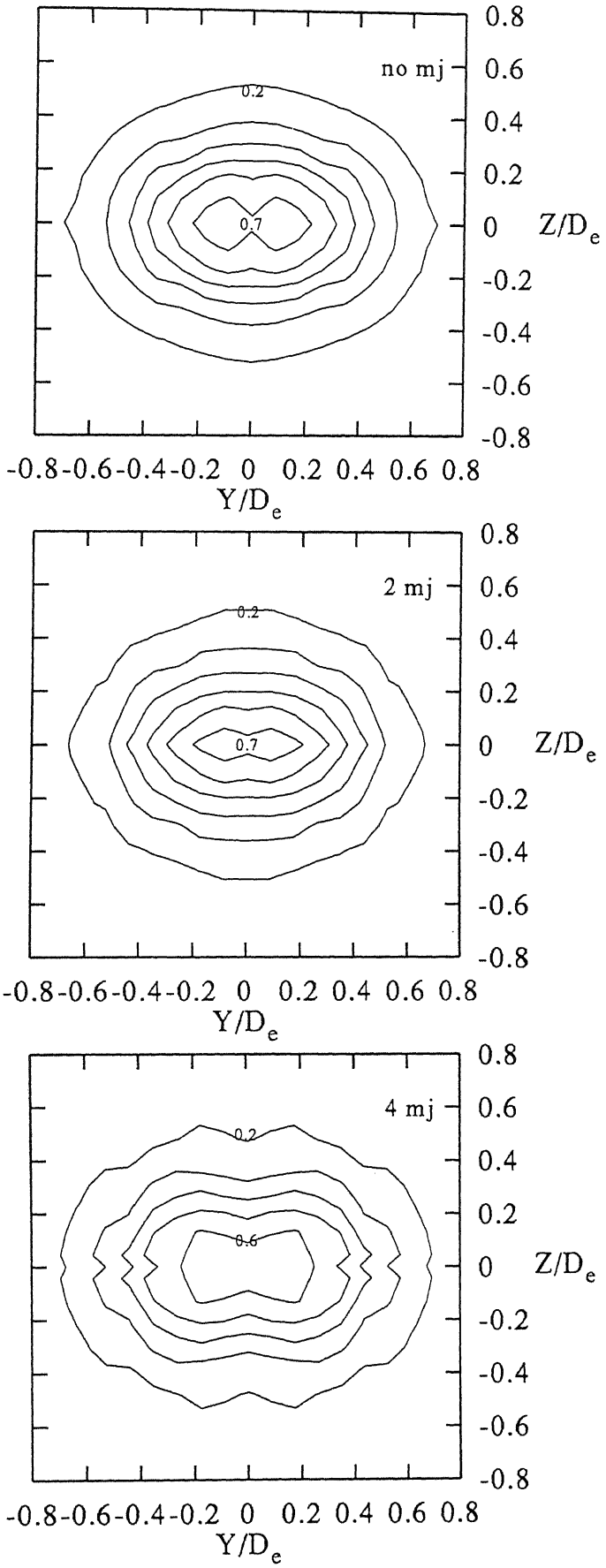

Fig 4.48. Contour Plots for NPR9, $X/D_e = 8$ and $r/r_e = 1.93$

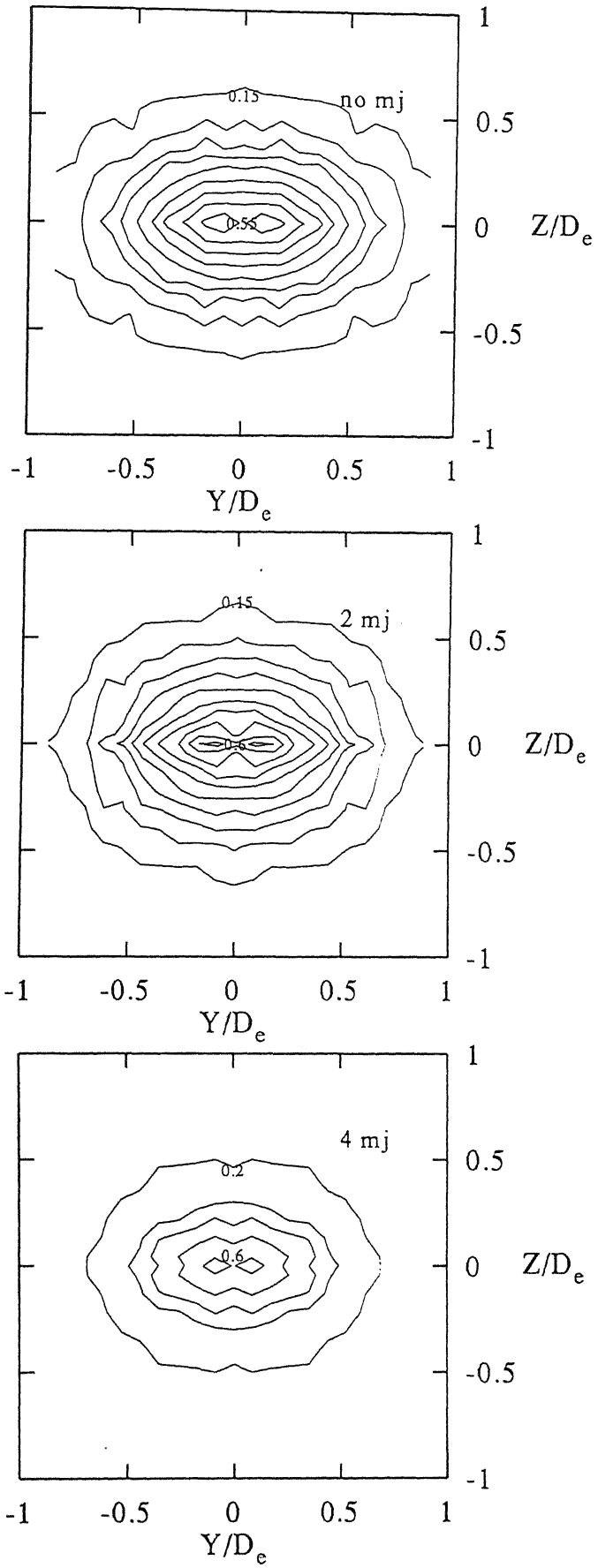

Fig 4.49. Contour Plots for NPR9, $X/D_e = 10$ and $r/r_e = 1.93$

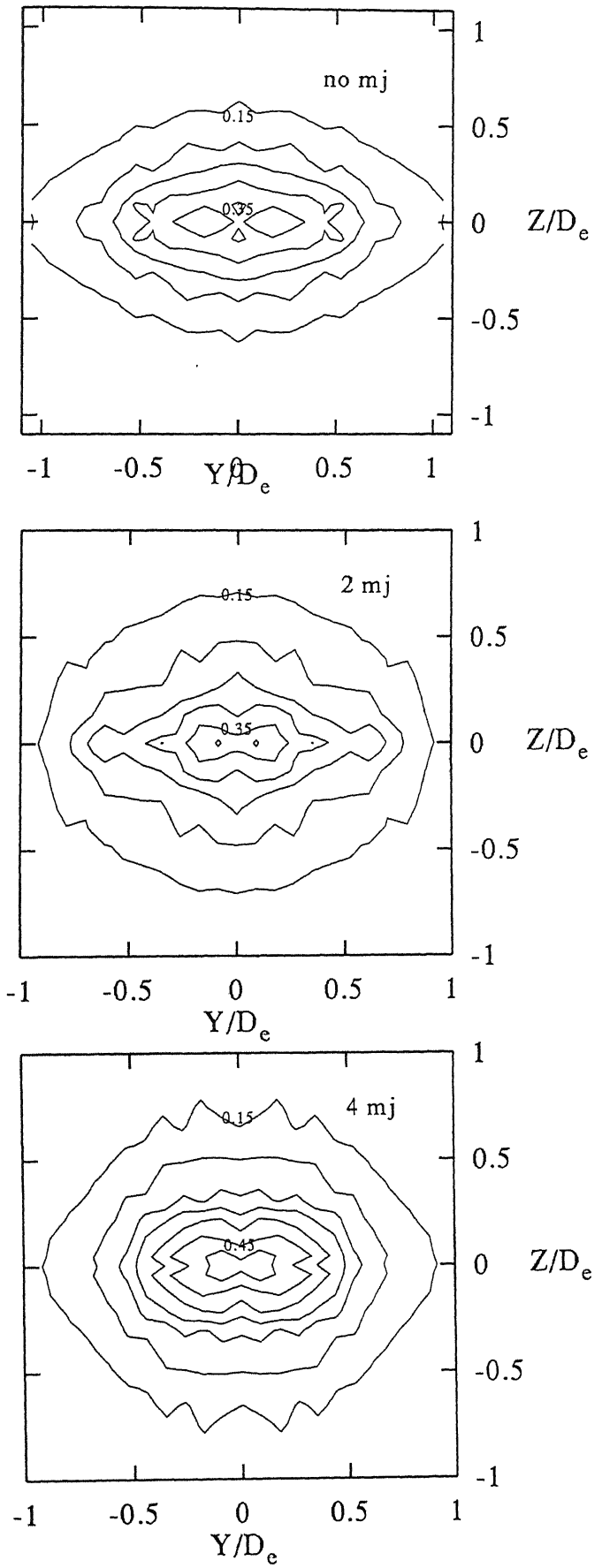

Fig 4.50. Contour Plots for NPR9, $X/D_e = 12$ and $r/r_e = 1.93$

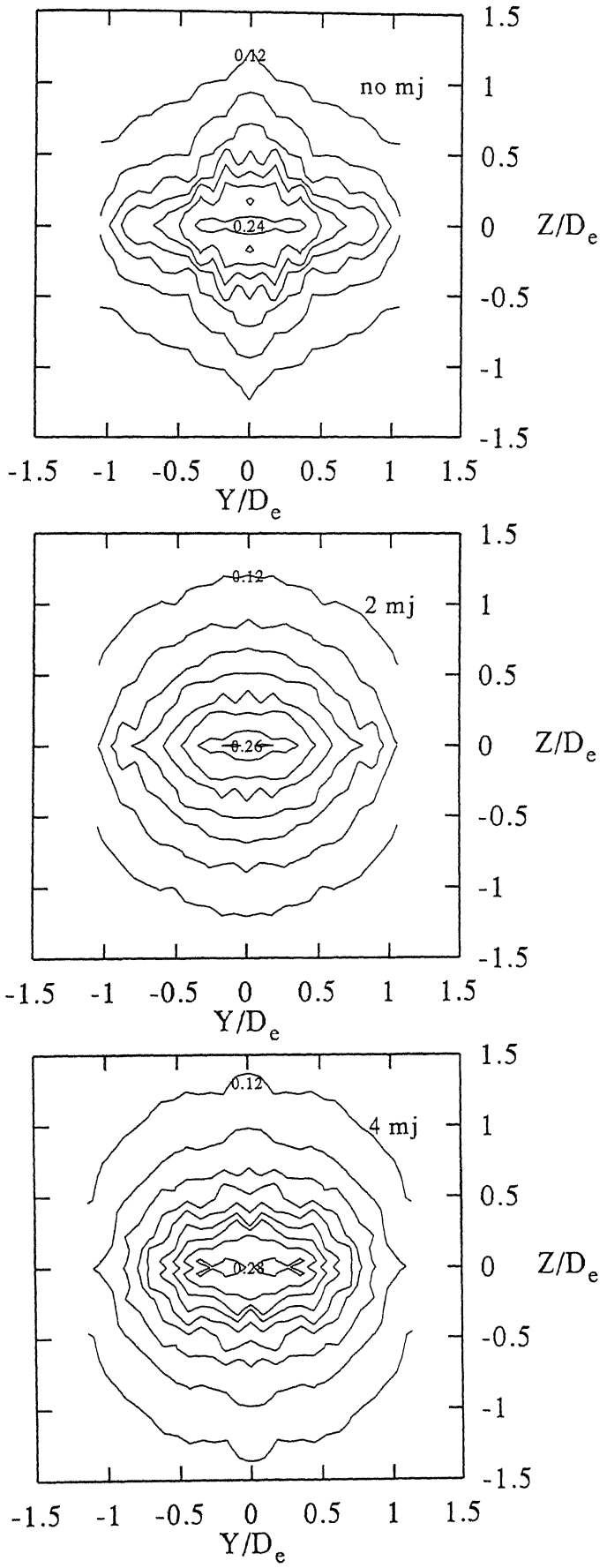

Fig 4.51. Contour Plots for NPR9, $X/D_e = 15$ and $r/r_e = 1.93$

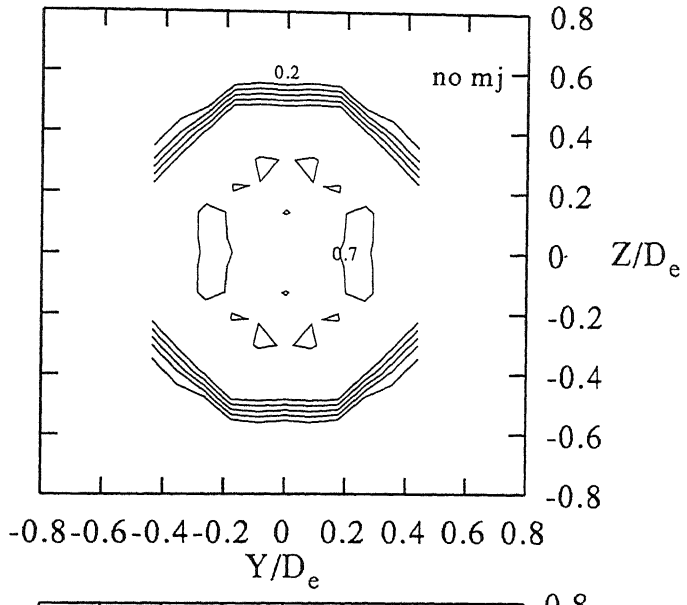

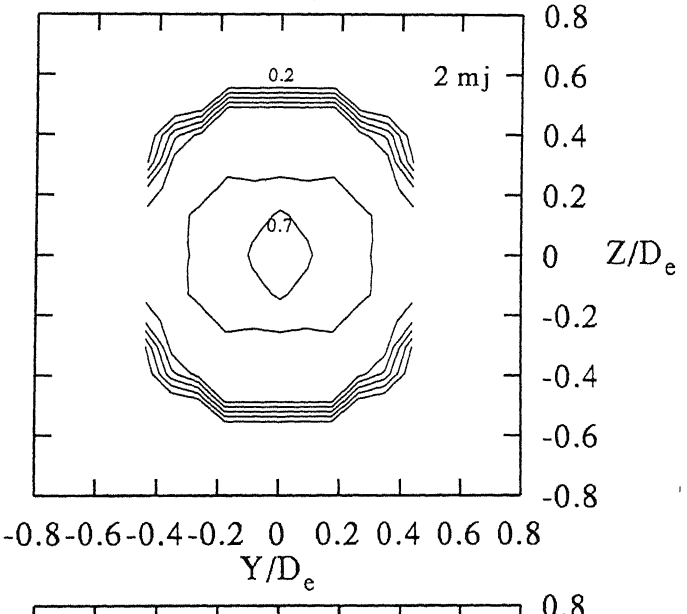

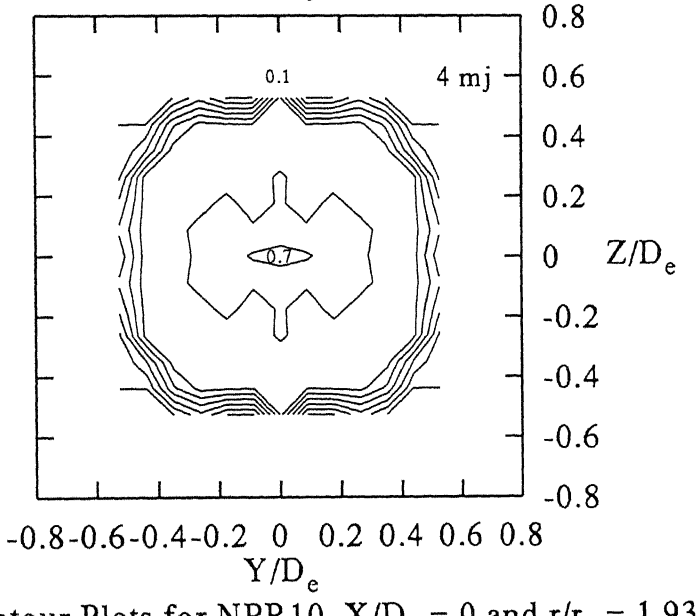

Fig 4.52. Contour Plots for NPR10, $X/D_e = 0$ and $r/r_e = 1.93$

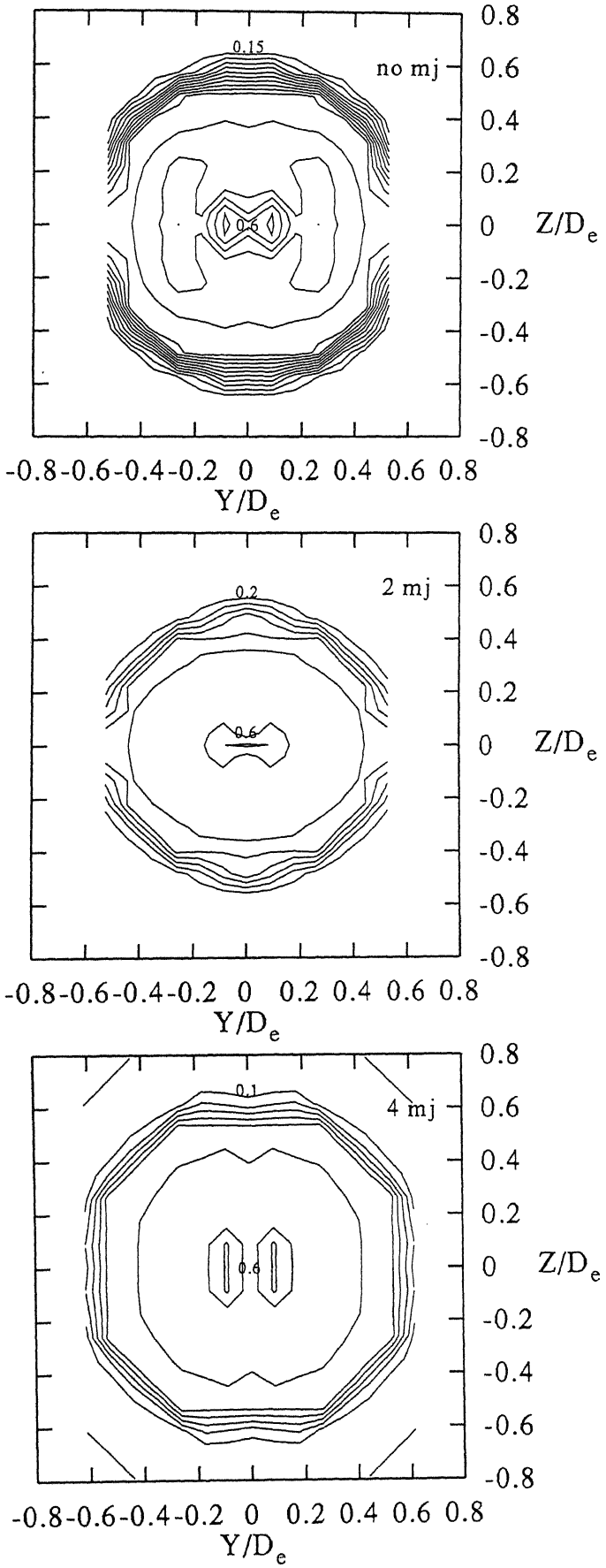

Fig 4.53. Contour Plots for NPR10, $X/D_e = 1$ and $r/r_e = 1.93$

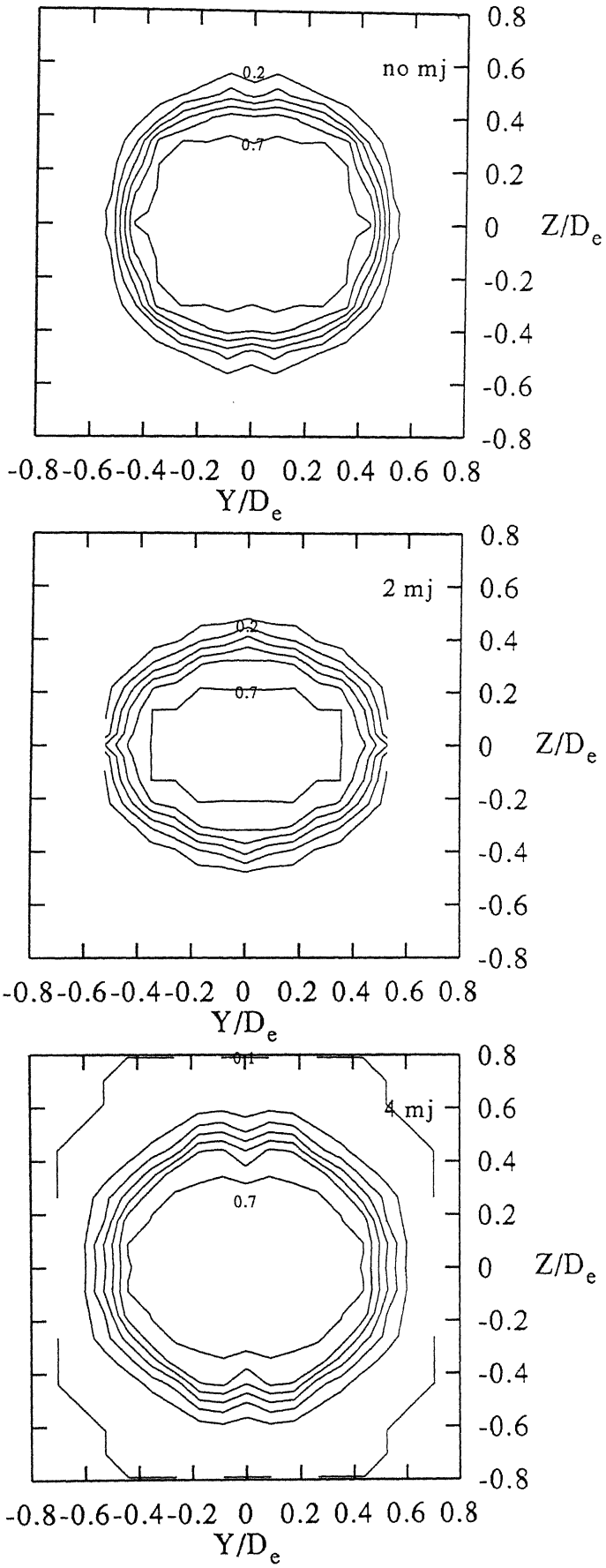

Fig 4.54. Contour Plots for NPR10, $X/D_e = 2$ and $r/r_e = 1.93$

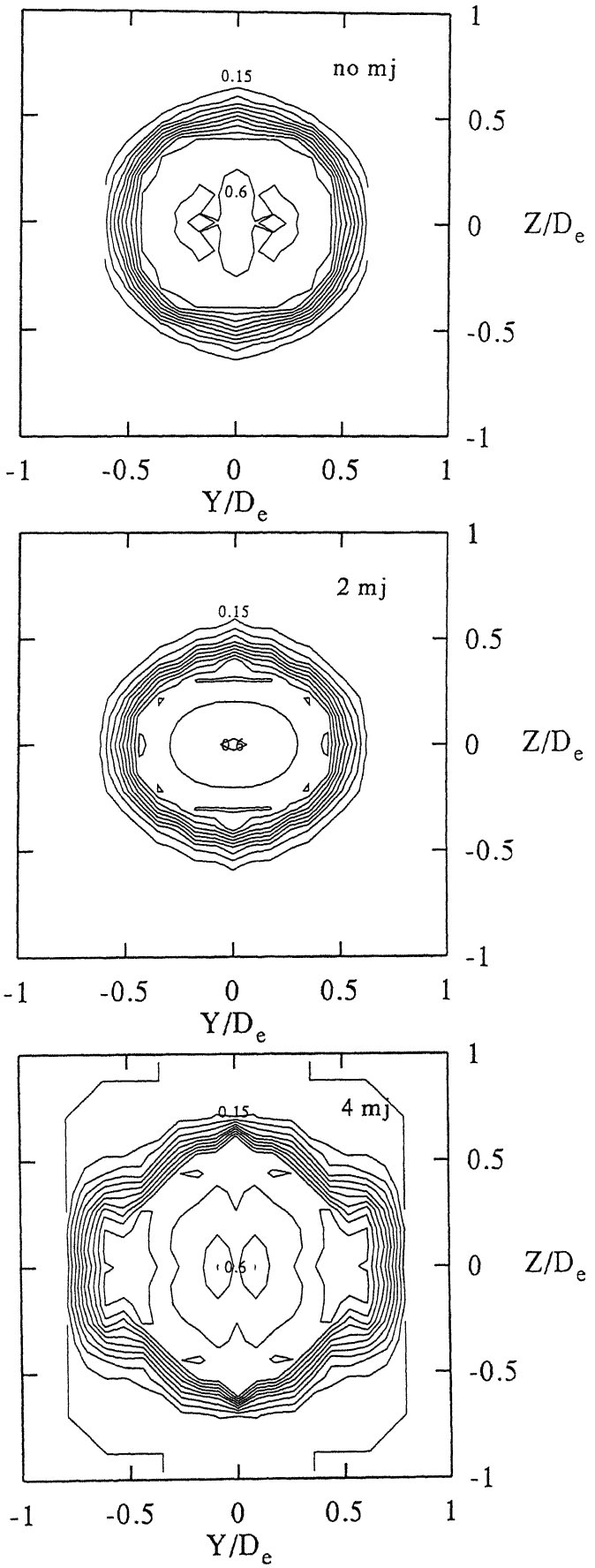

Fig 4.55. Contour Plots for NPR10, $X/D_e = 3$ and $r/r_e = 1.93$

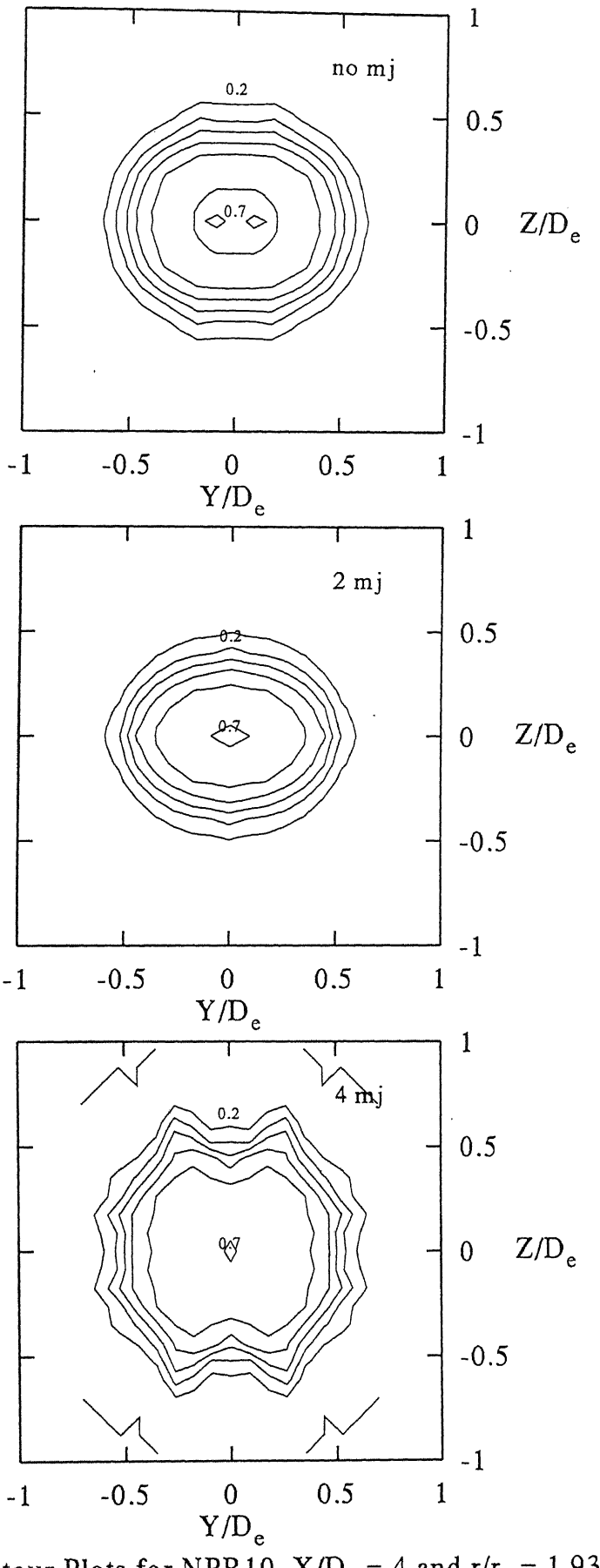

Fig 4.56. Contour Plots for NPR10, $X/D_e = 4$ and $r/r_e = 1.93$

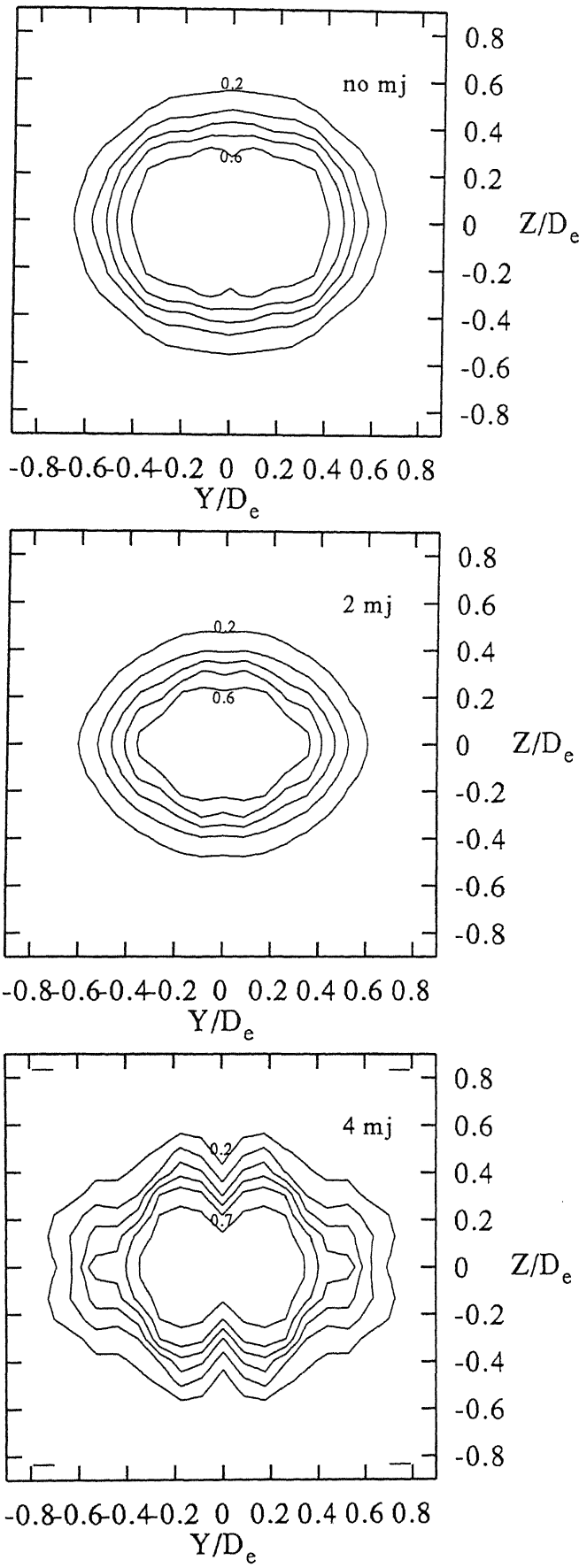

Fig 4.57. Contour Plots for NPR10, $X/D_e = 5$ and $r/r_e = 1.93$

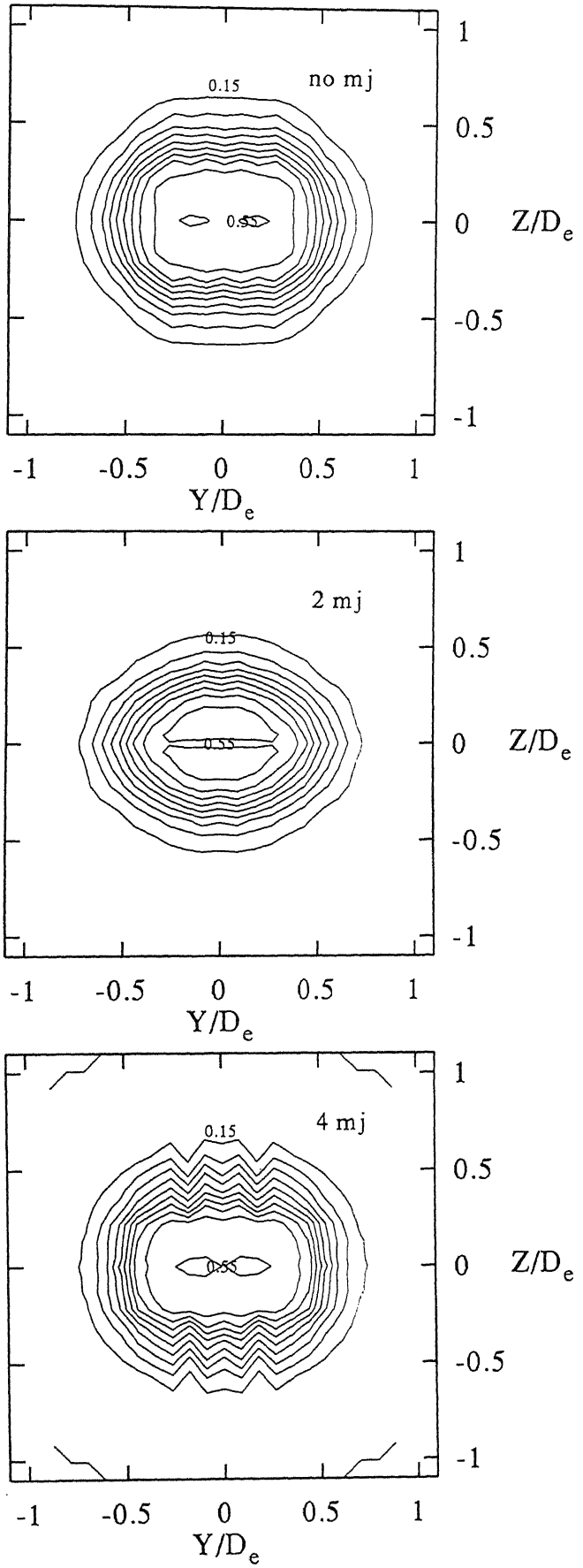

Fig 4.58. Contour Plots for NPR10, $X/D_e = 6$ and $r/r_e = 1.93$

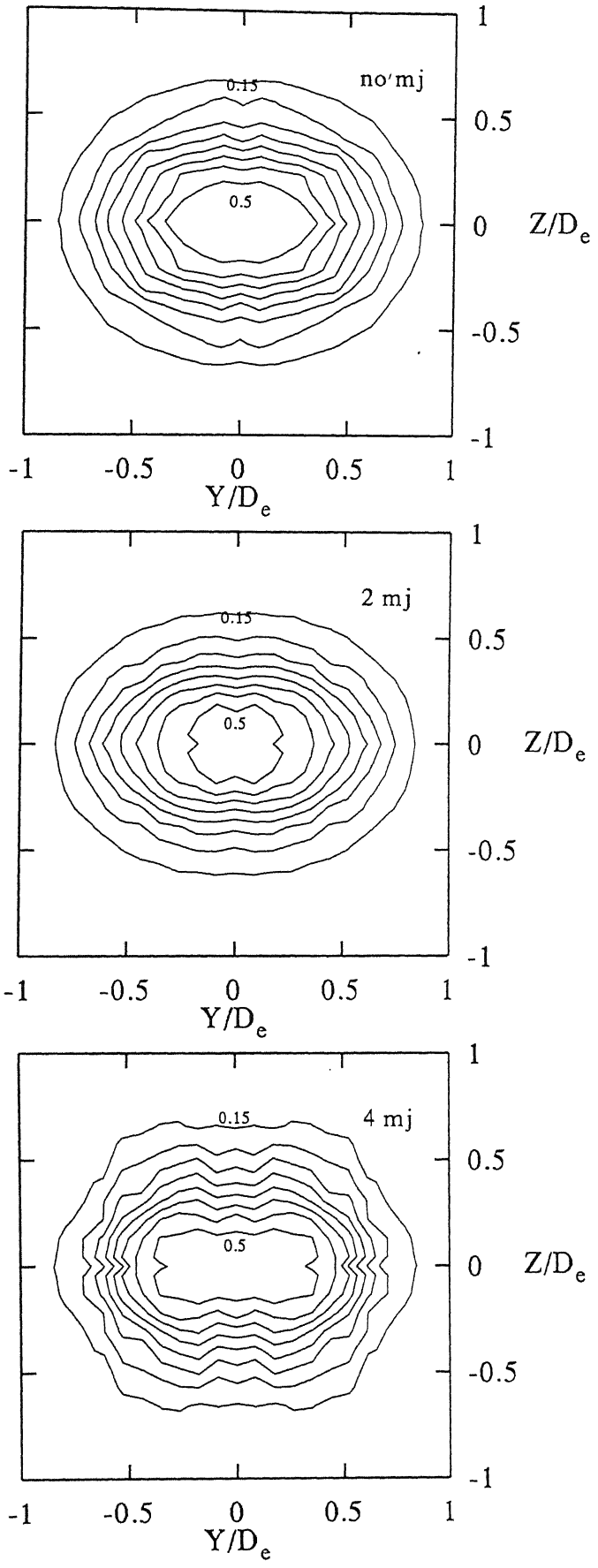

Fig 4.59. Contour Plots for NPR10, $X/D_e = 8$ and $r/r_e = 1.93$

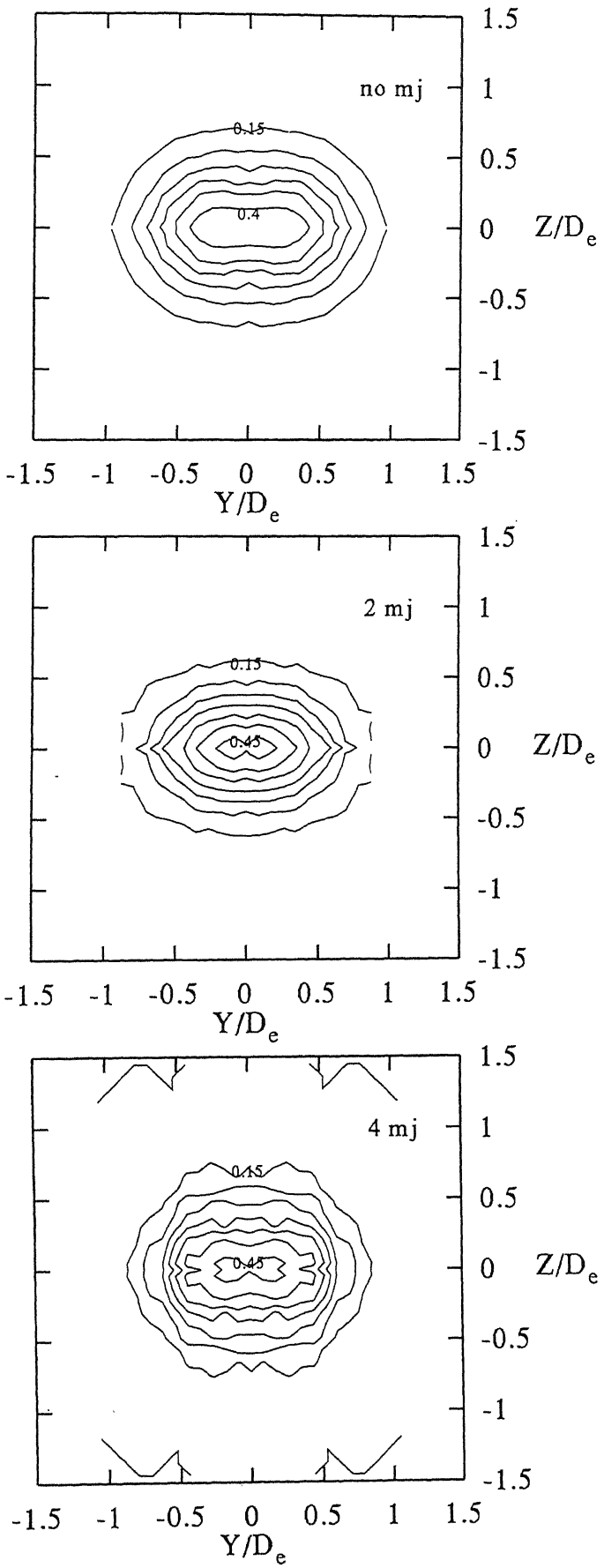

Fig 4.60. Contour Plots for NPR10, $X/D_e = 10$ and $r/r_e = 1.93$

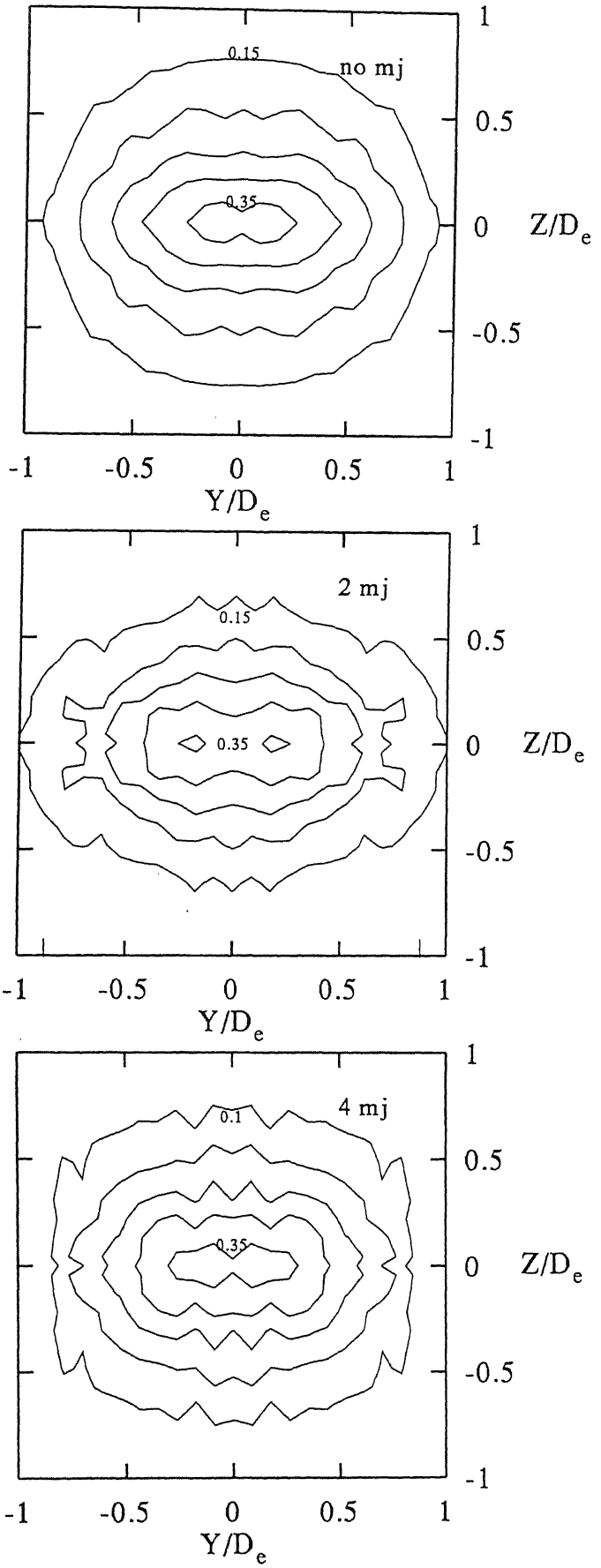

Fig 4.61. Contour Plots for NPR10, $X/D_e = 12$ and $r/r_e = 1.93$

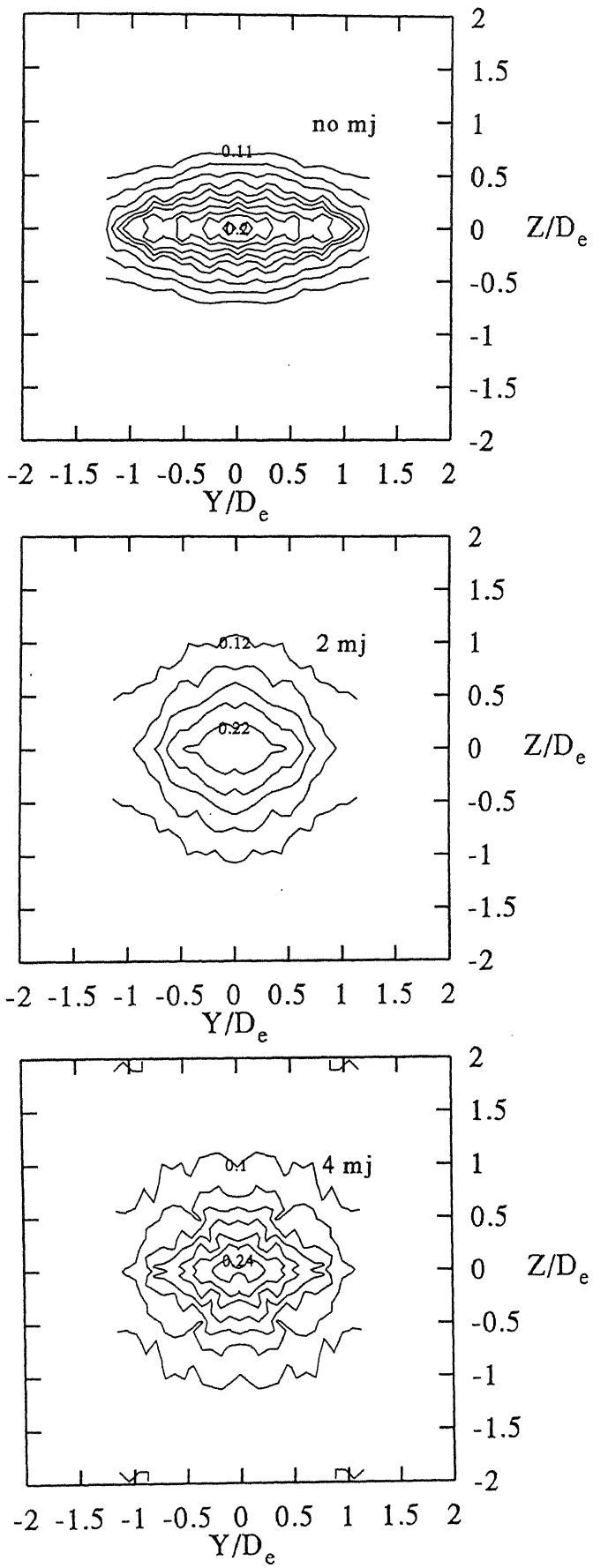

Fig 4.62. Contour Plots for NPR10, $X/D_e = 15$ and $r/r_e = 1.93$

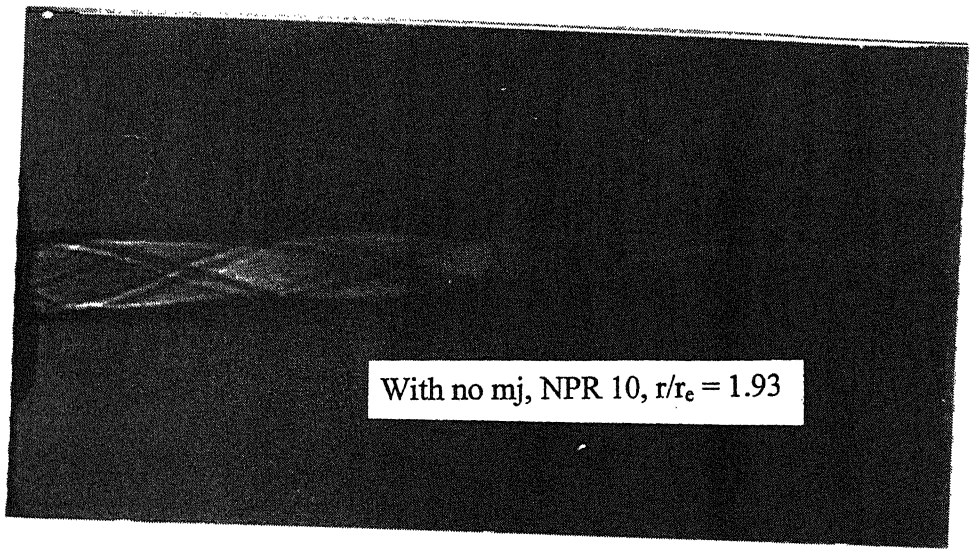

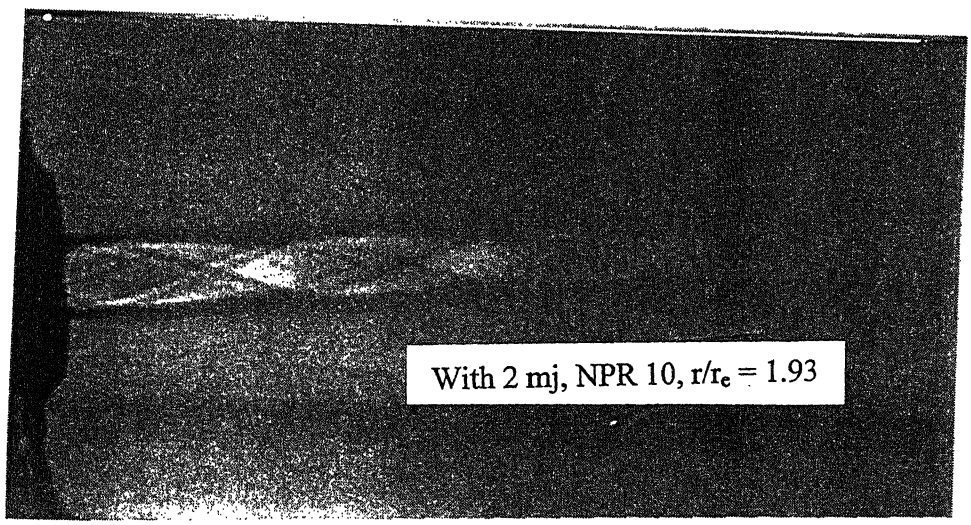

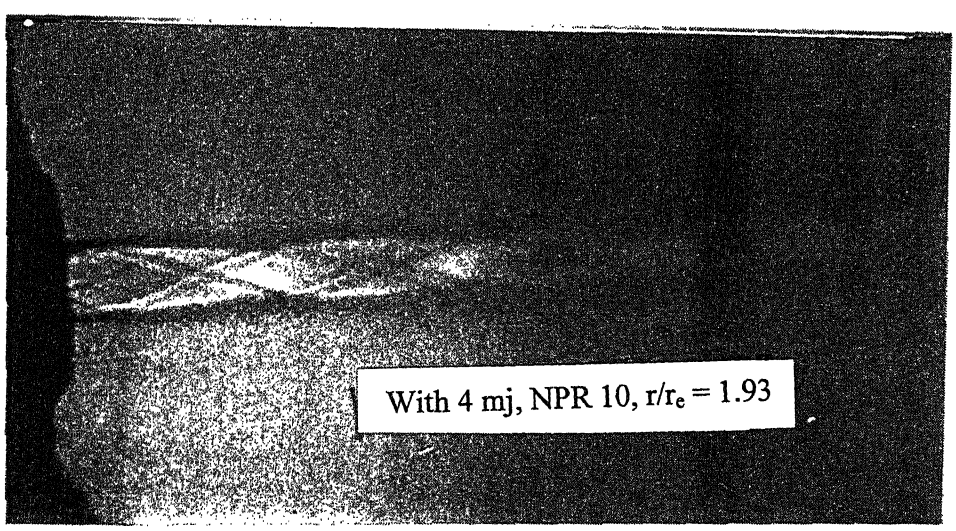

Fig. 4.63. Shadow graph Pictures for NPR 10.

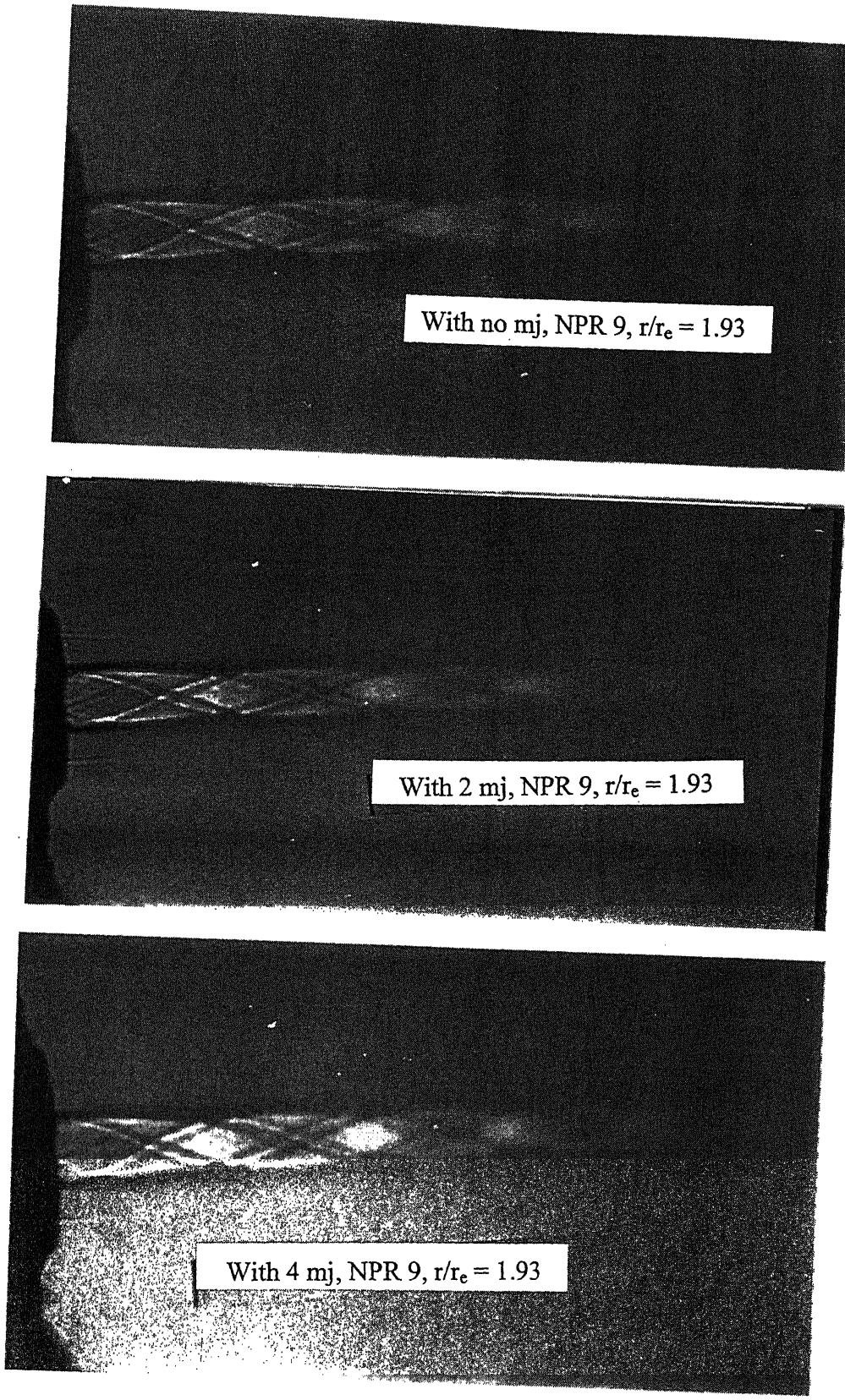

Fig. 4.64. Shadow graph Pictures for NPR 9.

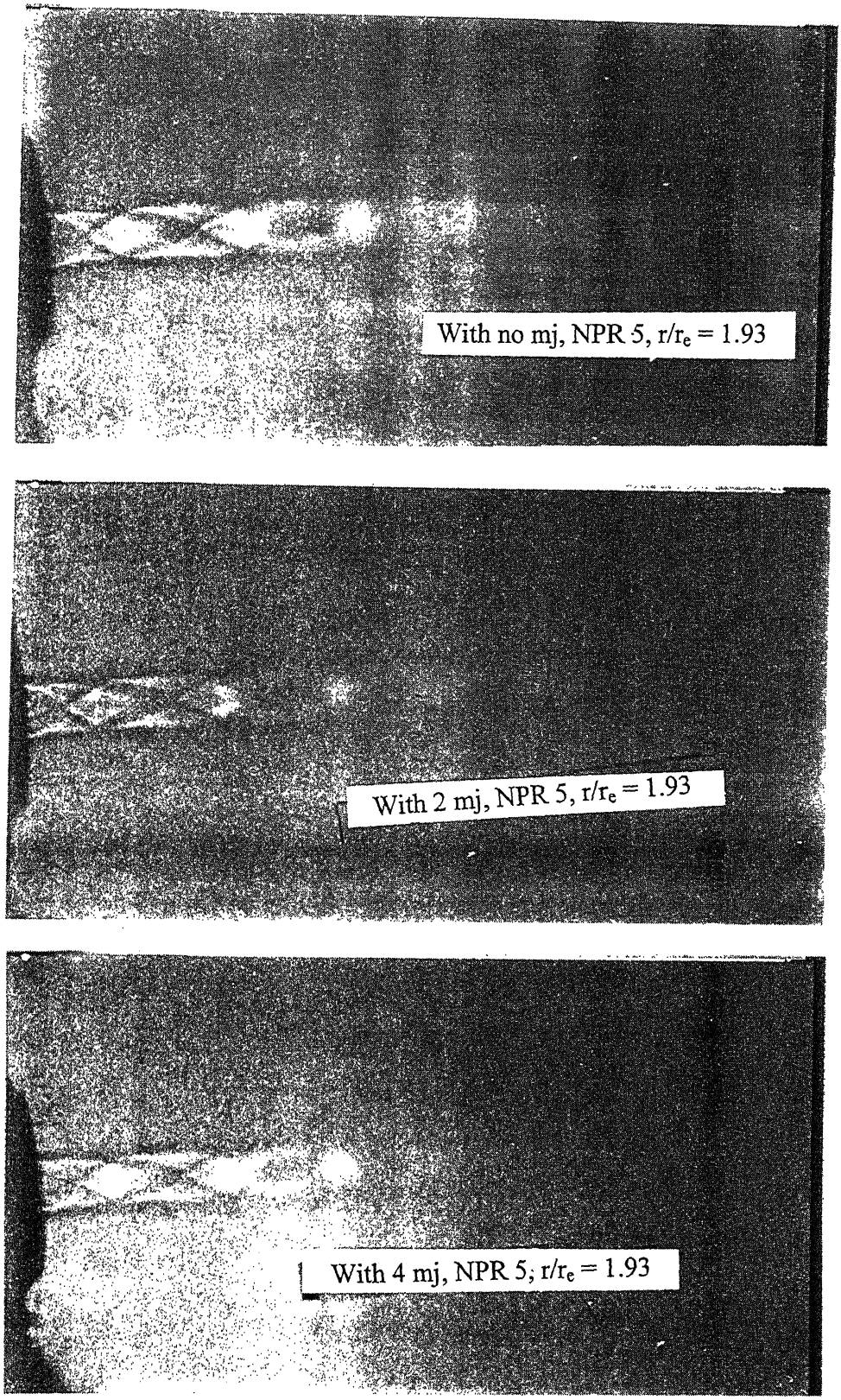

Fig. 4.66. Shadow graph Pictures for NPR 5.